NTNU

Norwegian University of
Science and Technology

Ecosystem restoration at Fundu Mare Island in the Inner Danube Delta near Braila (Romania)

Hydrodynamic optimisation

Muriel Zazie Madeleine Brückner

Civil and Environmental Engineering (2 year)
Submission date: February 2016
Supervisor: Jochen Aberle, IVM

Norwegian University of Science and Technology
Department of Hydraulic and Environmental Engineering

Abstract

Within the last century, the extensive implementation of engineering measures in European rivers has caused significant changes in river hydrology, water quality and local ecology, inducing major impact on the environment of wetlands. As a result, degradation of habitat quality in combination with loss of biodiversity are the major consequences. Along the Romanian Danube River, large parts of former wetlands, lakes and braided river reaches have disappeared, with the wetland Fundu Mare Island representing one of its last remains. In recent years, a reduction of the water levels and willow encroachment into the aquatic zone were observed, affecting the high biological diversity of the island. In order to protect biodiversity, the implementation of restoration measures in Fundu Mare Island is investigated within the project "Restoration of the aquatic and terrestrial ecosystems complex, from Fundu Mare Island, part of the Small Wetland of Brăila" funded by EEA-grants. As part of the project, this work aims at the investigation of a number of restoration scenarios that allow conservation of biodiversity. The implementation of a two-dimensional numerical model was examined in Delft3D. Due to the time restrictions of the thesis and unforeseen problems during model calibration, a general investigation by the application of a simplified water balance approach was applied. Based on the results, it can be concluded that the water levels on the island can be positively influenced by the implementation of weirs. In order to meet the requirements regarding security, hydrological uncertainty, and ecological demands, the installation of the bag weir is recommended. The demands of fish in the area can be met by seasonal opening of the channels on the island to enhance water exchange and provide connectivity between Fundu Mare Island and the Danube. However, further research needs to be carried out to analyse the feasibility of the implementation with regard to the simplifications made in this approach.

Table of content

List of figures

List of tables

List of equations

List of symbols

Symbol	Description	Dimension
$\sqrt{G_{\xi\xi}}, \sqrt{G_{\eta\eta}}$	coefficient to transform curvilinear to rectangular coord.	[-]
a	characteristic amplitude	[m]
A	channel cross section	[m²]
B_S	clear span between stones of bottom slide	[m]
C	Courant number	[-]
c	mass concentration	[m³/s]
c'_μ	constant	[-]
C_{2D}	Chézy-coefficient	[$m^{1/2}/s$]
d	depth below reference plane	[m]
$D_{V,H}$	vertical and horizontal diffusivity	[m²/s]
f	Coriolis coefficient	rad/s
$F_{\xi,\eta}$	horizontal Reynold's stresses	[m²/s²]
g	gravitational acceleration	[m/s²]
h	total water depth	[m]
h_0	backwater height upstream	[m]
h_m	mean water depth	[m]
h_u	backwater height downstream	[m]
I_b	bottom slope	[-]
k	turbulent energy	[m²/s²]
k_f	conductivity coefficient	[m/s]
L	mixing length	[m]
L_W	width of weir crest	[m]
$M_{\xi,\eta}$	external sources of momentum	[N/m]
n	Manning-coefficient	[$s/m^{1/3}$]
N	number of time-steps	[-]
n_1, n_2	relation x/y-coordinate	[-]
p	weir crest height	[m]
P	hydrostatic pressure	[N/m²]
$P_{\xi,\eta}$	horizontal pressure terms	[N/m²]
Q	total discharge	[m³/s]
Q_{in}	positive water discharge	[m³/s]

Q_{out}	negative water discharge	[m³/s]
S	source and sink terms	[kg m/s]
U	wetted perimeter	[m]
U,V	depth-averaged velocities	[m/s]
u,v	velocities in x-,y-coordinates	[m/s]
V_{ET}	volume of evaporation/precipitation	[m³/d]
V_{GW}	volume ground water loss	[m³/d]
V_n, V_{n-1}	water storage volume	[m³/d]
V_S	volume surface discharge	[m³/d]
Z	vertical axis	[m]
α	angle of Thomson weir	[°]
Δt	time-step	[s]
$\Delta x,y$	grid cell size	[m]
δ	threshold depth in velocity points	[m]
δ	discharge coefficient	[-]
ε	reduction factor for tailwater	[-]
ε	turbulent dissipation	[m²/s]
ζ	water surface elevation	[m]
$\nu_{v,H}$	vertical, horizontal eddy viscosity coefficient	[m²/s]
ξ,η	horizontal curvilinear coordinates	[m]
μ	discharge coefficient	[-]
ρ	density of water	[kg/m³]
σ	σ-coordinate	[m]
σ_{id}	overflow coefficient	[-]
$\tau_{bx,y}$	horizontal bed shear stresses	[N/m²]
ω	vertical velocity component	[m/s]

1 Introduction

Within the last century, the extensive implementation of engineering measures in European rivers caused significant changes in river hydrology, water quality and local ecology. With an alarming extent, the impact on the environment is quantified by a number of 60–90 % of natural habitats that have been lost in large parts of central Europe (Hoekstra et al. 2010). As a result, degradation of habitat quality in combination with loss of biodiversity are the major consequences. For example, in the Danube River (cp. Figure 1), which is the second largest river in Europe with a length of nearly 3,000 km and a catchment from Germany until its river mouth at the Black Sea (Schiemer et al., 1999), the introduction of dams and enhanced river straightening induced strong alterations of the flow regime. The measures had a major impact especially on the Lower Danube. In Romania, long stretches of the Danube were dammed and huge areas were set dry. Consequently, large parts of former wetlands, lakes and braided river reaches disappeared. The variety of wetlands and islands that provide habitat to many endangered species were strongly affected and caused alterations of the ecosystems and their functions for the local climate. Present problems for nature conservation in the Romanian Danube are related to modified flow and sedimentation processes, pollution, vegetation and changes in land use.

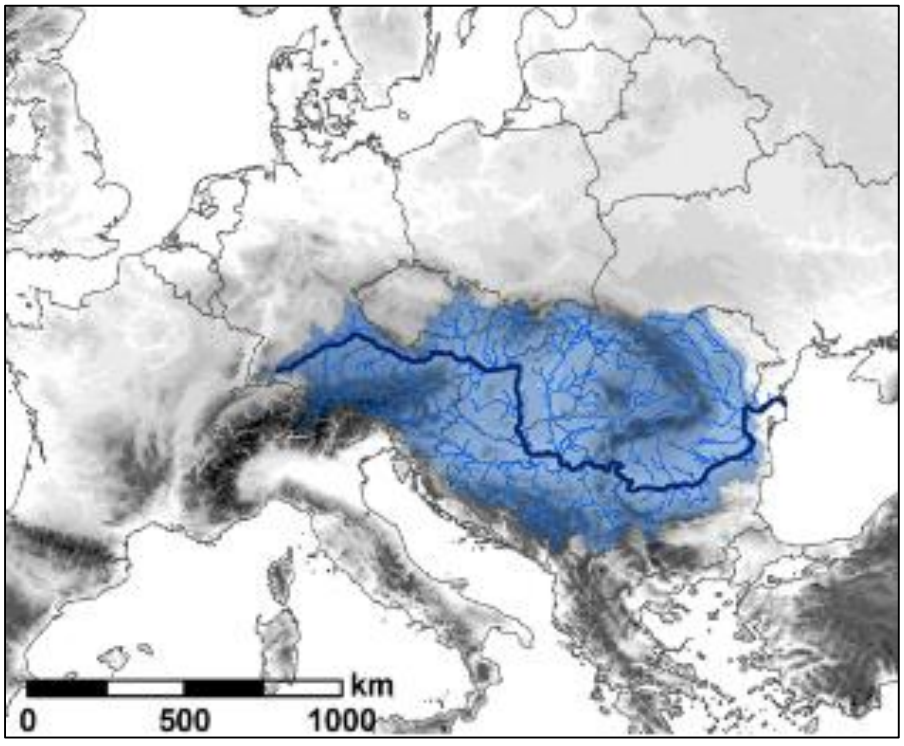

Figure 1. Danube River and catchment (Stagl & Hattermann, 2015)

The conservation of lakes and river systems is needed to protect ecosystem function and services to human society (Dungeon et al. 2006). One example of the ecosystem changes in the Danube is represented by the wetland Fundu Mare Island, which is one of the last remains of a previously larger wetland area. It is characterised by high biological diversity with a wide range

of plants and animal species. Today, it is especially important in providing habitat to a variety of endangered bird and fish species, which have lost great parts of their habitat by damming of the Danube. Within the last decade, significant changes in water retention on the island resulting from anthropogenic impact were recorded. An increased water loss led to a drying of the major lakes on the island during summer, which induced habitat loss of aquatic species and negatively altered biodiversity in the area. In recent years, an increase of ruderal plants in former aquatic habitat was observed. In combination with climatic changes, this trend is expected to increase and significantly affect biodiversity in the wetland in the long term (Stagl & Hatterman, 2015).

To protect and enhance biodiversity, the implementation of restoration measures in Fundu Mare Island is regarded as a necessity. The project "Restoration of the aquatic and terrestrial ecosystems complex, from Fundu Mare Island, part of the Small Wetland of Brăila", funded by EEA grants, is a Romanian-Norwegian cooperation between six different partners, including SINTEF Energy Research, Norwegian University of Science and Technology (NTNU), Norwegian Institute for Nature Research (NINA), Danube Durable Development Institute (IDDD), and "Dunărea de Jos" University of Galați (UDJG). The project is coordinated by the Romsilva National Forestry - Small Wetland of Brăila Natural Park Administration and carried out between May 2015 and May 2016. Due to a variety of engineering applications in wetland restoration, the investigation of the hydraulic characteristics and the ecological impact induced by possible construction measures is required to develop adequate site-specific measures for Fundu Mare Island. To investigate the hydraulics in Fundu Mare Island, different modelling approaches can be considered. Numerical modelling of wetlands is mostly carried out using one- and two-dimensional modelling, due to the high complexity of the hydraulic processes in wetlands. More simplified approaches are used to give insight into the reaction of basic flow parameters, i.e. water level, discharge and velocity, on alterations due to construction or restoration measures. In general, the appropriate method is decided upon based on the accuracy and resolution of the data and the accepted assumptions introduced by the method.

The task of this work is to study the effect of restoration measures in Fundu Mare Island on the hydraulic conditions and give advice on protection of local biodiversity. A comprehensive investigation of possible measures with regard to economy, ecology and society was carried out. To obtain most precise results, the feasibility of a hydrodynamic model based on the provided data is investigated. Moreover, to allow estimation of the hydraulic reaction to restoration measures, the application of alternative approaches was considered. Different restoration scenarios were analysed to study their effect on water retention on the island and to prevent drying out of the lakes. Therefore, chapter 2 gives a more precise description of research results with regard to restoration of wetlands, including suggestions on different construction measures. Furthermore, different modelling approaches are presented in detail. In chapter 3 the site and its temporal development are presented, leading to a precise description of the project's background. A summary of the available data and suitable software packages are described in chapter 4, which led to the selection of the appropriate software. The set-up of a two-dimensional model is closely looked at in chapter 5. Chapter 6 presents the analysis of the calibration process together with the implementation of a simplified approach. Additionally, the results are described and evaluated. A detailed discussion of the findings obtained by the

models and recommendation of suitable restoration measures is carried out in chapter 7, which leads to the final conclusion obtained in chapter 8.

2 State of the art

The following chapter gives an overview on the basic principles of river and wetland restoration as well as possible measures to recreate biodiversity. Moreover, the current development of numerical modelling in river engineering and its methodology is summarised.

2.1 Restoration of wetlands

Human activity in rivers has different purposes (e.g. hydroelectric power, agriculture, land reclamation, industry, flood protection) negatively affecting biota that is sensitive to habitat changes (Malmqvist & Rundle, 2002; Dudgeon et al., 2006). Biodiversity is not only limited to the main channel but interacts with the river catchment basin, including wetlands and floodplains (Buijse et al., 2002). Wetlands contribute to the global climate through carbon management, flood abatement, water quality improvement, and biodiversity support. They provide buffering functions in the hydrological cycle and natural resources, recharge ground water, reduce floods, and enhance dry season flows (Bullock & Acreman, 2003). These functions are determined as globally significant and negative impacts on the functionality of wetlands and rivers become a major issue (Zedler & Kercher, 2005). Restoration measures can diminish negative effects on local biodiversity and therefore are of great interest to sustain biological heritage.

2.1.1 Definition of wetlands and constraints

Cowardin et al. (1979, p. 3) defined wetlands as “lands where saturation with water is the dominant factor determining the nature of soil development and the types of plant and animal communities”. They are “lands transitional between terrestrial and aquatic systems, where the water table is usually at or near the surface or the land is covered by shallow water”. All over the world, flow regulation of large rivers has been carried out by construction of dams, channelization or floodplain reclamation (Gore & Shields, 1995; Buijse et al., 2002). In many dammed rivers, wetlands suffer from eutrophication followed by terrestrialization (Amoros et al., 1987), making them to one of the most endangered landscapes worldwide (Olson et al., 1998).

In combination with the direct anthropogenic impact the effects of climate change on wetlands is a controversial subject discussed in many research papers. Although ecological effects are apparent, the direct impact on local ecosystems is unbalanced and requires further analysis. The global change in temperature is predicted to range between 1°C and 5°C, inducing direct effects in coastal regions and secondary effects inland, e.g. changes in evaporation lead to increasing precipitation on higher altitudes, whereas lower altitudes experience a decrease in rainfall (Day et al., 2005). The main impact on wetlands due to climate change is alteration of the hydrological regime, including effects on the hydroperiod and increase of extreme events. Furthermore, regional effects influence the local climate, i.e. alteration of evaporation and biochemistry, increased temperature, and altered amounts and patterns of suspended sediment

loadings (IPOC, 1997; Burkett & Kusler, 2000). Future changes include declination of the number and functional capacity of wetlands as well as a geographical shift (Erwin, 2009).

To quantify the changes in wetland distribution the cross section of a river floodplain can be divided into different zones, determined by the water level of different flood frequencies (cp. Figure 2). The vegetation distribution can be defined by days of inundation throughout the year: inundation of 365 days is defined as aquatic zone, 30-150 days is classified as softwood, and 0-30 days per year is referred to as hardwood (Pott & Remy, 2000). For each zone different biota is representative according to the local ecosystem characteristics. With changes in flood frequency and duration due to the above effects, the number of inundation days can change and affect the distribution of vegetation. With a decreasing number of inundation days, hard- and softwood will move closer to the main channel and the wetland will shrink. As a result, vulnerable species will lose their habitat and become endangered from extinction. The functionality of the wetland for the local environment is reduced. If it comes to a dry-out of the entire wetland, a strong alteration in biodiversity is caused and whole regions may be affected.

With regard to the negative effects from flow regulation and climate change on water quality, biodiversity and groundwater, the restoration of rivers and their conservation becomes a priority (Gore & Shields, 1995).

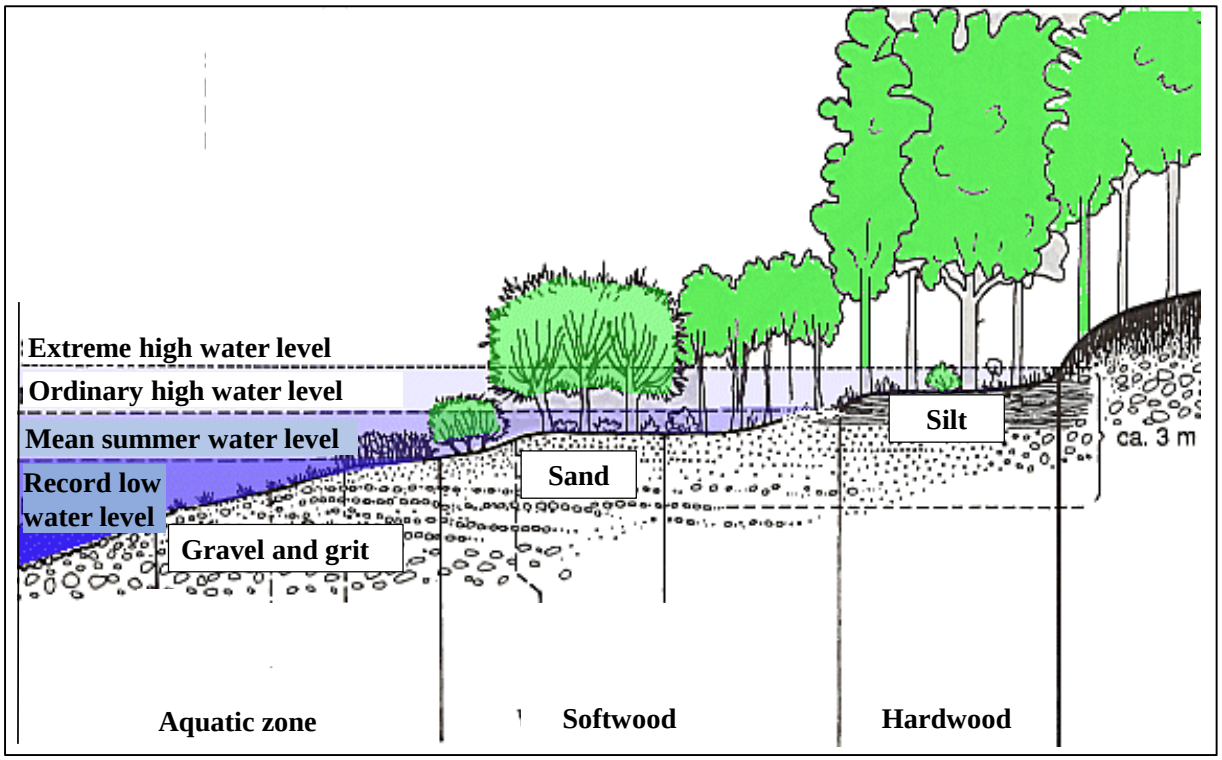

Figure 2. Cross section of a floodplain (Pott & Remy, 2000, modified)

2.1.2 Interaction between restoration and biodiversity

There exist different definitions for the term “restoration”. The European Centre for River Restoration (2014) defines river restoration as a high range of measures and practices, considering ecology, spatial and physical extent of the measures as well as management approaches. The objective of these measures is restoration of the natural state and of the functions in the river system by supporting biodiversity, flood protection, recreation and landscape development. Restoration of wetlands mainly target the increase of both biodiversity and ecosystem services. These objectives are not necessarily realizable on the same area, and require complex modelling (Ehrenfeld, 2000). Henry & Amoros (1995) see restoration of the dynamic equilibrium as major objective to stop the terrestrialization process. Terrestrialization describes the transformation from a wetland to a terrestrial ecosystem due to bottom aggradation caused by accumulation of organic matter, sediment deposition, or decrease in water level.

In the past, river conservation and restoration was primarily studied to manage economically important fauna, i.e. trout and salmon, or to protect endangered species. Generally, abiotic factors are determined as main drivers for abundance and distribution of biota in flood-prone rivers (Stanford et al., 1996). More specifically, biodiversity is controlled by temperature as well as presence of nutrients and other resources required for reproduction (Andrewartha & Birch, 1964). The genetic responses on changes of these factors depend on intensity and duration of environmental changes. However, the importance of the geological and climatic factors decreases with increasing time between abiotic disturbances (Ward & Stanford, 1983).

Floodplain systems, including main channel, shallow side arms, and floodplain lakes and ponds permit sustainability of endangered lotic species that are generally non-existing in large European rivers (Buijse et al., 2002). Highest heterogeneity occurs in alluvial segments within the river continuum, where seasonal temperature patterns and lateral habitat arrays create different environmental circumstances (Gore & Shields, 1995). Changing flow conditions define substratum changes hence forcing biota to adapt to physical forces and allowing different compositions in biodiversity (Statzner et al., 1988; Stanford et al., 1996; Glaeser & Wulf, 2009). This high complexity requires consideration of biological as well as chemical processes in the area. Together with the influence of human interaction, successful river restoration is possible (Stanford et al., 1996). Figure 3 shows resources and constraints influencing bioproduction.

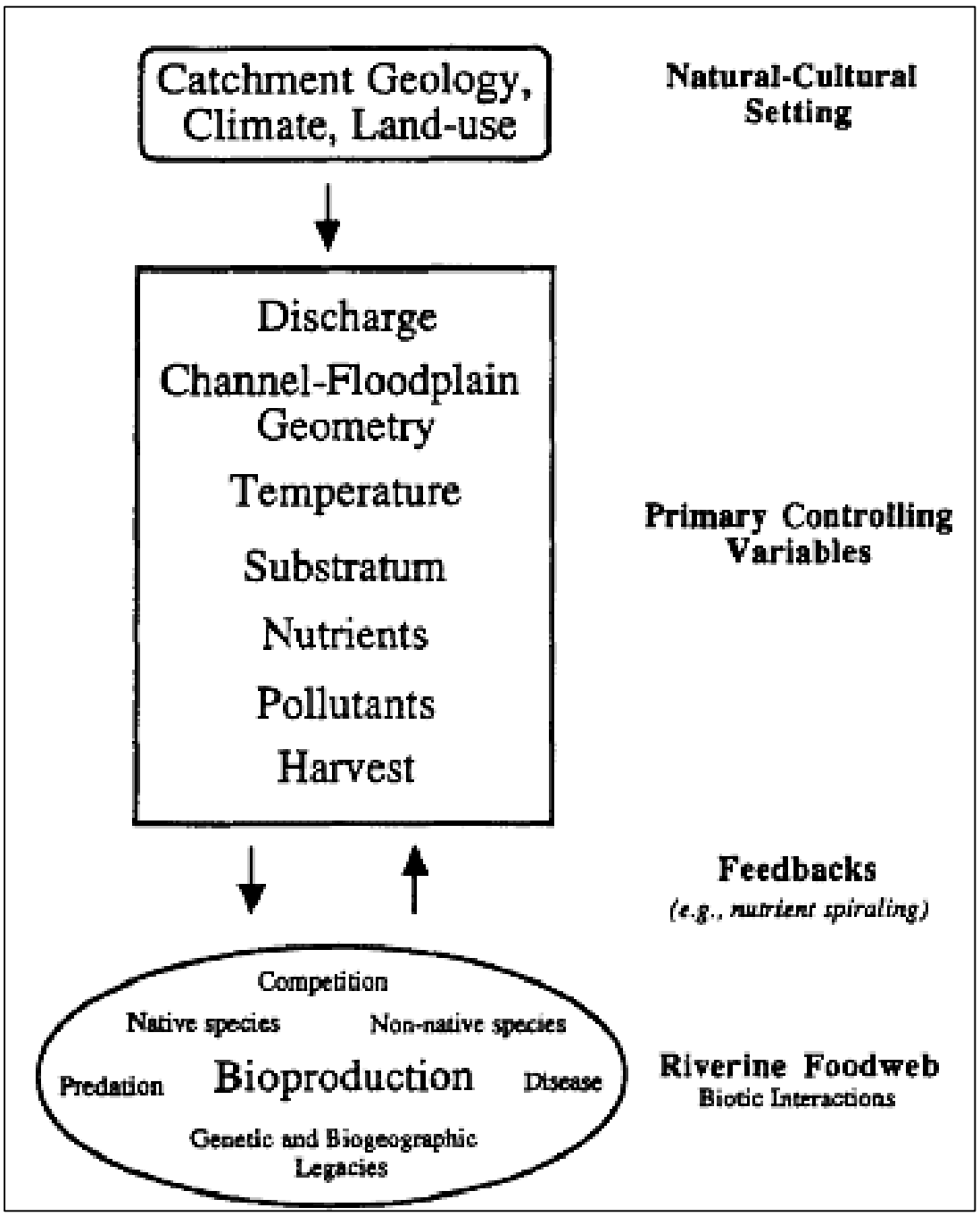

Figure 3. Important variables for successful bioproduction (Stanford et al., 1996)

Wetlands in lower river catchment areas in Europe have been primarily restored by re-opening or creating secondary channels to allow flow gradients. Examples from the lower Rhine report successful restoration by secondary channels in combination with sand-mining pits (Buijse et al., 2002), leading to an increase in biodiversity through bigger habitat ranges (Grift, 2001; Simons et al., 2001). In the Upper Danube River several restoration projects have been realized by improvement of hydrological connectivity and dynamics through lowering of embankments and reconnection of side arms (Tockner et al., 1998; Schiemer et al., 1999). In the Lower Danube water basin ecological restoration has been achieved by reconnection of river and

catchment area (Schneider-Binder, 2011). Furthermore, decommissioning of flood protection showed enhancement of biodiversity (Ebert et al., 2009). Water storage or diversion from other catchments enhances reduced water supply during summer due to climate change, as has been shown by projects in the United Kingdom (Buijse et al., 2002).

With special regard to terrestrialization, water management plays a key role in the restoration of wetlands (Acreman et al., 2007). Here, prolongation of the water retention time on the wetland is one of the main factors. Water retention is defined by geomorphic and hydrological properties of the river and describes an equilibrium between bed load transport and hydrology. In wide river beds, retentive zones can be established through accumulation of natural gravel bars or artificial construction of groynes (Zalewski, 2011). Additionally, reregulation of river discharges from storages according to natural patterns can create natural seasonality of flow and temperature patterns including overbank flow. Peak flows can interrupt terrestrialization (Buijse et al., 2002) by rearrangement of substratum and interconnection of floodplain and channel (Junk et al., 1989; Copp, 1989; Stanford et al., 1996). Moreover, several studies have shown that bird reproduction on wetlands is directly connected to water depth, degree of water level fluctuations, and plant communities during breeding season. The frequency of water level fluctuations implies variations in water depth, providing habitat for different species (Ntiamoa-Baidu et al., 1998). However, species nesting at or near the water surface react sensitively to nest flooding or drying (Desgranges et al., 2006). Consequently, a stable water level benefits breeding and increases water bird density (Connor & Gabor, 2006). In combination with river management also mortality by pollution and overharvest have to be eliminated.

It has been recognized that the management of the flow regime is essential to allow the conservation of biodiversity of fresh water environments. The maintenance of seasonal variability is a major aspect to underpin conservation strategies (Arthington & Pusey, 2003; Dudgeon et al., 2006). However, it has to be borne in mind that restoration of wetlands is highly complex, requiring high specification of the applied measures (Ehrenfeld, 2000). In general, restored sites should be self-sustaining in combination with well-functioning effective natural processes (Bailey, 1992; Henry & Amoros, 1995).

2.1.3 Hydraulic structures

In wetland management, the implementation of hydraulic structures to control the hydrological conditions is widely applied. These include floodgates, water pumps, canals and levees to create required water depths, water level fluctuations, and formation of desired topographical features. Furthermore, applied management that allows flooding during spring or summer can guarantee a suitable water table for germination, growth, and seed production. In combination with specific flooding measures in autumn and winter, an increase of water bird biodiversity and the abundance of wetlands is obtained (Coops et al., 2004; Kaminski et al., 2006).

The implementation of transverse structures in a river channel fulfils several purposes such as backwater of flow and stabilization of the bed level. To guarantee water retention by hydraulic measures, the construction of weirs or riverbed ramps is conceivable. Weirs can be classified in fixed and movable systems. Fixed structures are defined by a correlation between overflow and backwater height. With growing backwater level the discharge increases. On the other hand,

movable structures allow control of the overflow through adjustment to guarantee a fixed backwater level or discharge in the river (Strobl & Zunic, 2006). Figure 4 shows a sketch with an example of a fixed and a movable weir.

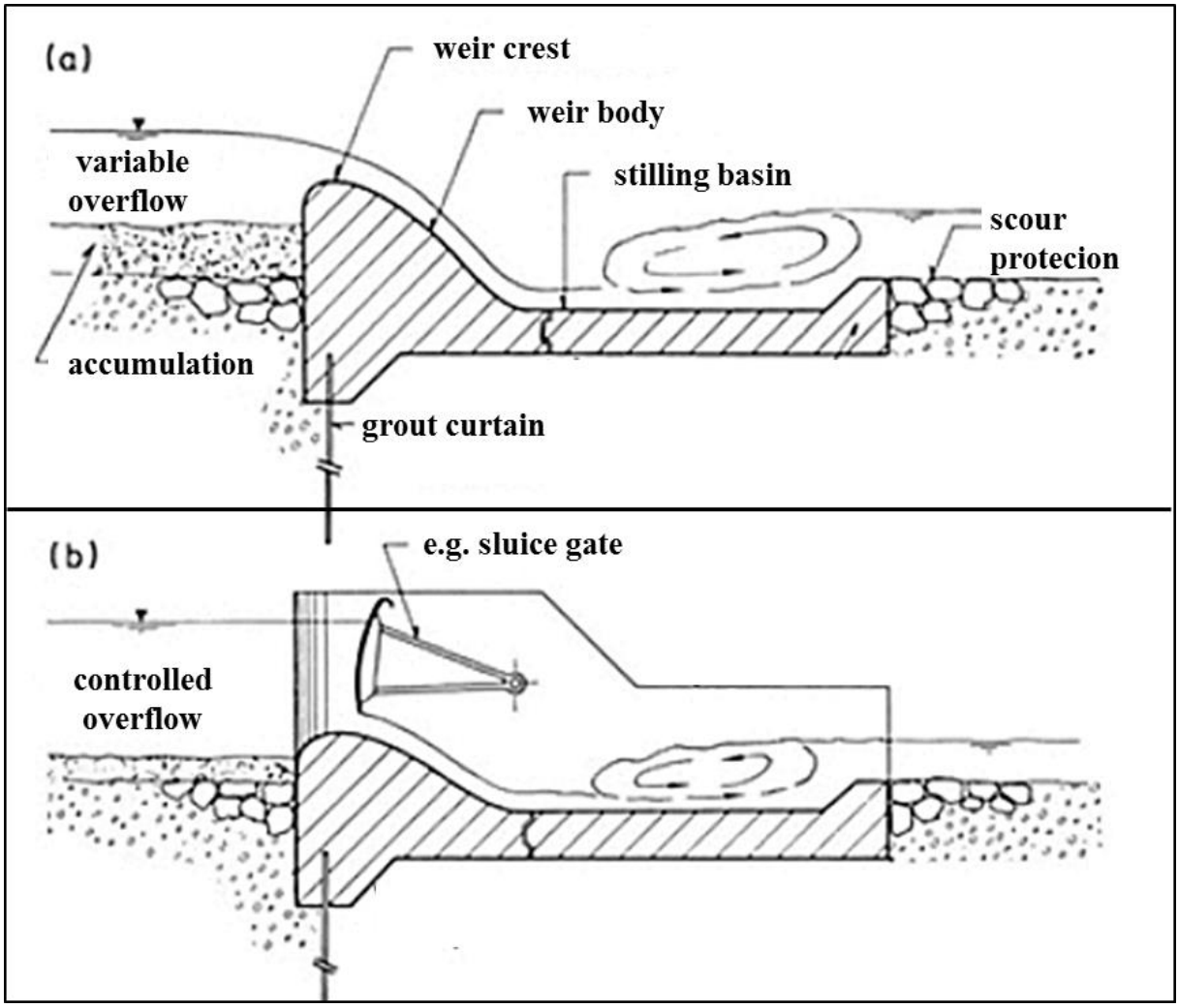

Figure 4. (a) Comparison of a fixed weir and (b) a movable weir (Vischer & Huber, 2013, modified)

Fixed structures are generally distinguished according to the form of the weir crest. Most commonly, the simplest designs of the crest are broad-crested weirs, sharp-crested weirs, and streamlined designs. An example of a broad-crested weir and a streamlined design is visualised in Figure 5a and Figure 5b. Fixed weirs guarantee an overflow when the backwater height is higher than the weir crest height. For lower water levels the water is retained and a specific water level upstream the weir is set. In general, fixed weirs are robust and require less maintenance and control than movable weirs. However, a combination of a fixed with a movable weir structure is possible (Dittrich et al., 2007).

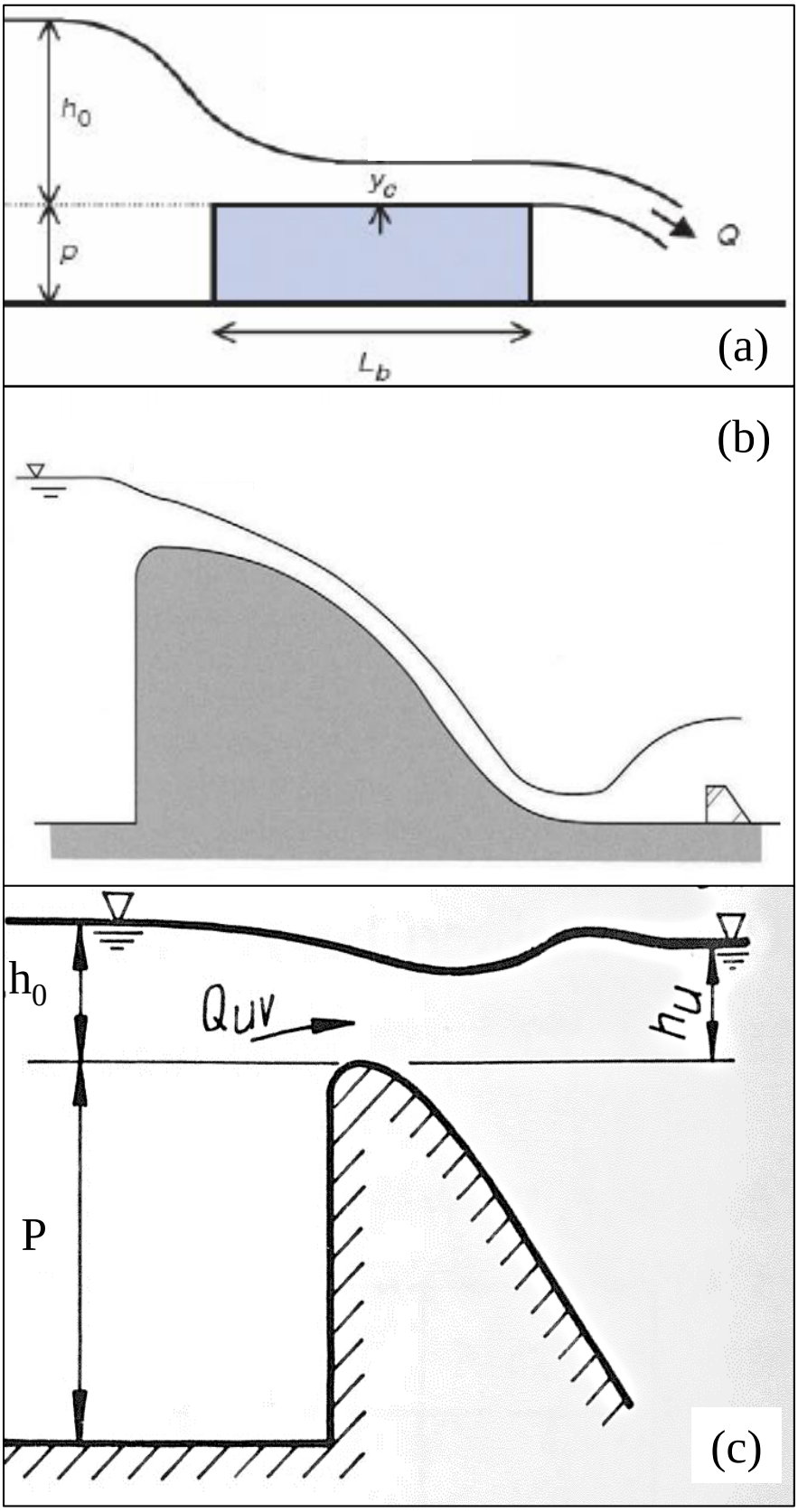

Figure 5. Sketch of different weir crest types. (a) broad-crested weir, (b) streamlined design (Novak et al., 2007, modified), (c) effect of high tailwater (Bollrich, 2007, modified)

The general equation to describe the discharge over a weir crest is determined by the Poleni-equation (Bollrich, 2007):

$$Q = \frac{2}{3}\sigma_{id}\mu\sqrt{2g}L_w h_0^{3/2} \tag{2.1}$$

where, L_W is the length of the weir crest and h_0 the overflow height. μ is a discharge coefficient accounting for the shape of the flow velocity head, head-loss, and vertical contraction of the flow. The overflow coefficient σ_{id} describes the reduction of the discharge in case of large tailwater heights (cp. Figure 5c). σ_{id} depends on the weir type, weir height, and water level quotient. For broad-crested weirs μ is determined to around 0.5 and σ_{id} has to be applied for (h_u - p) = 0.7-0.85(h_0 - p). For a more streamlined design a discharge coefficient between 0.70 and 0.75 is suggested (Strobl & Zunic, 2006) and the influence of the tailwater has to be taken into account when (h_u-p)/(h_0-p) = 0.5 (Bollrich, 2007).

A sharp-crested weir is displayed in the left part of Figure 6. On the right part, a special type of the sharp-crested weir is shown. The Thomson weir has a triangular weir crest defined by the angle α. The total weir height is determined by the maximum water level, whereas the weir crest height w is the desired water level upstream. The width of the weir crest is not constant and correlates with the overflow height. The Poleni-formula for the Thomson weir is (Bollrich, 2007):

$$Q = \frac{8}{15}\mu \cdot \sqrt{2g} \cdot h_0^{3/2} \cdot \tan\alpha \tag{2.2}$$

For sharp-crested weirs values of μ = 0.64 are applied (Strobl & Zunic, 2006). Sharp-crested weirs are usually applied for discharge measurements as they guarantee free and aerated flow over the crest.

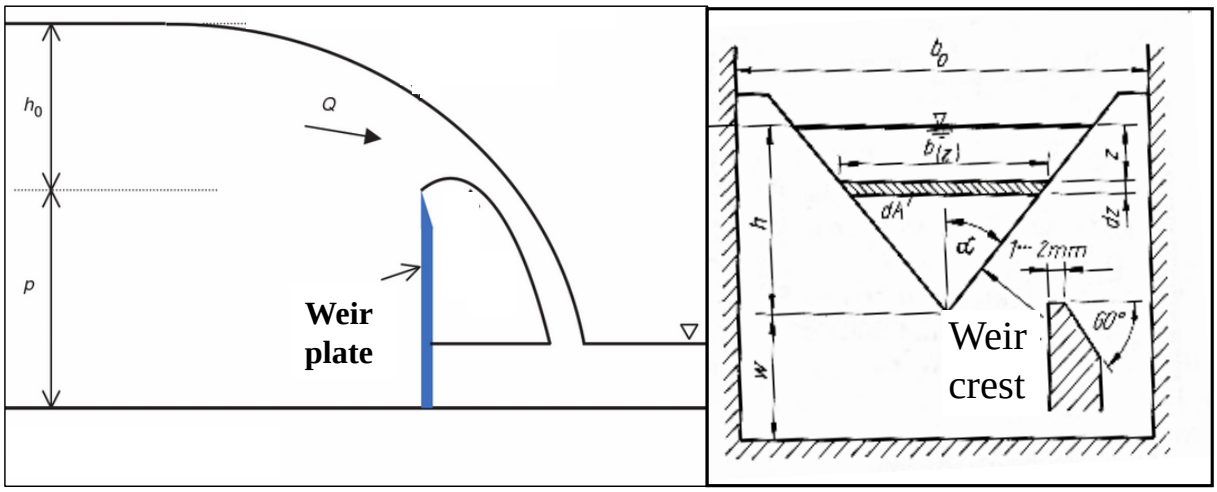

Figure 6. left: sharp-crested weir (Akan, 2006, modified); right: Thomson weir overfall (Bollrich, 2007, modified)

The use of movable structures (e.g. flap, segment gate, drum gate) is regarded as reasonable in case of a required constant water level or discharge in the river. In general, they require high maintenance effort and control by special trained staff. A more independent working weir type

is the so-called bag or membrane weir. These are inflatable dams that are applicable in rivers with backwater heights lower than 4.0 m and channel widths greater than 8.0 m. Figure 7 shows the profile of the bag weir with the upstream water level and an example from the Aller River. Membrane weirs consist of an inflatable bag that is filled with either water or air. Automatic drainage with rising water levels in combination with a pump system for refilling control the weir crest height. This weir type is favourable and less costly due to simple construction in the channel and low maintenance efforts. Additionally, low structures guarantee a good fitting in natural sites, low corrosion and low risk of deconstruction by thieves (Dittrich et al., 2007). Some installations allow navigational passage through lowering of the bag on the channel ground. The discharge coefficient of a bag weir depends on the ratio between the overfall height and backwater height. Generally, the coefficient is highest for small discharges. The maximum coefficient was determined as $\mu = 0.85$ for a ratio of 0.6 (Gebhardt, 2006).

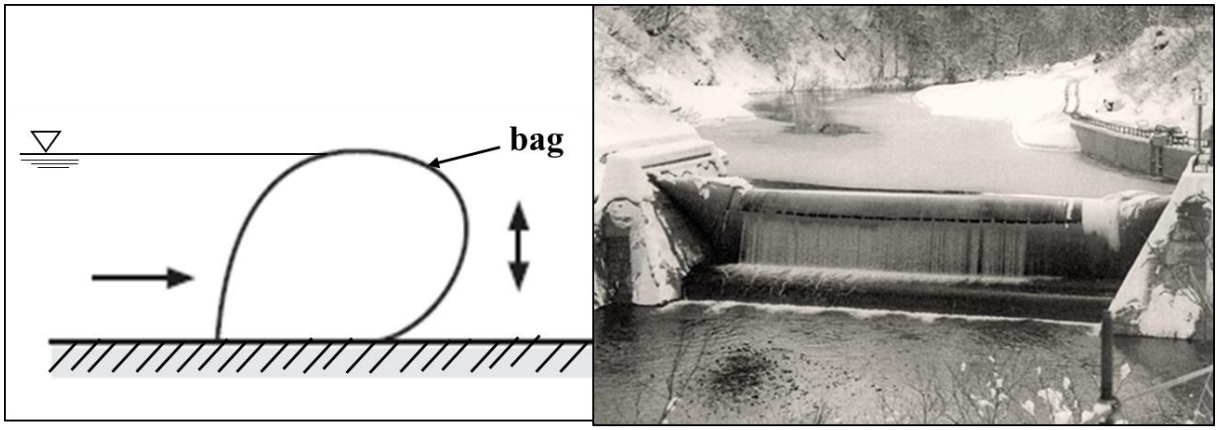

Figure 7. Bag weir; left picture is a sketch (Giesecke et al., 2014, modified) and the right pictures shows an example of an air-filled membrane weir near the Kurotani dam, Japan (Gebhardt, 2006)

Natural hydraulic engineering includes the use of natural materials to enhance the dynamics of the river. Here, dead materials can be chosen, i.e. stones, textiles, fascines of deadwood. In general, living material is favourable when sufficient resistance against the occurring stresses is guaranteed (Patt & Gonsowski, 2010). The construction of riverbed ramps and riverbed slides allows stabilization of the bottom material and guarantees water retention (Figure 8). Their structures have low visual impact and sufficiently small slope gradients guarantee ecologic connectivity. The determination of the discharge over bottom slides is discussed in many research papers and a general approach is not applicable (Aberle & Kulisch, 2007). The Poleni-equation is one simplified approach that can be applied to define the discharge over a structured slide as follows:

$$Q = \frac{2}{3}\sigma_{id}\mu\sqrt{2g}B_S h_0^{3/2} \tag{2.3}$$

here, B_S is the open width between the stones. The discharge coefficient for slides with broken stone is suggested between 0.5-0.6 (Dittrich et al., 2007).

Figure 8. Rockfilled slide in the Aich River (LUBW, 2005)

To analyse the capacity of the river channel, different flow formulas are applicable. These allow investigation of the discharge for open channel flow and give a basis for the technical design of hydraulic structures. One widely-used example is the Manning's formula:

$$Q = A \cdot \frac{1}{n} \cdot \sqrt{I_b} \cdot \left(\frac{A}{U} \right)^{2/3} \tag{2.4}$$

A is the cross sectional area of the channel, *n* is the Manning-coefficient, I_b the bottom slope, and *U* the wetted perimeter. This equation is based on the assumption of uniform flow. However, this requirement is not fulfilled for natural river beds (Chow, 1959).

2.2 Modelling approaches for wetland restoration

Modelling allows the description of the reality through simplified approaches and is an important tool in river engineering. Different methods can be applied to investigate hydraulic processes. The next chapter describes applied theories in modelling as well as different numerical approaches. Moreover, an overview on former research projects within numerical simulation of wetlands is given.

2.2.1 Overview

Rock et al. (2008) defines a model as a simplified image of a (partial) reality. For engineering measures, modelling can be divided into physical or empirical modelling and theoretical or analytical modelling. Examples of physical modelling are laboratory and in situ model tests, providing useful information to develop empirical or semi-empirical algorithms. On the other

hand, analytical modelling consists of the construction of a mathematical model with appropriate assumptions in the form of differential or algebraic equations. Strongly simplified mathematical models can be solved analytically, whereas highly complex methods require the development of an appropriate numerical model or an approximation to the mathematical model. Figure 9 shows a general course of action in numerical investigations. To allow a sufficient representation of the reality, every numerical model usually needs to be accurately calibrated and validated against pre-existing data or analytical results (Rock et al., 2008). Especially, the results obtained by an analytical approach require careful evaluation due to strong simplification and assumptions. It has to be borne in mind that only a rough representation of the reality is given.

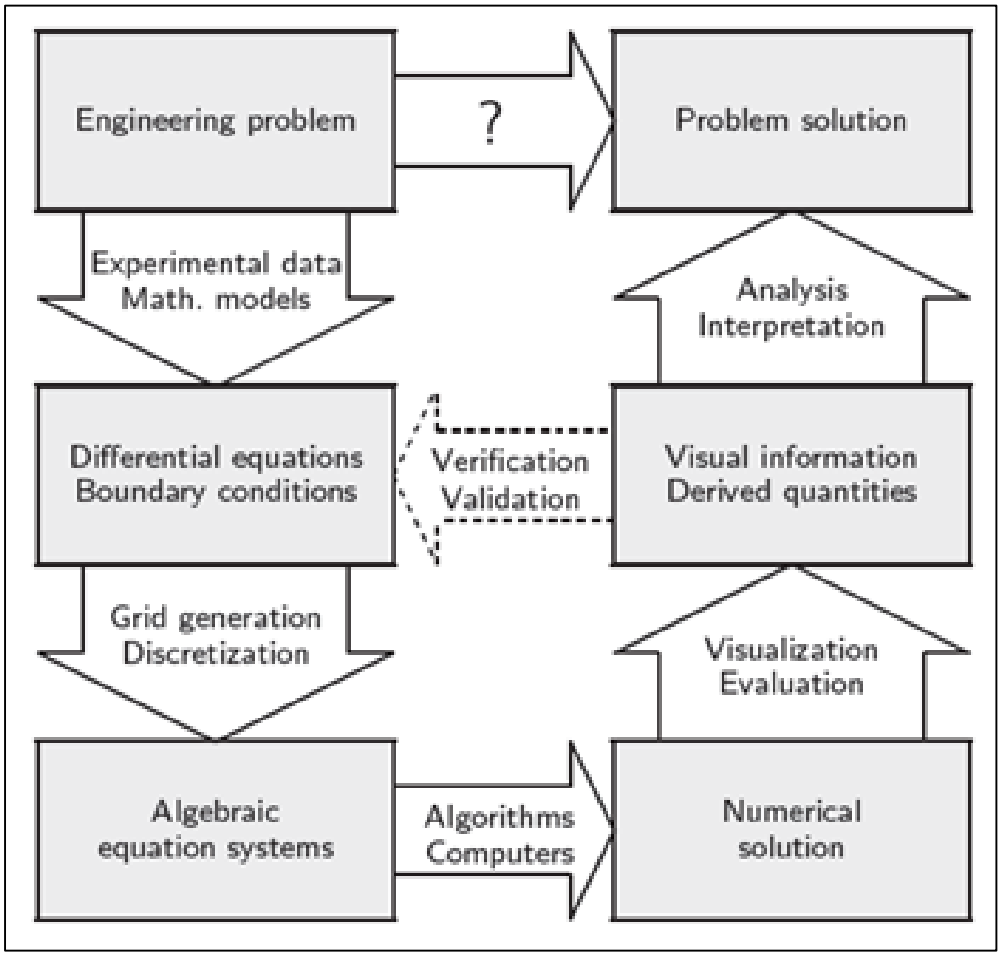

Figure 9. General procedure to solve an engineering problem numerically (Schäfer, 2006)

At present, the knowledge about hydraulic characteristics of natural floodplains is limited, due to difficulties in monitoring of flow depth, velocities, and turbulence parameters. As a general methods, simplified mathematical models can estimate the hydraulics in open channel flow. To further enhance the understanding of flow processes, the investigation by laboratory flume studies is widely applied (e.g. Knight & Shiono, 1996). On the other hand, numerical models allow simulation of more complex boundary conditions and therefore can give better representation of natural floodplain environments. Especially limitations in simulating multiple channel flow and gradual inundation of wetlands suggest analysis through computational

approaches (Nicholas & Mitchell, 2003). The next part gives an overview on simple approaches followed by a section explaining numerical methods in greater detail.

2.2.2 Simple water balance approach

With regard to the investigation of hydraulic characteristics of wetlands, simple equations can be applied to obtain results for basic flow parameters. An investigation of the discharge on wetlands is possible by a model based on mass balance. With this method, the wetland is generally considered as a black box, resulting in the assumption that the incoming water mass equals the outgoing water mass:

$$Q = Q_{in} - A(P - ET - GW) - Q_{out} \tag{2.5}$$

Q is the flow rate, Q_i the flow rate at the inlet, Q_{out} the flow rate at the outlet, A the surface of the wetland, P precipitation, ET evapotranspiration and GW ground water loss. For steady conditions with $Q = V_{n-1} - V_n$ and $Q_{in} = 0$, the general equation to describe the stored water volume in a wetland at a defined point in time can be obtained as:

$$V_n = V_{n-1} - V_{ET} - V_{GW} - V_S \tag{2.6}$$

with V_n being the water volume for t = n, V_{n-1} the water volume for t = n-1, V_{ET} the evapotranspiration/precipitation, V_{GW} ground water loss, and V_S surface runoff between Δt=n-(n-1). The water balance is visualised in Figure 10. With regard to wetlands, the water volume represents the inundated areas, which are assumed to be storages that are filled with water to a certain water level with a horizontal water surface. If the relation between the water volume in the storage and the according water levels is known, a stage-volume relationship can be obtained. Hence, a time-series of daily water levels depending on the evaporation/precipitation, ground water loss and the surface discharge on the wetland is determined. With this method, the inundated area can be identified and further analysis of the changes of the hydrological conditions on the wetland can be carried out.

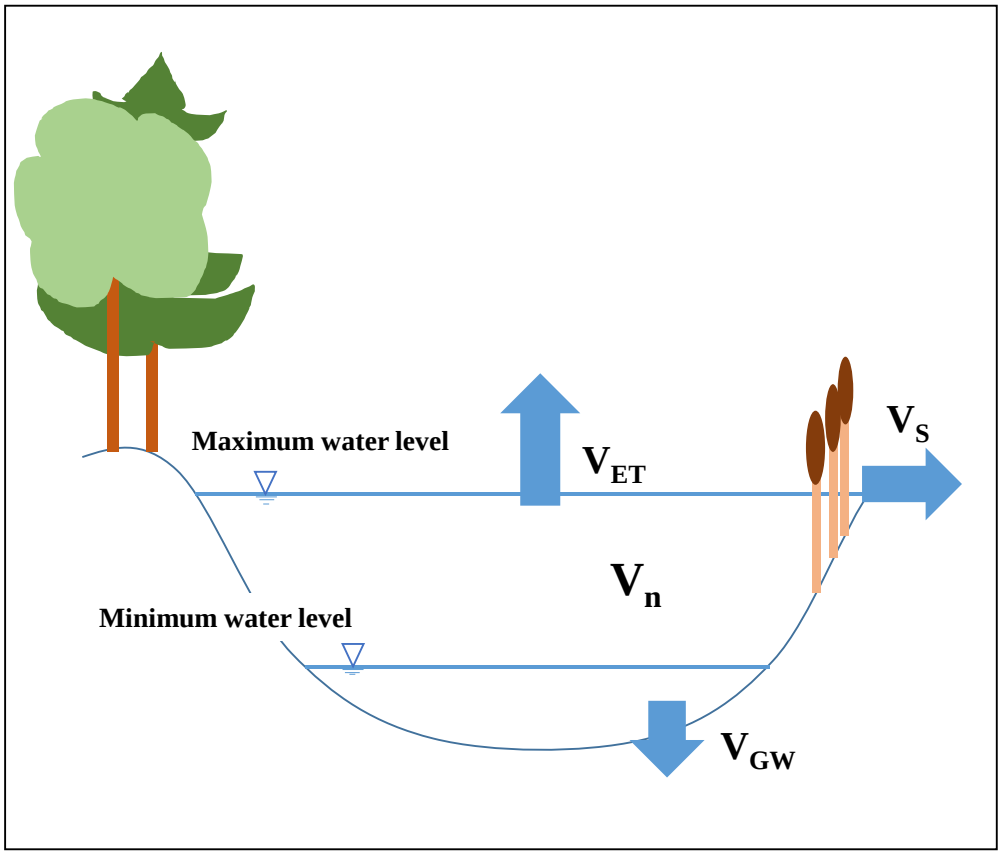

Figure 10. Sketch of the water balance in a wetland (eq. 2.6)

2.2.3 Numerical modelling

Within the last decades, the investigation of hydraulic problems by numerical simulation became more and more important, as it represents an inexpensive and effective solution to give insight in critical design issues at an early stage (Teklemariam et al., 2002). To allow numerical description of engineering problems, the general principle to obtain discrete numerical values is to approximate the exact solution. With this method, a discretization of the problem, both for the domain and the differential equations, is necessary.

The spatio-temporal continuum has to be discretized by the definition of a space step Δx and a time-step Δt representing the smallest scales in the numerical method (Allaire, 2007). The discrete geometry representation is described by a numerical grid over the problem domain. In practice, being faced with complex geometries, grid generation can be time-consuming. In general, grids can be distinguished in structured or unstructured grids. Structured grids are defined by a regular arrangement of the grid cells and therefore require less computational effort. Unstructured grids have no regularity in the arrangement of the grid points allowing higher modelling flexibility. For the grid selection, the following rule has to be taken into account: “The more regular the grid, the more efficient the solution algorithms for the computation, but the more inflexible it is with respect to the modeling of complex geometries” (Schäfer, 2006, p.61). Hence, a reasonable compromise between required accuracy and effort must be found.

In addition to the domain, also the equations have to be discretized. To determine the numerical values for the unknown quantities, three different discretization methods exist: The finite elements- (FEM), finite volume- (FVM), and the finite differences-method (FDM):

FEM is based on the division of the domain into elements. Every sub domain is described by an element equation which can be recombined into a global system of equations. The system can be solved by using the initial values of the problem. FEM is mostly used for numerical computations in solid mechanics and is suitable for unstructured grids. FVM is based on the conservation principle. Division into control volumes and formulation of the integral balance equations for each domain allow the creation of a discrete algebraic system. In order to obtain a solution, the function values are approximated by numerical integration (Schäfer, 2006). FDM is the oldest method to solve the partial differential equations. The basic principle is the approximation of the solution based on the Taylor series through replacement of the derivations at each grid point by finite difference quotients. Here, every grid point is connected to an unknown variable which is described by an algebraic equation. Through these equations the unknowns of every neighbour cell are related. The approach is suitable for each grid type and known as simple and effective on structured grids (Ferziger & Peric, 2002).

In open channel flow, the solution of turbulences must be taken into account. However, flow with high Reynolds numbers is highly complex and requires further considerations. Three different approaches apply for the investigation of turbulent flow: Direct-numerical-simulation (DNS), Large-eddy-simulation (LES), and Reynolds-Averaged-Navier-Stokes models (RANS).

In conventional engineering problems, the approach based on the RANS equations is widely applied. For this theory, the turbulent flow is defined by a mean value and a fluctuation part. The mean part can be described by the equations, whereas the fluctuations require a turbulence model based on the dependency between turbulence and velocity. The basic principles of turbulence closure are described in chapter 4.3.2 (Griebel et al., 1998). DNS requires strong computational effort and is primarily applied in research or for small Reynolds numbers (Nguyen, 2015). LES can be described as the intermediate approach between DNS and RANS model. This approach is suitable for small-scaled bathymetries with small Reynold's numbers, but for calculations of large and complicated bathymetries computational time is significantly increased (Nguyen, 2015). Consequently, for computations of complex flows on wetlands primarily RANS models are employed.

State-of-the-art computer models usually resolve one- or two-dimensional calculations but have limited capability in solving complex hydrodynamic flow phenomena. On the other hand, due to large calibration effort and large computational time, fully three-dimensional simulations are often expensive (Giardino, 2010). Wetland hydrodynamics depend both on internal factors, i.e. bathymetry, vegetation distribution, and inlet and outlet conditions and external impact, i.e. wind shear and hydraulic loads. Due to complex flow patterns, stagnant water and circuit flows are characteristic for the flow field of wetlands (Somes et al., 1999).
Several two-dimensional models have been developed to represent the hydraulics of natural floodplains. The complexity of the models varies from simple one-dimensional diffusion-wave approaches to solving the shallow water Navier-Stokes equations. Moreover, different scales

of bathymetries with varying resolutions of the numerical grid have been investigated. Low spatial resolution cannot resolve small-scale topographic features, which control overbank inundation of wetland surfaces. On the other hand, due to the computational effort high resolutions have mostly been applied for short river reaches (Nicholas & Mitchell, 2003). Somes et al. (1999) successfully modelled a wetland using the depth-averaged, finite-differences software MIKE21 on a staggered grid. The Alternate Direction Implicit (ADI) method is used. Eddy viscosity represented the main calibration factor for the model. Also Nicholas and Mitchell (2003) validated two-dimensional modelling of flooding of wetlands solving the shallow water equations and a k-ε turbulence closure model. Rameshwaran & Naden (2003) analysed inbank and overbank flow for a channel with high aspect ratio. Finite-volume discretization in combination with a RANS model and a standard k-ε turbulence closure model was capable of representing velocity distribution and shear stress. Bed shear stress due to vegetation on floodplains can be sufficiently described by Reynolds Stress Models through implementation of the drag force induced by cylindrical vegetation (Kang & Choi, 2005).

A high range of software packages are used in hydrodynamic modelling. One well-known example is Delft3D, which has been validated for several applications in coastal and river engineering. Edmonds et al. (2010) investigated the response of river-dominated delta formation to variable discharges. The area was successfully represented and rearrangement of the channel network was observed. Temmerman et al. (2005) produced reasonable results with regard to vegetation, flow and sediment patterns. Even in depth-averaged mode, the representation of currents was accurate (Elias et al., 2000). With regard to sediment transport, Lesser et al. (2004) validated Delft3D for changing flow conditions, spiral flow in bends, entrainment, transport, and settling of sediment. Furthermore, varying levels of uniform bed shear stress, and bed slope effects have been investigated. A part of the Danube Delta has been monitored in Delft3D by Cioaca et al. (2010) to analyse changes in water levels and hydraulic connection by climate change. The analysis of bed forming processes is of great interest for the prevention of disasters due to floods, design and management of hydraulic structures, as well as maintenance of the river ecosystems (Jang & Shimizu, 2005). Due to time restrictions, the simulation of bed forming processes was not carried out in this work.

Modelling of hydrological interactions related to restoration of wetlands represents an inexpensive solution to determine the impact of engineering measures. Nevertheless, it has to be borne in mind that such a modelling is still in its development and requires further research on implementing three-dimensional modelling of large-scale projects with highly complex bathymetries. However, the application of the appropriate numerical method depends on the characteristics of the site and has to be selected carefully. In order to provide understanding for the choices made for this work, the site and the project frame are described in the following chapter.

3 Site and project

The following chapter presents the project area in its historical context. The project framework and its objectives are presented with regard to the processes described in the previous chapter.

3.1 Problem definition of the site

The area investigated in this work, Fundu Mare Island, is located between kilometre 175 and 190 upstream the river mouth of the Danube River in the eastern part of Romania. The island is part of the Small Wetland of Brăila Natural Park, which is located in the inner delta of the Danube River (Figure 11). The natural park is a wetland with a size of 241 km² within the so-called Lower Danube Wetland System (LDWS), which is situated between the Black Sea and the hydroelectric power station Iron Gate II (Vadineanu et al., 2003). The natural park represents one of the areas with highest biodiversity in the Romanian wetland system and was declared as natural reserve in 1994. Within the last century, a range of measures have been implemented in this area to improve fisheries and agriculture, water way transportation, flood control, and land reclamation. The anthropogenic impact caused significant alterations in the Small Wetland of Brăila and in the structure and functions of the Danube River (Vadineanu, 2001).

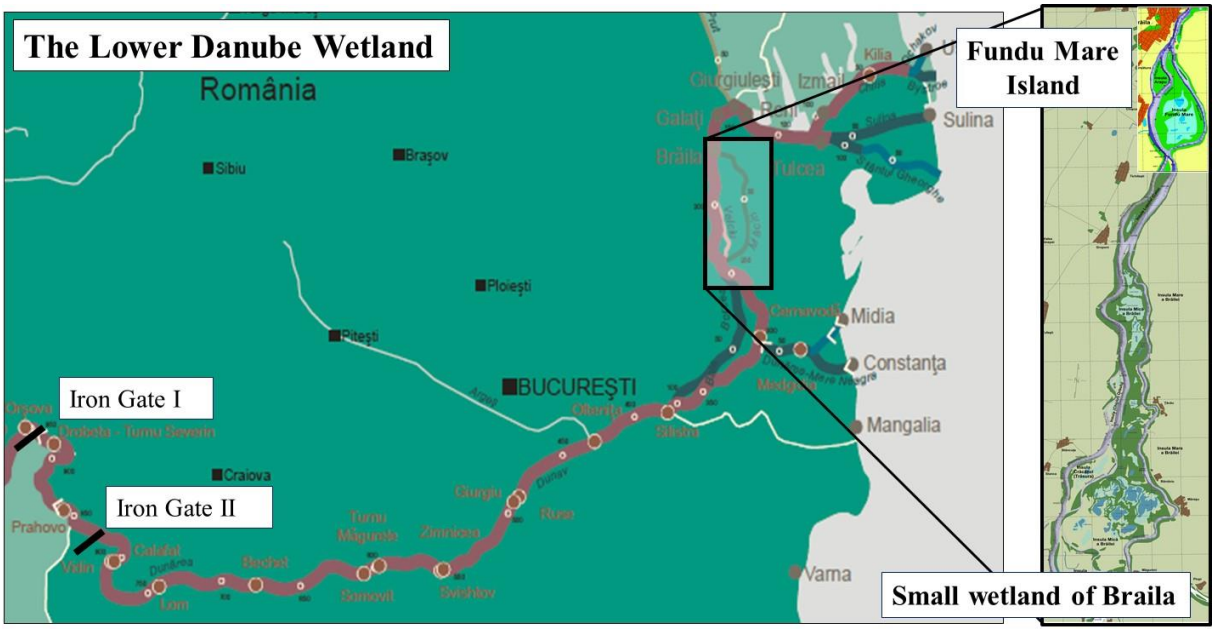

Figure 11. Location of Fundu Mare Island (Maps: via donau (2015); ERDF (2013), modified)

Due to its location between the Danube branches, the Small Wetland of Brăila has been less exposed to anthropogenic impact and preserves a characteristic morpho-hydrodynamic structure, including a network of banks and natural dams, ponds and canals (Iordache et al., 2005; Bodescu & Iordache, 2010). The Natural Park provides a habitat for the spawning, feeding and nesting of bird and fish species, as well as more than 1,500 plant species and almost

4,000 animal species (Vadineanu et al., 2003). Due to its location on the migratory routes between Africa and northern Europe, the area has a main importance in protection of migratory birds. By preserving 10% of the former Inner Danube Delta it represents the last wetland complex in the area.

In the beginning of the 20th century, the lower Danube has been modified by river straightening and dredging to improve navigation between the Black Sea and the port of Brăila (Vadineanu, 2001). In order to achieve land reclamation for agriculture, the construction of dams was implemented in the 1960's and 1970's. Primarily, the drainage of the so-called Large Wetland of Brăila was achieved, which led to a reduction in size of the natural floodplain in the inner Danube Delta by more than 80% (cp. Figure 12). As a result, the Small Wetland of Brăila was disconnected from the surrounding lands by large dykes, which prevent water and nutrient exchange by separating surface connectivity. The lack of drainage systems induced water stagnation and soil salinization of the surroundings (Vadineanu, 2001).

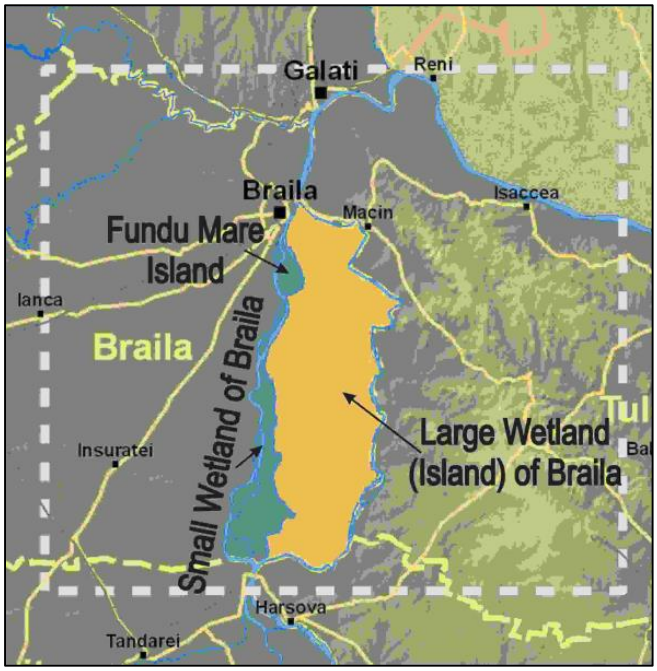

Figure 12. Location of the Large Wetland of Brăila (NMAR, 2015, modified)

The two hydropower stations, Iron Gate I and II, along with water reservoirs for irrigation and industrial water supply, were built between the 1960's and 1980's (Vadineanu, 2001; Andrei, 2011). These affected the hydrological cycle of the Danube and reduced seasonal flow patterns and sediment transport. Furthermore, short-cutting and dredging of river arms and channels were applied to enhance navigation and fishing in the LDWS. This increased surface runoff and led to a reduction of water retention time (Bondar, 1996 cited in Vadineanu et al., 2003).

As a result of these anthropogenic measures, the hydrological and the sediment regime were both heavily altered. Increased water levels in the main channel, reduced inundation of the area and erosion of the wetlands have been observed (Vadineanu et al., 2003; Andronache, 2009; Habersack et al., 2016). This effects will be enhanced by a predicted decrease of the flood in

summer (Stagl and Hatterman, 2015). In addition to the hydrological changes, chemical pressures have been exerted on the local ecosystems. Eutrophication and pollution by agricultural and industrial activities affect the nutrient cycle and reduce water quality in the wetlands. Together with high amounts of dissolved and particulate organic matter, higher turbidity is induced, severely affecting biodiversity. As a result, taxonomic composition and species richness were significantly altered (Vadineanu, 2001).

In order to protect the lower Danube Wetlands, governmental decisions have been implemented within the last decades. These included the minimization of pollution and eutrophication as well as biodiversity conservation. The Small Wetland of Brăila was declared as special protection area and pilot region to establish sustainable development (Vadineanu, 2001). To protect its high biologic diversity, Fundu Mare Island has been declared as RAMSAR site and Natura 2000 site (Vadineanu, 2001). Furthermore, it has been classified as "a protected area where the interaction of people and nature over time has produced an area of distinct character with significant ecological, biological, cultural and scenic value" by the International Union for Conservation of Nature and Natural Resources (IUCN, 2012). Additionally, the Small Wetland of Brăila was candidate in different programmes for conservation and reconstruction of biodiversity (BmB, 2010). Today, the overall goals for sustainable development in the Small Wetland of Brăila are improvement of biodiversity, reconstruction of natural wetlands and application of multi-functional farming contributing to the ecosystems, introduction of a holistic bio-economic management system, and enhancement of social equity (Vadineanu et al., 2003).

3.2 Project background

Construction measures and climate change, respectively, induced major changes in the LDWS. One major issue is the terrestrialization process of Fundu Mare Island.

Bed erosion in the Danube channel, due to the upstream damming in combination with a greater width of the river induced lower water levels (Schwarz, 2008). As a result, rapid water loss occurs during summer due to higher soil elevation of the wetlands than water level elevation in the Danube River (Vadineanu, 2001). Before the construction works, the former Brăila wetland was flooded every one to three years and at least 50% of the area was inundated annually (Andronache, 2009). These alterations caused silting on the wetland and drying out of the lakes during summer. Furthermore, the combination of hydraulic, sedimentary and chemical alterations in the Danube wetlands led to significant changes in vegetation including replacement of reed and marsh vegetation by ruderal plants (Vadineanu, 2001). In the Small Wetland of Brăila the propagation of willows into the aquatic zone has been recorded. These alterations in vegetation cause problems for aquatic birds in finding nesting and feeding areas. Due to its high sensitivity, dredging of the site is not applicable and other solutions have to be evaluated (Andrei, 2011).

Due to the ecological importance of Fundu Mare Island the interdisciplinary project "Restoration of the aquatic and terrestrial ecosystem complex of Fundu Mare Island" was launched in 2015. The project aims at analysing the flow characteristic and a proposal of

restoration measures to enhance the hydrological and sediment regime in the wetland to stop the terrestrialization process. Fundu Mare Island is characteristic for its large aquatic zones represented by two major lakes that are connected by artificial channels built before 1989. The lakes are flooded during spring and the water levels are controlled by the flow regulation in the Danube through two channels: the Hogioaia-channel and the LIFE-channel (cp. Figure 13). One part of the Hogioaia-channel is dammed by a provisional weir structure displayed in Figure 13a. Upstream the weir an undammed side arm guarantees connection with the Danube River. The influence of the channels on drainage and water retention of the lakes on the island are of special interest for the project.

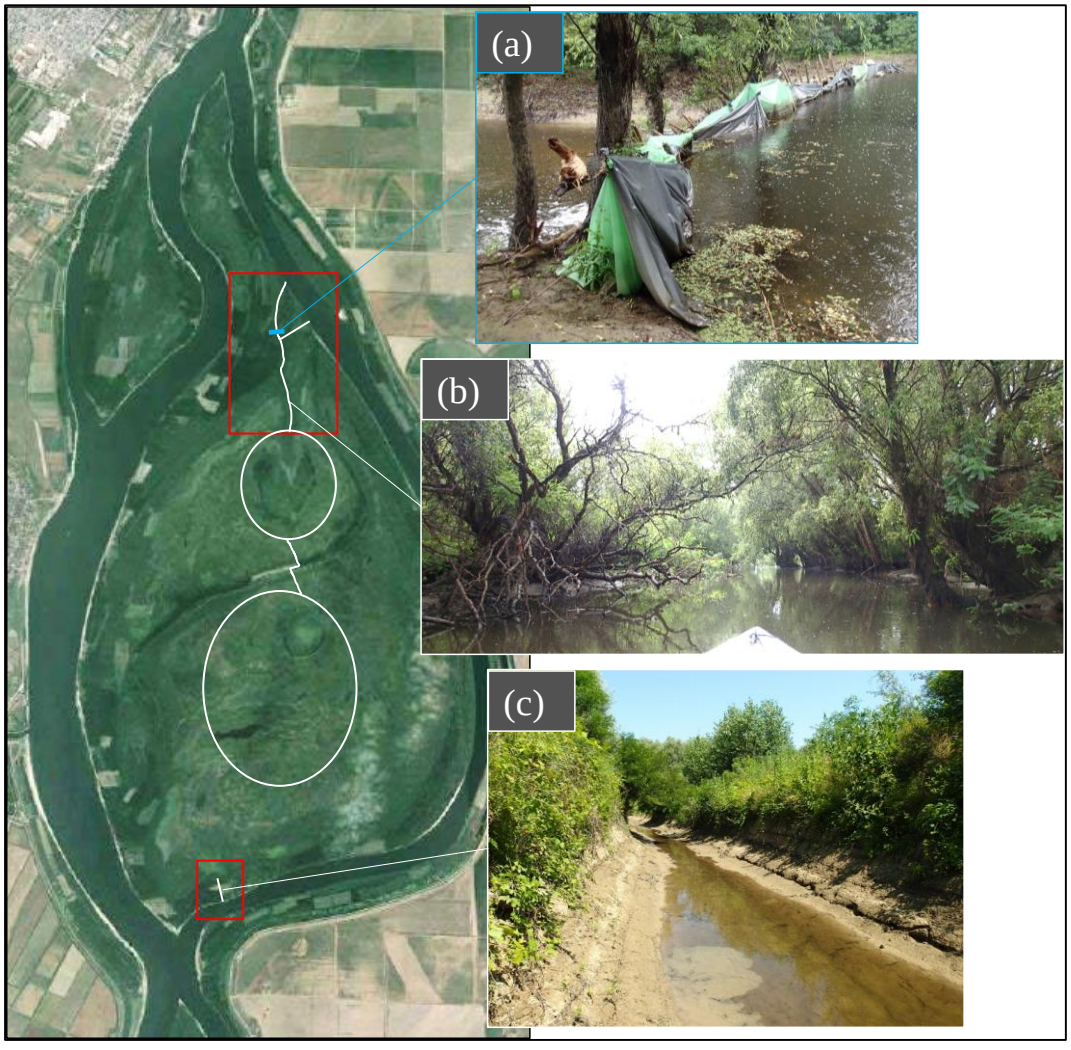

Figure 13. Areas of main interest for the hydraulic computations (Google Earth, 2014) (a) weir structure in the Hogioaia-channel, (b) Hogioaia-channel between lakes and weir, (c) LIFE-channel (Pictures: Zinke & Aberle, 2015). The lakes and their connection channels are simplified as circles.

In order to analyse the flow characteristics on the island, the Hogioaia- and the LIFE-channel, in combination with the weir structure have to be investigated. By implementing different hydraulic structures, the effect of different restoration measures is examined. The influence of anthropogenic impact and climate change on the local hydrological regime has to be considered when setting up management and restoration plans for the area.

4 Data review and software selection

In order to get an overview on the available data in the project, a data review was carried out. A summary of the provided data in comparison with the requirements implied by numerical models is given. The uncertainty related to the data sources is evaluated. In a next step, the appropriate software package was selected.

4.1 Data review

In order to set up a numerical model, the following information on the investigated area is required (Habersack et al., 2014):

- Digital terrain elevation model
- Structural boundaries
- Upstream discharge
- Downstream water surface elevation
- Measurements of flow velocities and water surface elevation measurements for model calibration and validation
- Bed roughness distribution and vegetation

Within the project data were obtained from different sources which had to be checked against plausibility. In the following parts, a brief description of the available data and their accuracy is given. In summary, the following data were collected from literature or made available to the author by project partners:

- A morphological model based on a Digital Elevation Model (DEM) of Fundu Mare Island
- Specifications of the channel geometry in Fundu Mare Island
- Evaporation, precipitation and temperature data from the Danube Delta
- Long-term water level-discharge relations of the Danube River recorded in Brăila
- ADCP-measurements in the Danube River

Furthermore, results of a field survey carried out in July 2015 were provided by Zinke & Aberle (2015), including:

- ADCP-data in the Hogioaia-channel
- Water level recordings from pressure loggers in the lakes on the island
- Water level- storage volume relation for the lakes on the island
- Water level-discharge relation for the Hogioaia-channel
- Estimated roughness distribution on the island in the form of Manning values

The data collection points of the ADCP-measurements and of the water levels in Fundu Mare Island are shown in Figure 14. The locations of the ADCP-measurements are marked red. The pressure loggers are marked with numbers.

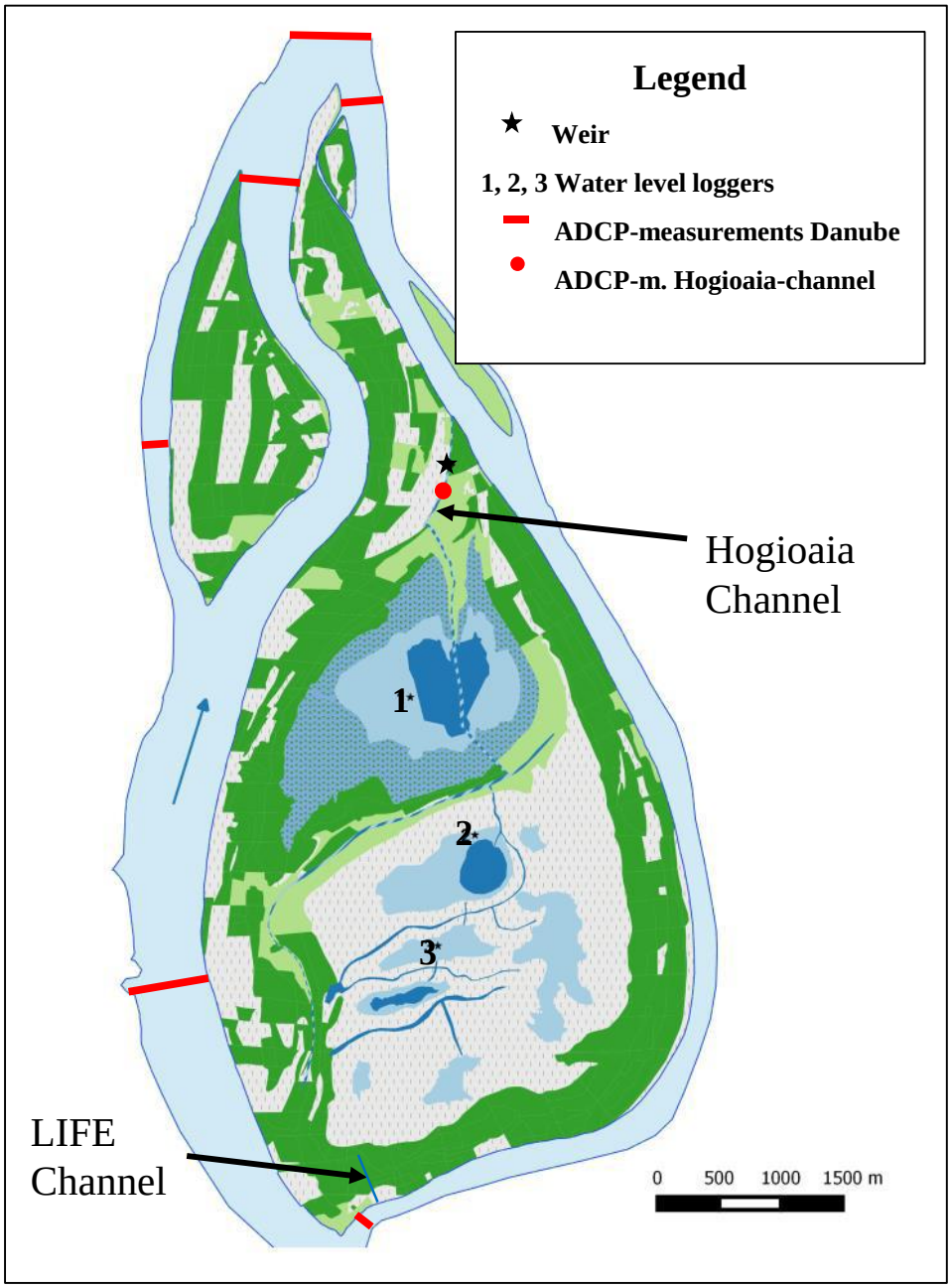

Figure 14. Data collection points (Zinke et al., 2016, modified)

4.1.1 Bathymetry data

A Digital Elevation Model (DEM) of Fundu Mare Island based on data from the Danube Delta National Institute (DDNI) was available for the study. The elevation values refer to the Black Sea Sulina (MNS). In the following the abbreviation MNS is defined as "meters above the Black Sea Sulina". The DEM was obtained in 2007 with a spatial resolution of 10 m and had been transformed into a morphological model within the Geographical Information System QGIS. The accuracy of the model is specified by Zinke et al. (2016) with 0.05-0.2 m. The median elevation of the island is around 4.6 MNS, but large areas are characterised by values between 4.4 and 4.8 MNS (Zinke et al., 2016). Levees with a height of 6.5 to 7.5 MNS occur

along the shore of the Danube. The riverbed of the Hogioaia-channel is at elevations of 2.4-2.9 MNS and the LIFE-channel is estimated to bed levels between 3.8-4.4 MNS. The deepest lakes are at bed elevations of about 3.2 MNS. The structural boundaries are defined by the dykes that separate the Small Island of Brăila from the Large Island of Brăila (cp. Figure 12).

The cross section of the Hogioaia-channel was extracted from ADCP-measurements recorded during the field survey on the island (Zinke & Aberle, 2015). Figure 15 shows the recorded cross section and an estimated geometry. The blue and green lines represent the measured data. From the data the cross section was estimated with the assumption of a trapezoidal channel (red line). For greater water depth, the channel dimensions are unknown, but a steeper gradient of the foothills is possible.

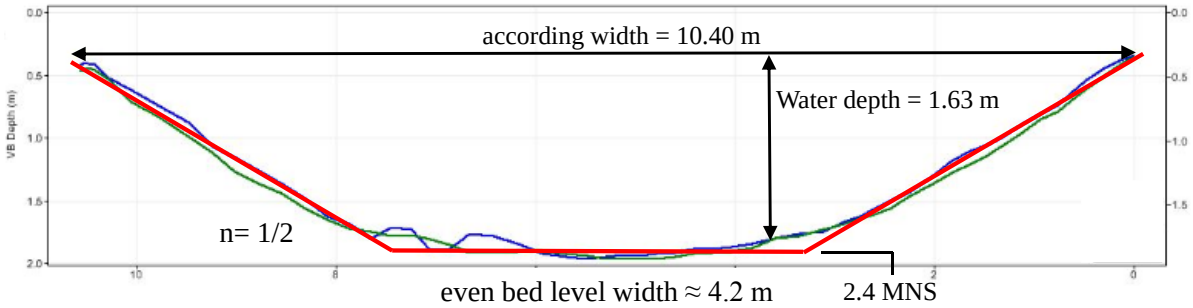

Figure 15. Cross section from the ADCP-measurements in the Hogioaia-channel

For water levels higher than approximately 3.8 MNS the hydraulic connection between the LIFE-channel and the Danube River is given. The cross section of the LIFE-channel was estimated from pictures of the field survey (Zinke, 2015a):

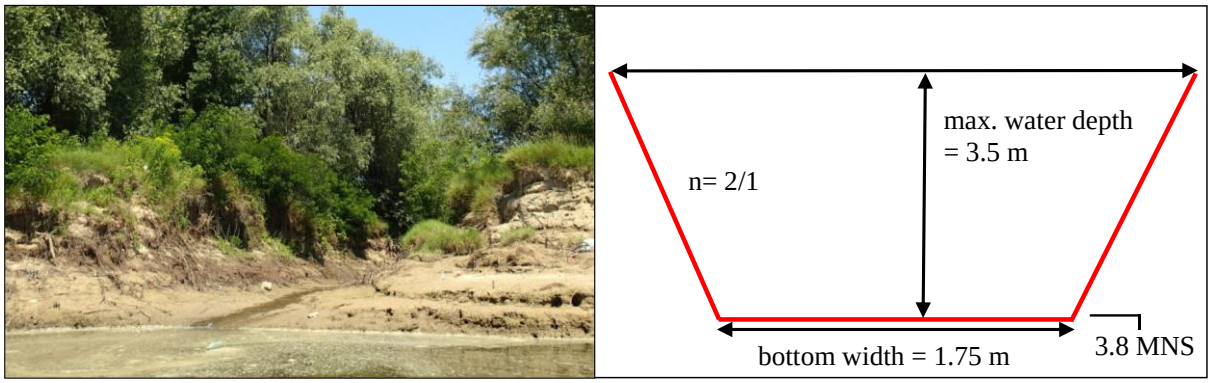

Figure 16. Cross section of the LIFE-channel (Photo: Zinke & Aberle, 2015)

In case of flooding, the water from the Danube enters the Hogioaia channel and the LIFE channel. With increasing water levels, the flood wave overtops the lower levees north of the lakes (Zinke et al., 2016). In Figure 17 the inundated areas for different water levels is visualised. In the left picture the inundation for a water level of 4.6 MNS is shown, which represents the average elevation on the island. For a water level of 5.6 MNS in the Danube River a hydraulic connection between island and main channel over the levees is given (cp.

Figure 17b). The water level gradient over the area is estimated to be ca. 1.6 cm/km (Habersack, 2014; Zinke et al., 2016).

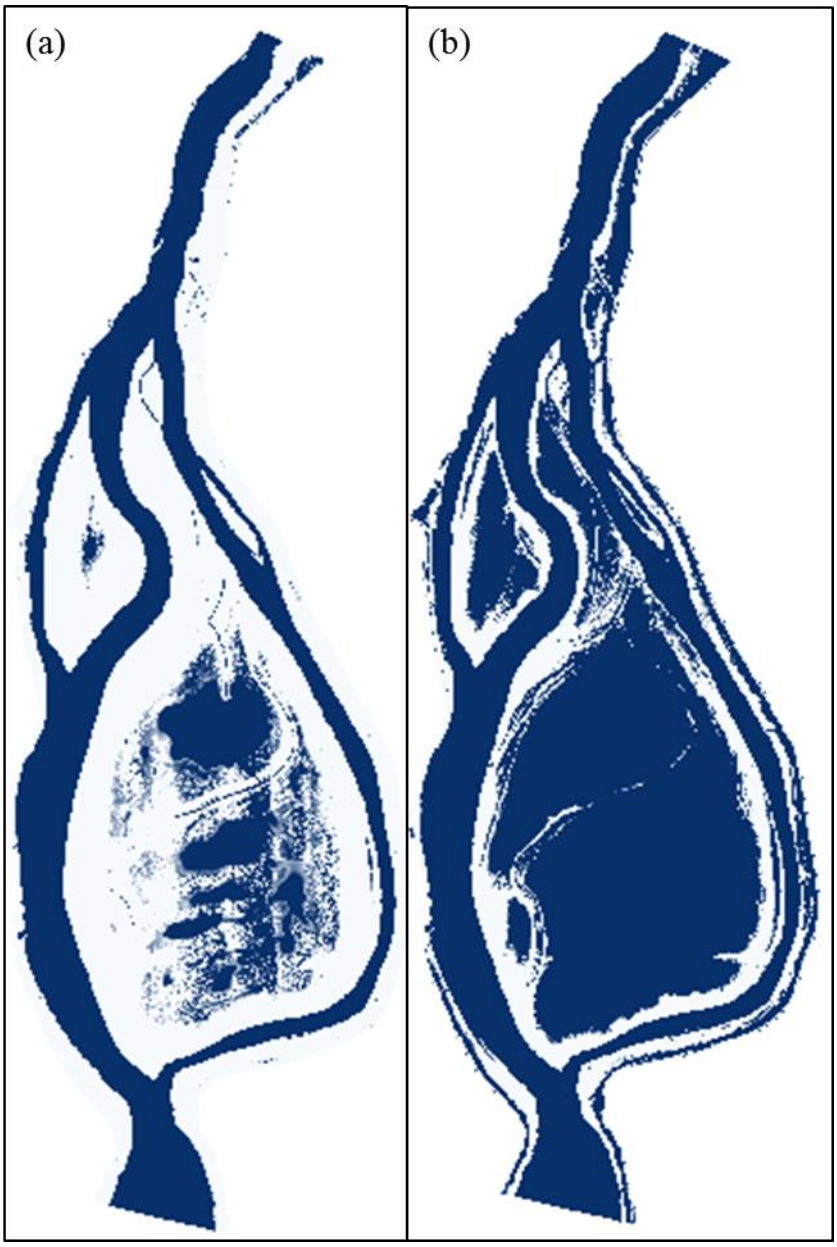

Figure 17. Inundation in Fundu Mare Island for two different water levels. (a) 4.6 MNS and (b) 5.6 MNS in Brăila. The blue parts represent inundated, the white parts dry areas.

4.1.2 Hydrology data

Evaporation, precipitation and temperature data at Fundu Mare Island are based on long-term data for the Danube Delta provided by Hooijer (2002). Ground water loss was estimated using Darcy's law based on an estimated hydraulic gradient between the Danube and the lakes with a k_f-value of $1 \cdot 10^{-5} m/s$ for silt-sand soil suggested by Busch et al. (1993).

At Brăila, the water levels of the Danube were made available as mean daily values by the River Administration of the Lower Danube in Galati (AFDJ). The decades between 1970 and 2015 were described by decennial mean daily values in Zinke et al. (2016), which are displayed in Figure 18.

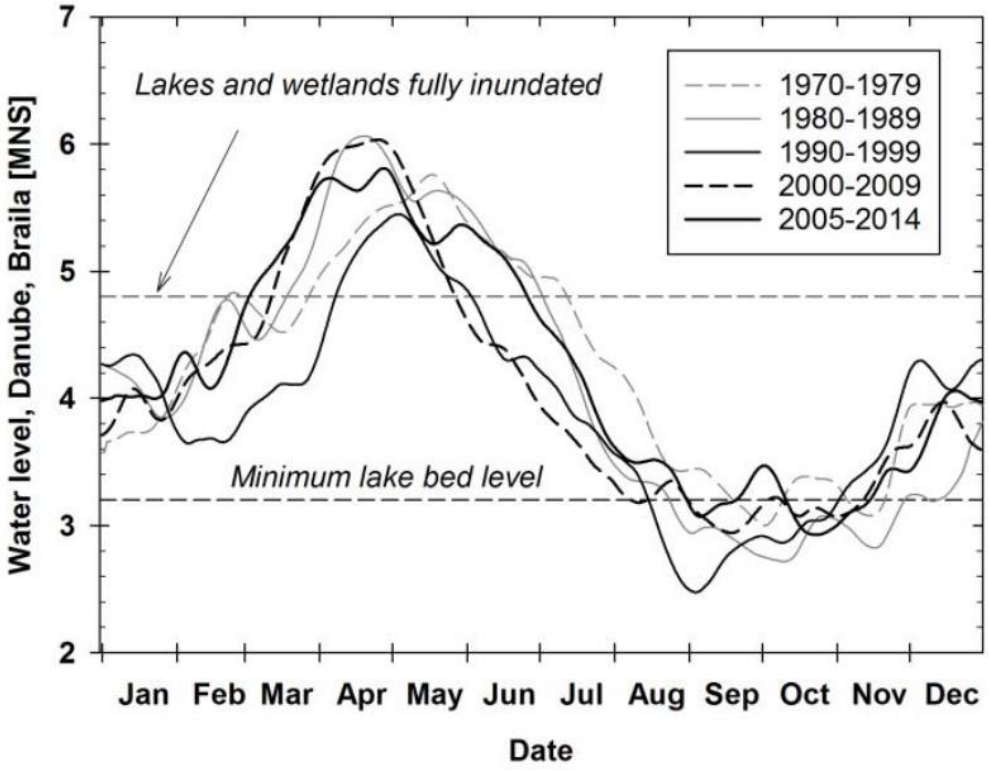

Figure 18. Hydrograph at Brăila (10 days moving average of the mean daily value) for several decades after 1969 (Zinke et al., 2016)

For Fundu Mare Island water level data up from the 9th of June 2015 were provided by three pressure sensors (Zinke & Aberle, 2015). Additionally, water depths, discharges and flow velocities from Acoustic Doppler Current Profiler (ADCP) and handheld Acoustic Doppler Velocimeter were available for the Hogioaia channel on the island for July 2015. Moreover, ADCP-measurements in the Danube were extraced from Nichersu (2016). The measurements on from 2015 include uncertainties with regard to the acquisition methods. The ADCP-measurements in the Danube were implausible and were not used for further investigation.

Based on the available bathymetric and hydrological data for 2015, the correlation between water volume and water levels on the island was visualised by a stage-volume relationship (Zinke & Aberle, 2015). The function is shown in the left part of Figure 19 and is assumed to be representative for different hydrological events. In the right part of the figure, the correlation of the water level in Fundu Mare Island with the inundated area is displayed, which is based on the modified morphological model by (Zinke & Aberle, 2015).

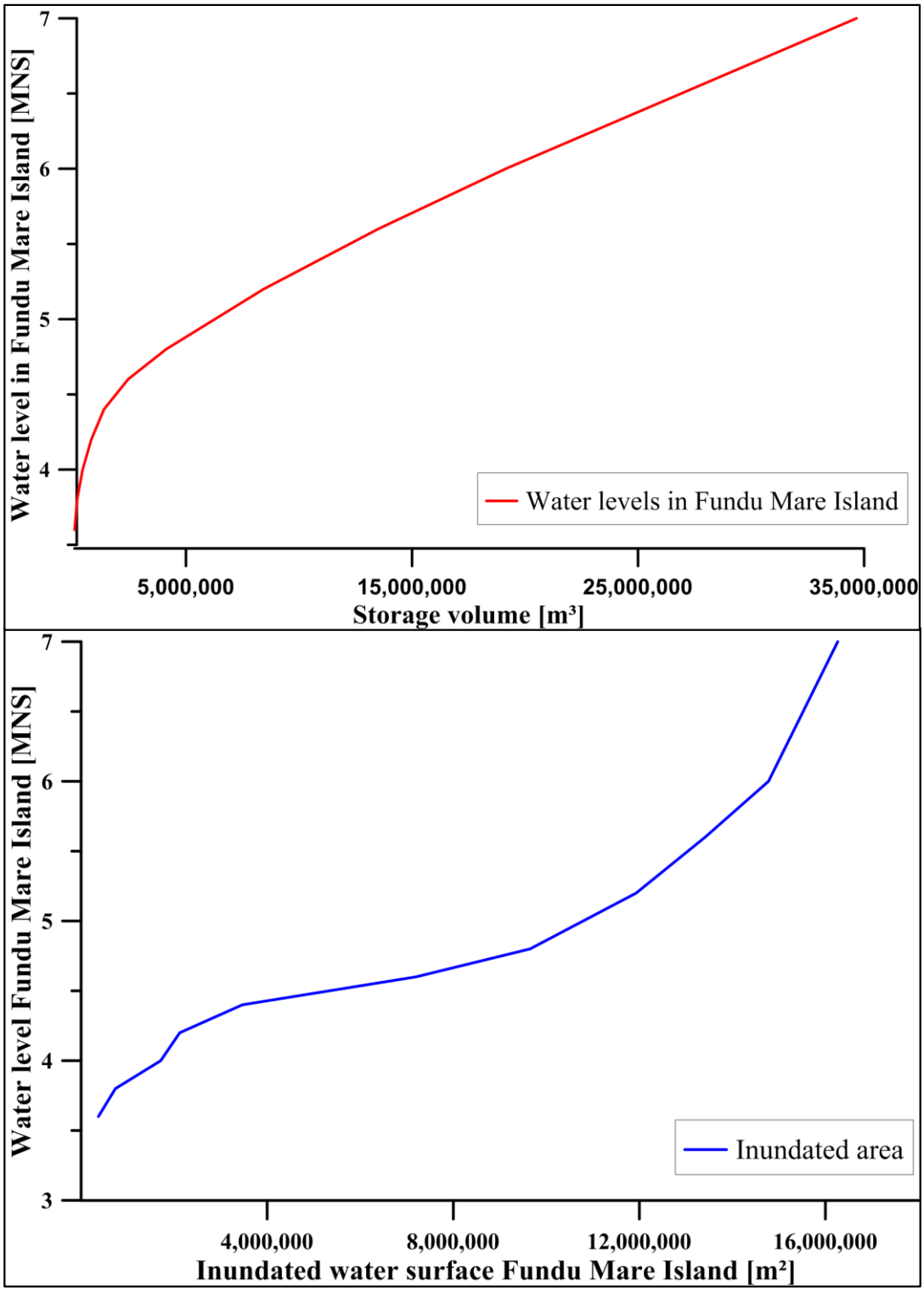

Figure 19. above: stage-volume relationship on the island according to the estimated GIS-morphology and corrections by measurements in 2015; below: relation of water level in correlation with the inundated surface

4.1.3 Vegetation and roughness data

The habitat classification of the island is based on nature types provided through digital maps, which contain a summary of the main biota types in the area (EU, 2013). Furthermore, vegetation in the lakes and in the wetland as well as the respective water levels, were recorded during punctual measurements in July 2015 (Zinke et al., 2016). Based on this habitat classification, a list of estimated Manning values was made available, determining the roughness distribution on the island. Moreover, the bed roughness in the main channel was made available by Zinke (2015b). Figure 20 shows the habitat classification and the according roughness data.

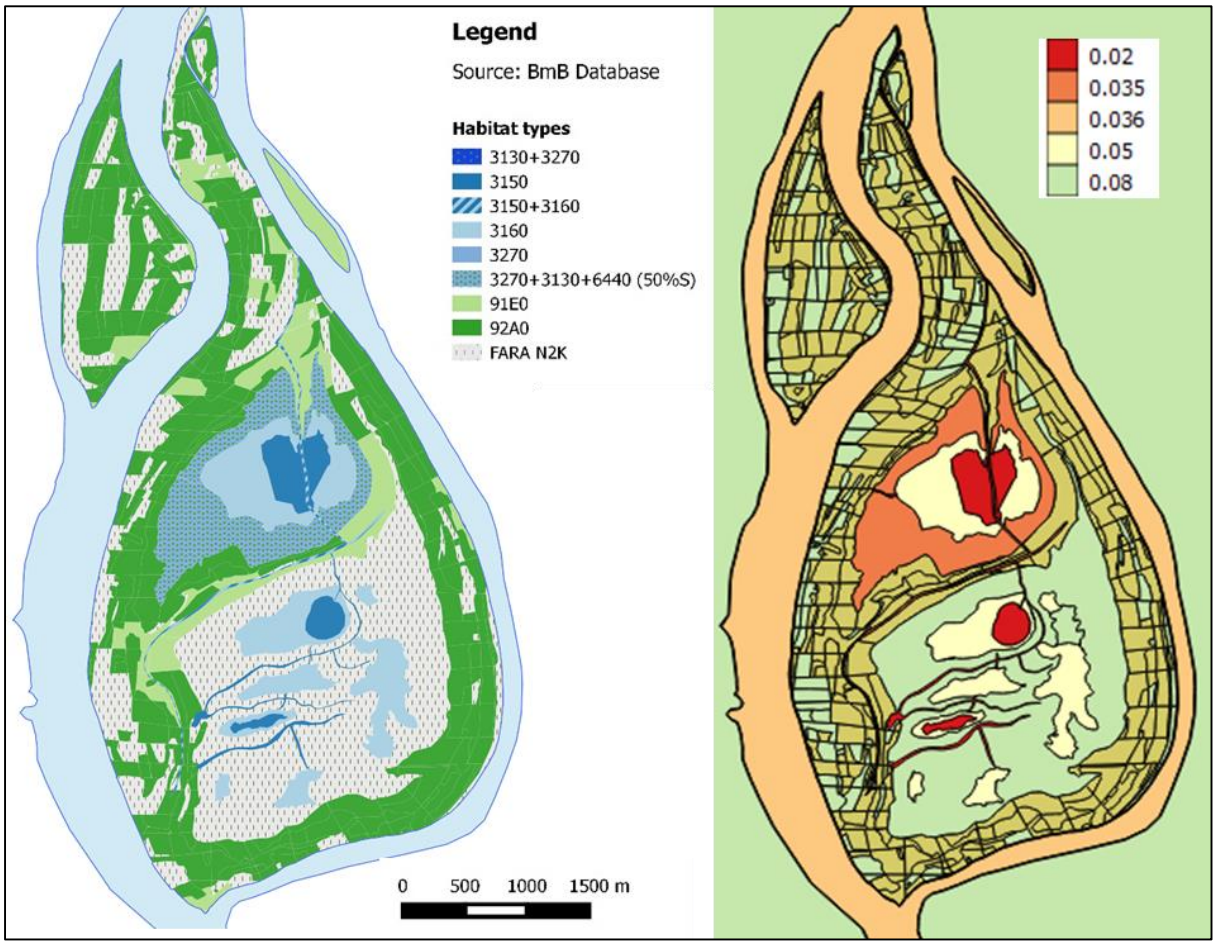

Figure 20. Habitat classification (left) (Zinke et al., 2016). For further explanation please refer to the reference. Provided initial Manning value distribution [$s/m^{1/3}$] on the island (right) (Zinke, 2015b).

The estimations made during data acquisition and processing have to be taken into consideration when implementing and calibrating the hydrodynamic model. The selection process of the software and a detailed description of the tools are presented in the next chapter.

4.2 Selection of modelling software

The selection of the appropriate software for simulating the given data required precise analysis and comparison of different types of software. Based on the project's requirements, specific criteria were defined:

- 2D and possible 3D-modelling
- open-source software to allow personal adjustment of the code in case of specific problems
- free of charge
- comprises sediment transport model
- good usability and user support
- available tools to simulate ground water flow

Various kinds of software have been examined, including packages and codes that require pre- and post-processing tools. In this matter, the compatibility of input and output files with non-commercial pre- and post-processing software was also examined. In Annex A, the considered software packages can be found in Table 4. In order to avoid simplifications in the modelling of vertical flow and its effects on secondary flow introduced by models of lower dimensionality (1D,2D) (Habersack et al., 2014), a software that can provide 3D-modeling was preferred. Finally, two well-known non-commercial packages were closely examined. SSIIM (Olsen, 2014) and Delft3D (Deltares, 2014a), which are powerful tools that can be used for the description of river flow and sediment transport and have been validated in several studies. Table 5 in the Annex A summarises some of their specifications.

The River Administration of the Lower Danube (AFDJ) recommended the software Delft3D for this project. In order to facilitate communication and understanding within the collaboration, Delft3D was prioritised for this work. In addition, good user support by the developers is provided, which is an important aspect considering limited previous experience with the utilisation of Delft3D. In general, Delft3D has been tested for several applications and therefore represents a reliable tool for the simulation of the hydrodynamics in Fundu Mare Island (cp. chapter 2.2.3). In order to gain a better understanding of the calculations, a summary of the analytics as well as the different tools of Delft3D applied in this work is given in the following chapter.

4.3 Delft3D by Deltares

Delft3D consists of several software modules simulating hydrodynamic flow, sediment transport, waves, water quality, morphological developments and ecology. The Delft3D-module FLOW resolves unsteady flow and transport phenomena by solving the shallow-water equations. In this work, the hydrodynamic processes within the area have been investigated with the help of the FLOW-module. The important aspects about the analytics and properties, and also the limits of the software are described below. Additional pre-processing software packages used in this work are also briefly discussed.

4.3.1 Pre-processing tools

In order to produce the orthogonal and curvilinear grid for Delft3D-FLOW, the pre-processing software RGFGRID (Deltares, 2014b) has been used. This package allows the creation of structured and unstructured grids, including personal adjustment within the areas of interest. By local refinement of the grid along vertical and horizontal grid lines, the computing time is reduced and the accuracy of the results at specific locations is increased. To reduce boundary effects, the area of interest is located as far as possible from the open boundaries. The grid resolution can be specified related to bottom bathymetry and desired accuracy. Mesh quality is determined by orthogonality, aspect ratio of the cells (cell length/cell height) and smooth grid cell transition in both horizontal directions. The bathymetry of the model was prepared by a software package called QUICKIN (Deltares, 2014c). It allows assignment of sample data to the grid points by interpolation. Missing data can be interpolated by internal diffusion using the surrounding values on the grid. In case of sudden bathymetry changes a smoothing option is implemented to treat the bathymetry, allowing stability within the computations.

RFGGRID and QUICKIN, respectively, are required to pre-process the data and allow creation of the required data files for Delft3D-FLOW. Further information on the pre-processing can be found in the user manuals.

4.3.2 The hydrodynamic module Delft3D-FLOW

The software Delft3D-FLOW is the hydrodynamic module of Delft3D. It offers applications to allow representation of a variety of engineering problems. All features are embedded in Graphical User Interface (GUI). Switching between two-dimensional (2D) depth-averaged and three-dimensional (3D) mode through representation of the bathymetry by σ-coordinate transformation is possible. Turbulence is represented by the LES or RANS method including several turbulence closure models. Bottom roughness and shear stress are based on the concepts of Chézy, Manning or White-Colebrook. For this work, a 2D depth-averaged approach is sufficient as stratification can be neglected. Therefore, to describe the investigated area a depth-averaged model has been created to save computing time and disc space. However, the adjustment of the model for further investigations in three dimensions can be easily performed. Therefore, the governing equations in three dimensions are summarised below.

Theoretical background

The software solves the shallow water equations in two and three dimensions, which are simplified versions of the time-averaged Navier-Stokes equations for incompressible free-surface flow. The module consists of the horizontal momentum equation, the continuity equation, the transport equation and a turbulence closure model. Within Delft3D the use of a σ-coordinate system is implemented that has been described by Deleersnijder & Beckers (1992) or Stelling & Kester (1994) to approximate horizontal gradients. With this method, the three-dimensional flow domain consists of a constant number of layers over the horizontal computational area within the vertical σ-coordinates $(-1 < \sigma \leq 0)$ (cp. Figure 21):

$$\sigma = \frac{z - \zeta}{h} \tag{4.1}$$

with z being the vertical axis, ζ the water surface elevation at reference date, and h total water depth in meters. A set of coupled conservation equations is solved for each layer, where the partial derivatives are described in σ-coordinates within the Cartesian coordinate system, introducing additional terms (Stelling & Kester, 1994)

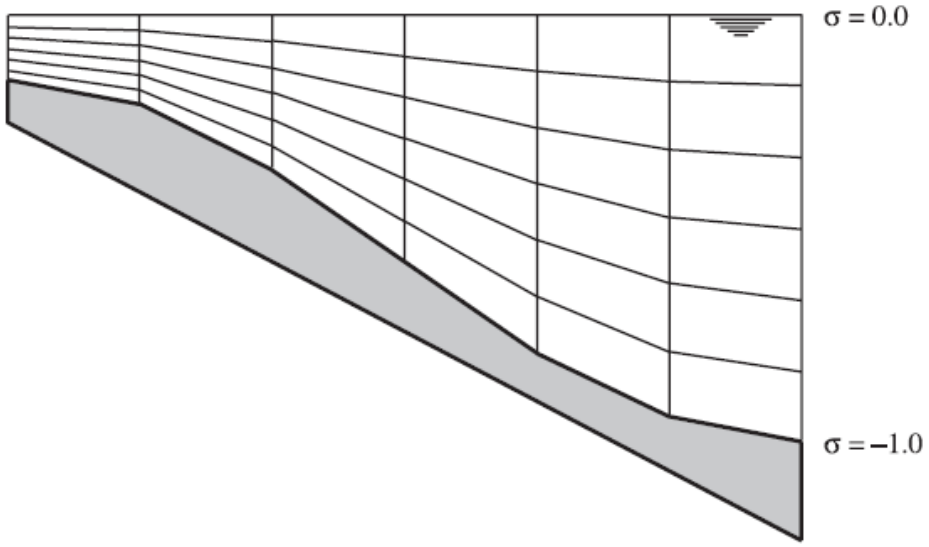

Figure 21. σ-coordinates with six layers (Lesser et al., 2004)

Vertical accelerations due to buoyancy effects or strong variations in bottom topography are assumed to be small compared to gravitational acceleration reducing the vertical momentum equation to the hydrostatic pressure relation:

$$\frac{\partial P}{\partial \sigma} = -\rho g h \tag{4.2}$$

with ρ representing water density and g gravitational acceleration. As a result, vertical accelerations are neglected. Therefore, Delft3D-FLOW is suitable for the prediction of flow in shallow lakes and rivers, where horizontal length and time scales are significantly larger than the vertical scales (Lesser et al., 2004).

The coordinates for the curvilinear grid in a Cartesian coordinate system are defined as ξ-direction and η-direction. The depth-averaged continuity equation with Q representing the contribution of discharge/withdrawal of water, evaporation and precipitation per unit area is defined as (Deltares, 2015):

$$\frac{\partial \zeta}{\partial t} + \frac{1}{\sqrt{G_{\xi\xi}}\sqrt{G_{\eta\eta}}} \frac{\partial \left[(d+\zeta) U \sqrt{G_{\eta\eta}} \right]}{\partial \xi} + \frac{1}{\sqrt{G_{\xi\xi}}\sqrt{G_{\eta\eta}}} \frac{\partial \left[(d+\zeta) V \sqrt{G_{\xi\xi}} \right]}{\partial \eta} = (d+\zeta) Q \tag{4.3}$$

where U and V are the depth-averaged velocities in flow and lateral direction respectively:

$$U = \frac{1}{d+\zeta}\int_{d}^{\zeta} u\ dz = \int_{-1}^{0} u\ d\sigma \tag{4.4}$$

$$V = \frac{1}{d+\zeta}\int_{d}^{\zeta} v\ dz = \int_{-1}^{0} v\ d\sigma \tag{4.5}$$

with d being depth below reference plane and $\sqrt{G_{\xi\xi,\eta\eta}}$ coefficients used to transform curvilinear to rectangular coordinates. The horizontal momentum equations are defined as:

$$\begin{aligned}&\frac{\partial u}{\partial t}+\frac{u}{\sqrt{G_{\xi\xi}}}\frac{\partial u}{\partial \xi}+\frac{v}{\sqrt{G_{\eta\eta}}}\frac{\partial u}{\partial \eta}+\frac{\omega}{h}\frac{\partial u}{\partial \sigma}-\frac{v^2}{\sqrt{G_{\xi\xi}}\sqrt{G_{\eta\eta}}}\frac{\partial\sqrt{G_{\eta\eta}}}{\partial \xi}+\frac{uv}{\sqrt{G_{\xi\xi}}\sqrt{G_{\eta\eta}}}\frac{\partial\sqrt{G_{\xi\xi}}}{\partial \eta}-fv\\&=-\frac{1}{\rho_0\sqrt{G_{\xi\xi}}}P_\xi+F_\xi+M_\xi+\frac{1}{h^2}\frac{\partial}{\partial\sigma}\left(\nu_v\frac{\partial u}{\partial\sigma}\right)\end{aligned} \tag{4.6}$$

$$\begin{aligned}&\frac{\partial v}{\partial t}+\frac{u}{\sqrt{G_{\xi\xi}}}\frac{\partial v}{\partial \xi}+\frac{v}{\sqrt{G_{\eta\eta}}}\frac{\partial v}{\partial \eta}+\frac{\omega}{h}\frac{\partial v}{\partial \sigma}-\frac{u^2}{\sqrt{G_{\xi\xi}}\sqrt{G_{\eta\eta}}}\frac{\partial\sqrt{G_{\xi\xi}}}{\partial \eta}+\frac{uv}{\sqrt{G_{\xi\xi}}\sqrt{G_{\eta\eta}}}\frac{\partial\sqrt{G_{\eta\eta}}}{\partial \xi}+fu\\&=-\frac{1}{\rho_0\sqrt{G_{\eta\eta}}}P_\eta+F_\eta+M_\eta+\frac{1}{h^2}\frac{\partial}{\partial\sigma}\left(\nu_v\frac{\partial v}{\partial\sigma}\right)\end{aligned} \tag{4.7}$$

ν_v represents the vertical eddy viscosity coefficient, ω the vertical velocity component in σ-coordinates, f Coriolis coefficient, F_ξ and F_η the unbalance of horizontal Reynold's stresses, P_ξ and P_η the horizontal pressure term, and M_ξ and M_η describe external sources or sinks of momentum (i.e. discharges, wave stresses, etc.).

For simulations on a large scale where shear stresses at the closed boundaries are neglected, the stresses can be simplified to

$$F_\xi = \nu_H\left(\frac{1}{\sqrt{G_{\xi\xi}}\sqrt{G_{\xi\xi}}}\frac{\partial^2 u}{\partial\xi^2}+\frac{1}{\sqrt{G_{\eta\eta}}\sqrt{G_{\eta\eta}}}\frac{\partial^2 u}{\partial\eta^2}\right) \tag{4.8}$$

$$F_\eta = \nu_H\left(\frac{1}{\sqrt{G_{\xi\xi}}\sqrt{G_{\xi\xi}}}\frac{\partial^2 v}{\partial\xi^2}+\frac{1}{\sqrt{G_{\eta\eta}}\sqrt{G_{\eta\eta}}}\frac{\partial^2 v}{\partial\eta^2}\right) \tag{4.9}$$

with the horizontal eddy viscosity ν_H assumed to be constant.

Transport of dissolved substances, salinity and heat, parameterised with c in eq. 4.10, is computed by the advection-diffusion equation. For the three coordinate directions it can be written as:

$$\frac{\partial[hc]}{\partial t}+\frac{1}{\sqrt{G_{\xi\xi}}\sqrt{G_{\eta\eta}}}\left\{\frac{\partial\left[\sqrt{G_{\eta\eta}}huc\right]}{\partial\xi}+\frac{\partial\left[\sqrt{G_{\xi\xi}}hvc\right]}{\partial\eta}\right\}+\frac{\partial[\omega c]}{\partial\sigma}$$
$$=\frac{h}{\sqrt{G_{\xi\xi}}\sqrt{G_{\eta\eta}}}\left[\frac{\partial}{\partial\xi}\left(D_H\frac{\sqrt{G_{\eta\eta}}}{\sqrt{G_{\xi\xi}}}\frac{\partial c}{\partial\xi}\right)+\frac{\partial}{\partial\eta}\left(D_H\frac{\sqrt{G_{\xi\xi}}}{\sqrt{G_{\eta\eta}}}\frac{\partial c}{\partial\eta}\right)\right]+\frac{1}{h}\frac{\partial}{\partial\sigma}\left[D_v\frac{\partial c}{\partial\sigma}\right]+hS \quad (4.10)$$

with *S* summarizing sink and source terms per unit area (discharge/withdrawal of water and heat exchange). D_H and D_V are the horizontal and vertical diffusivity.

Horizontal and vertical viscosity and diffusivity are described as a superposition of three different parts in Delft3D-FLOW, including kinematic viscosity, "3D turbulence", and "2D turbulence". The kinematic viscosity of water is constant with 10^{-6} m^2/s, whereas "3D turbulence" is defined by a selected turbulence closure model and "2D turbulence" describes horizontal mixing that is not computed by advection. "2D turbulence" can either be specified by the user or can be computed by horizontal large eddy simulation (HLES).

In Delft3D-FLOW the model is discretized by finite differences and a rectangular, curvilinear or a spherical grid. The grid is arranged as a staggered grid with water level points in the centre of the cells and velocity components in x-direction (u-velocity) and in y-direction (v-velocity) perpendicular to the cell faces as shown in Figure 22 (Lesser et al., 2004). The cell corners represent the bottom depth of the bathymetry. The water level points are defined in the centre of each cell, whereas the current components are defined at the cell faces. In order to determine the total water depth in the cell centre the surrounding depth values are required.

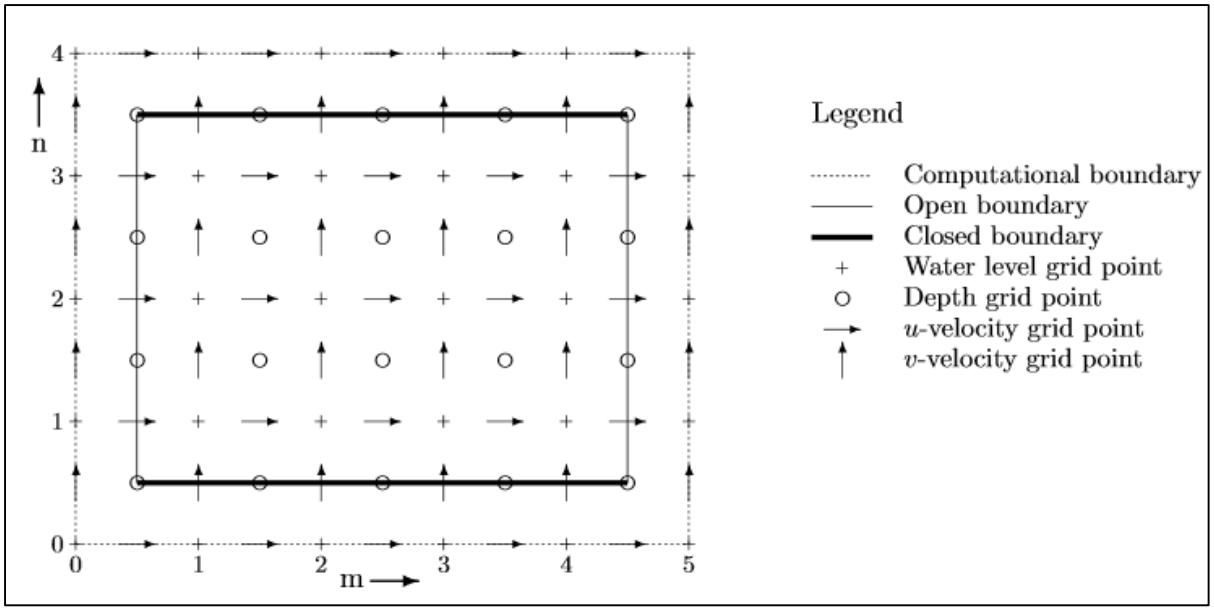

Figure 22. Concept of a staggered grid (Broomans et al., 2004)

The finite-difference discretization is solved by Alternate Direction Implicit (ADI) integration (Stelling & Leendertse, 1992 cited in Geleynse et al., 2011). The wetting and drying process is computed by so-called half-time steps. With this method, water levels and velocities in x-

direction are implicitly solved within the first half of the time step, whereas y-directional water levels and velocities are computed in the second half. To control the wetting and drying process the velocity points are set dry when falling below a user-defined threshold. This value is interfering with the model stability and is specified according to a rule of thumb:

$$\delta \geq \left|\frac{\partial \zeta}{\partial t}\right| \Delta t \approx \frac{2\pi |a|}{N} \tag{4.11}$$

with $\left|\frac{\partial \zeta}{\partial t}\right|$ being changes of the water level over time, *a* characteristic amplitude and *N* number of time-steps. This method is extremely stable and requires less computational effort than for instance the Crank-Nicholson method. More detail about this method can be found in Stelling (1983). For the 3D-shallow water equations the horizontal velocity components are coupled vertically by the vertical advection and viscosity term which is solved by a fully implicit time integration method.

In Delft3D-FLOW several turbulence models are implemented, which are all based on the "eddy viscosity" concept (Kolmogorov, 1941; Prandtl & Wieghardt, 1947). The eddy viscosity is defined as

$$\nu_v = c_\mu ' L\sqrt{k} \tag{4.12}$$

with c'_μ being a constant set by calibration, *L* mixing length and *k* the turbulent kinetic energy. The mixing length is determined by the turbulent dissipation ε and a calibration constant c_D:

$$L = c_D \frac{k\sqrt{k}}{\varepsilon} \tag{4.13}$$

In two-dimensional computations, the turbulence is determined by the horizontal eddy viscosity which is defined by the user. The horizontal eddy viscosity coefficient includes 2D-turbulence and dispersion.

The roughness is applied as 2D-Chézy coefficient with the use of Manning's value *n*:

$$C_{2D} = \frac{\sqrt[6]{h}}{n} \tag{4.14}$$

Secondary flow is defined as a function of the velocity component perpendicular to the main flow:

$$I = \int_{-1}^{0} |v(\sigma)| \, d\sigma \tag{4.15}$$

Where *I* is the magnitude of this velocity in the vertical plane.

Boundary conditions

Boundary conditions are required to solve the system of equations. Delft3D-FLOW distinguishes between closed and open boundaries, where closed boundaries enclose the model area and open boundaries allow definition of exchange between model and "outer world". According to the type of model and the needs of the user water level, velocity, flux, and weakly reflective boundary conditions can be chosen. The selection of different kinds of boundary conditions within one model is suggested by Deltares (2015) to prevent model instability by mass conservation. The bed and surface boundaries are defined by the σ-planes reducing the vertical velocity to

$$\omega(-1) = 0 \quad \text{and} \quad \omega(0) = 0 \tag{4.16}$$

Friction at the bed is represented by

$$\frac{\nu_v}{h}\frac{\partial u}{\partial \sigma}\bigg|_{\sigma=-1} = \frac{\tau_{bx}}{\rho} \quad \text{and} \quad \frac{\nu_v}{h}\frac{\partial v}{\partial \sigma}\bigg|_{\sigma=-1} = \frac{\tau_{by}}{\rho} \tag{4.17}$$

with τ_{bx} and τ_{by} representing bed shear stresses including wave-current interaction. Friction due to wind stress at the water surface may be included in a similar manner. Along the lateral component at closed boundaries the velocity component perpendicular to the boundary is set to zero.

Numerical stability and computational effort

The Courant number is an indicator for the stability of the model and is defined as:

$$C = 2\Delta t\sqrt{gh\left(\frac{1}{\Delta x^2} + \frac{1}{\Delta y^2}\right)} \tag{4.18}$$

where Δx and Δy are the size of the cell faces and Δt the time-step. The relation between the propagation speed and time-step is represented, which determine the computational time. Therefore, to reduce computational effort, the largest time-step possible without the loss of stability and accuracy is desired (Stelling, 1983).

The run time of the model depends on the number of grid points, layers, and processes. Also the time-step and the hardware configuration play a role in the simulation run time. The simulation performance depends on the CPU time, the grid points, time-steps and constituents.

5 Model set-up

The model of the investigated area of the project was implemented in the software package Delft3D-FLOW in combination with the application of the pre-processing modules RGFGRID and QUICKIN. Before the creation of the model, the input data required by the software was summarised to give an overview on the procedure and tasks. Delft3D-FLOW requires information about the boundaries of wet and dry cells as well as open boundaries, the bathymetry and geometrical details, e.g. structures, discharges and breakwaters as well as location of storage of results. Furthermore, a numerical grid has to be defined, that summarises the location-related parameters. The basic steps to create a model can be summarised as (Deltares, 2014a):

1) Definition of the extent of the area
2) Definition and location of the boundary conditions
3) Creation of the numerical grid
4) Generation of the bathymetry on the numerical grid
5) Description of grid related parameters, i.e. open boundaries, monitoring points, discharge locations or drogue release points
6) Time-frame definition, e.g. start and stop time, discharges or salinity

The pre-processing of bathymetry and roughness data were conducted using the GIS operator QGIS. The bed level data were interpolated to create a higher resolution of the bathymetry data (Zinke, 2015a). These data were provided by Zinke & Aberle (2015).

5.1 Grid set-up

The area extent was defined by land boundaries representing the surrounding dike crest, which defines the closed boundaries of the model. Its location was determined based on GIS data. The open boundaries are located south of the island to define water inflow as well as specification of the outflow close to the gauging station at Brăila. In order to solve stability problems observed during test runs, the location of the boundaries should be as far away as possible from the investigated area (Deltares, 2015). An artificial expansion of the grid had been implemented and the open boundaries were shifted away from the island. Moreover, Delft3D requires open boundaries that are along one direction of the cell faces over the whole domain, i.e. the whole boundary can only be along either x- or y-direction. Therefore, the grid was expanded north and south to guarantee horizontal alignment. The process is displayed in Figure 23. The red lines describe the open boundaries prior to and after processing.

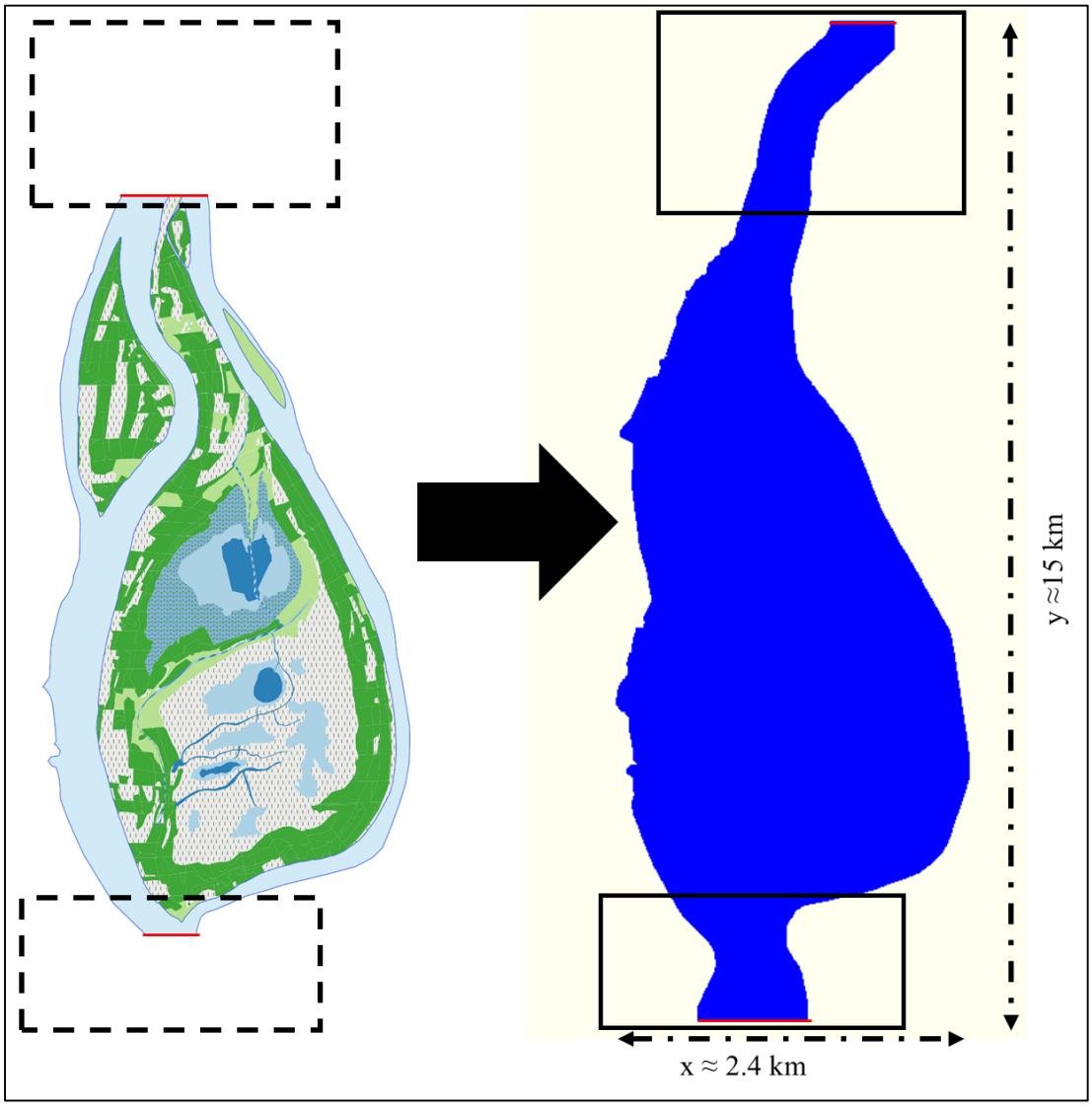

Figure 23. Expansion of the numerical domain north and south of the Fundu Mare Island

To set up the orthogonal grid, the grid generator RGFGRID was used. A Cartesian grid had been chosen as suggested by Deltares (2015) for smaller scale areas. As a basis, a rectangular grid over the whole area was created. The land boundaries were prepared in a GIS and inserted to evaluate the exact location of the domain. To fit the grid as close to the boundaries as possible, the grid has been refined to $\Delta x = \Delta y = 10\ m$ and all grid cells located outside the domain have been erased. The cells have been deleted when approximately half of the cross section was located outside the investigated area. Figure 24 displays the final grid with an example of the adapted method.

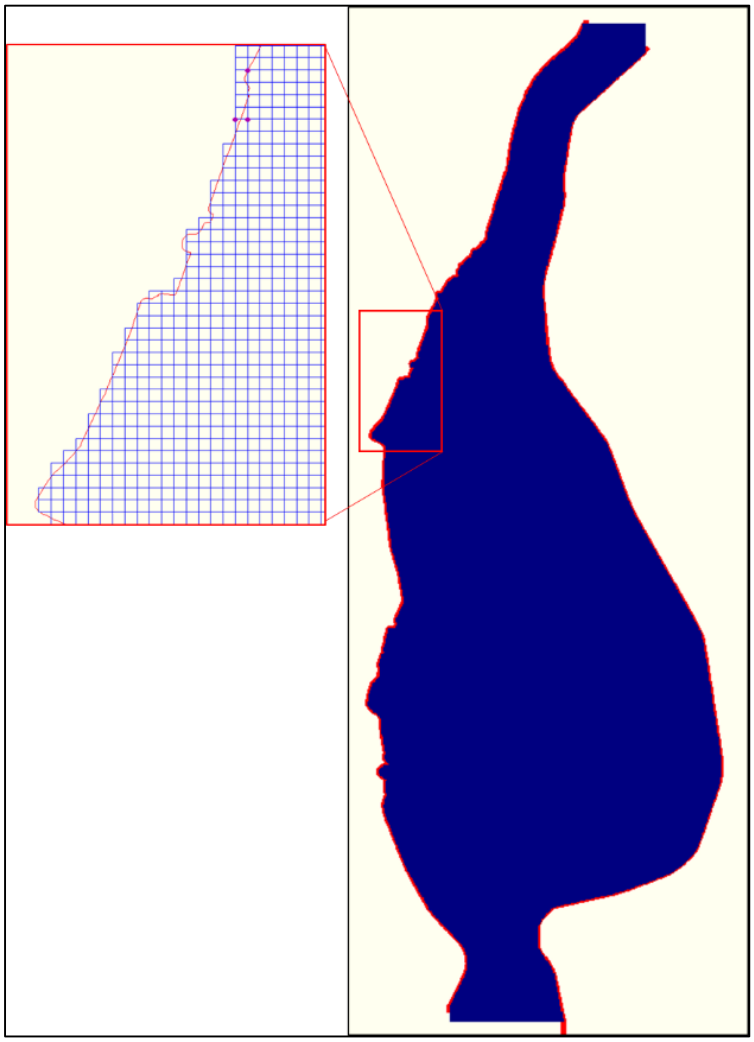

Figure 24. Refined grid (blue lines) with land boundaries (red lines)

For the whole area cells with 10m-faces were retained. To allow investigation of the Hogioaia- and the LIFE-channel on the island, the mesh was refined locally to a cell length of 5m. The whole grid has been smoothed to achieve a regular transition between the different cell sizes. This function was used repeatedly until the suggested ratio between cell sizes of less than 1.2 was achieved for most of the grid cells. Orthogonality is described as the cosine of the cell corners. A value close to zero is required for sufficient grid quality of the mesh. Furthermore, aspect ratio of the grid cell is supposed to be between 1 and 2. Deltares (2014b) states that some exceptions in grid cell variations are acceptable. The mesh of the area was determined to sufficient mesh quality for further investigations. Figure 25 shows the final grid and its resolution. Due to the automatic adjustment of the mesh quality, the grid cell sizes vary throughout the domain in a range of some decimetres. The refinement of the grid cells is restricted to a refinement of the entire axis in either horizontal or vertical direction. Therefore, to refine the grid cells for the channels on the island, the specific grid cells had to be refined over the whole domain. As a result, the "cross-pattern" was created. Further information about the smoothening process and the quality of the mesh can be found in the Annex.

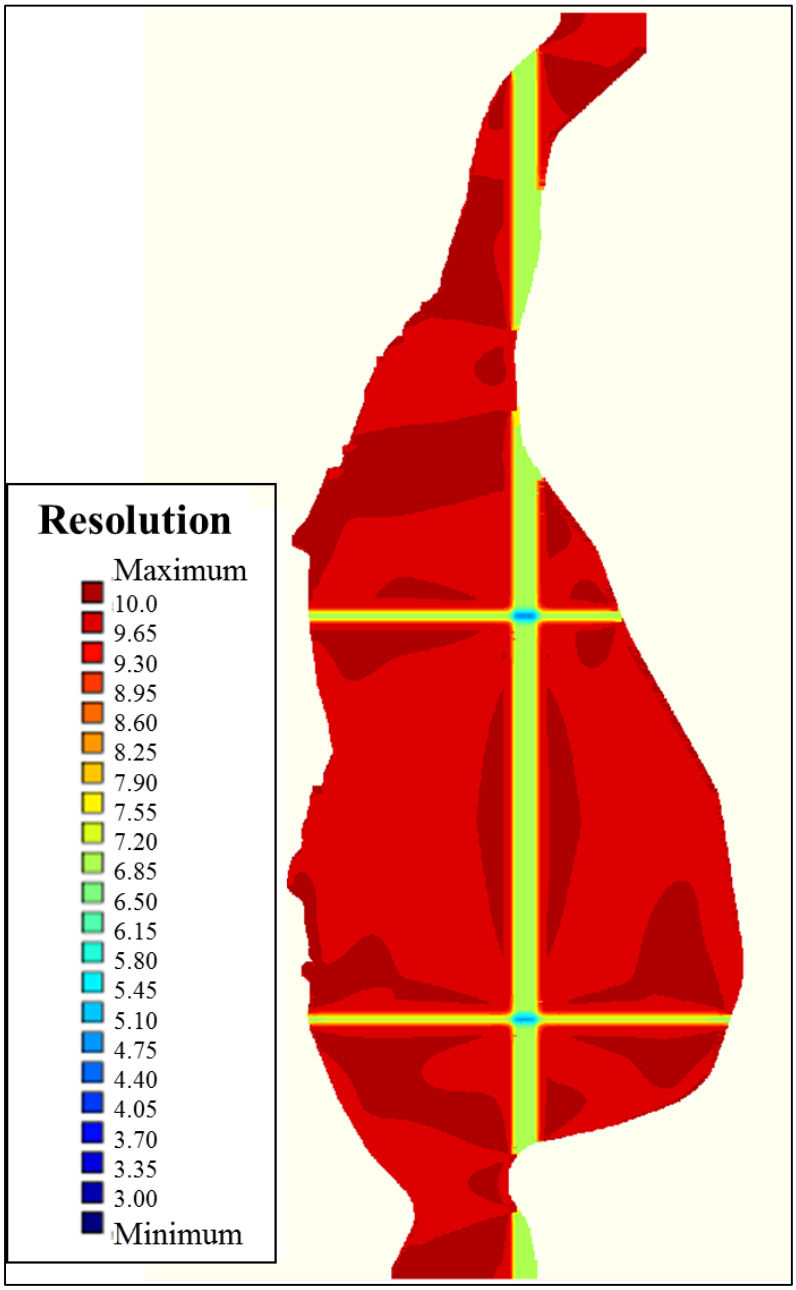

Figure 25. Final grid resolution

5.2 Bathymetry

The bathymetry was processed with the help of the QUICKIN tool that is included in the Delft3D-package. The DEM was exported from a GIS-operator and implemented in QUICKIN as a sample-file. The depth samples had to be processed to make them suitable for the beforehand created grid. Additionally, the depth-values had to be assigned to the grid cells by interpolation. Several tools within QUICKIN were used to redistribute the depth-values to the grid cells: QUICKIN allows averaging of high numbers of sample values and triangular interpolation in case of a small sample density. Internal diffusion was used to assign depth-values at grid cells with no value. The last step was necessary mainly in locations, where the

grid was expanded. As a consequence, the depth values at the open boundaries had to be manually adjusted to allow smooth in- and outflow of the discharge. In Figure 26 the final bathymetry is displayed.

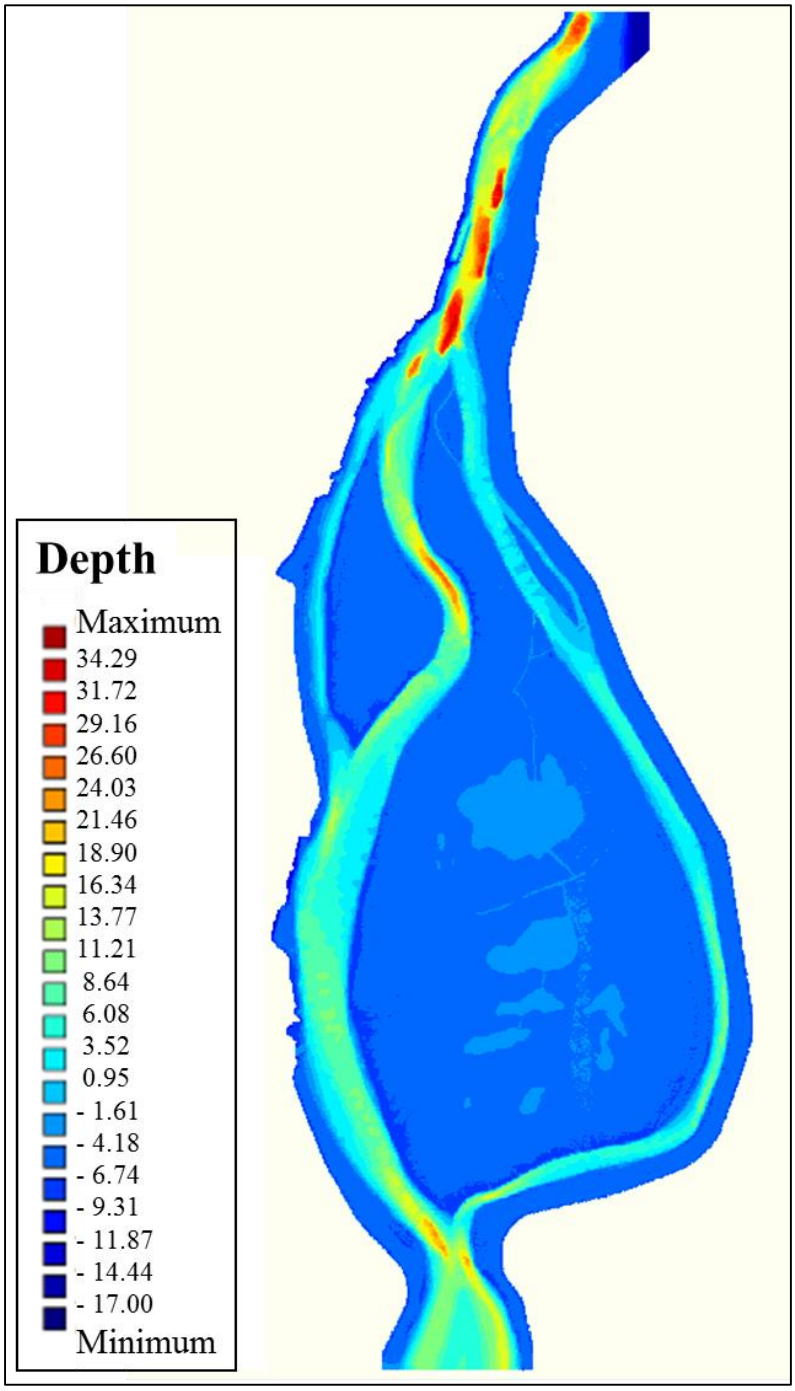

Figure 26. Depth value distribution on the grid in MNS

Due to the interpolation process in the GIS-operator and during pre-processing, small scaled details were not sufficiently represented. This included the depth-values of the artificial channels and the weir height as well as the channels between the lakes on the island. The values had to be corrected manually to guarantee a hydraulic connection between the lakes on the

island and the Danube branches. Therefore, the channels were “dug” by assigning values to the grid points, whereas the surrounding grid points were interpolated by the software to guarantee a smooth transition (cp. Figure 27 and Figure 28). This tool did not work correctly during the model set-up and induced higher time effort for the model creation.

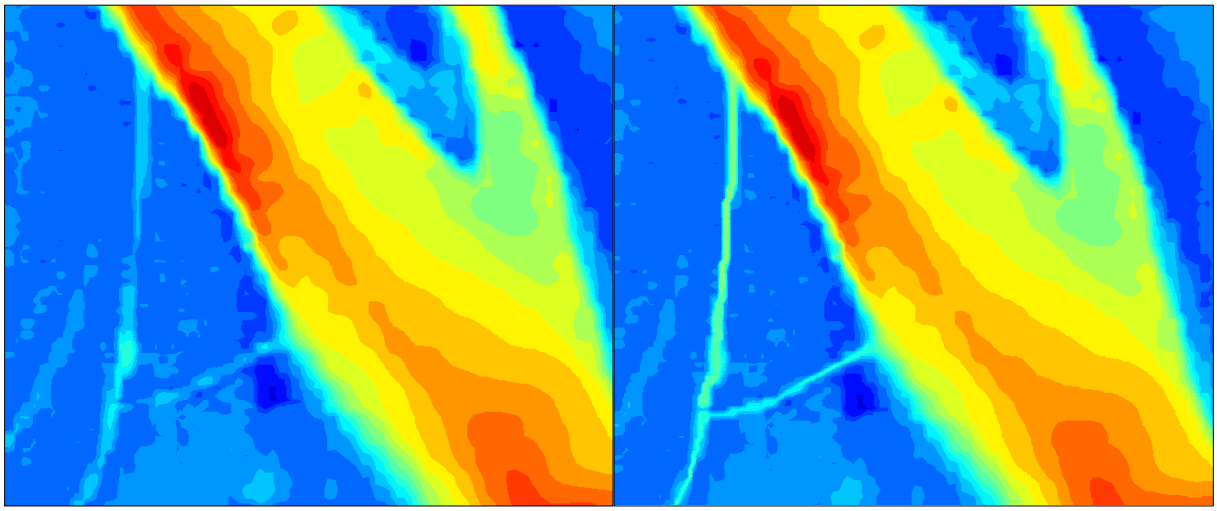

Figure 27. Depth-values of the channel and the weir on the island before (left) and after correction (right)

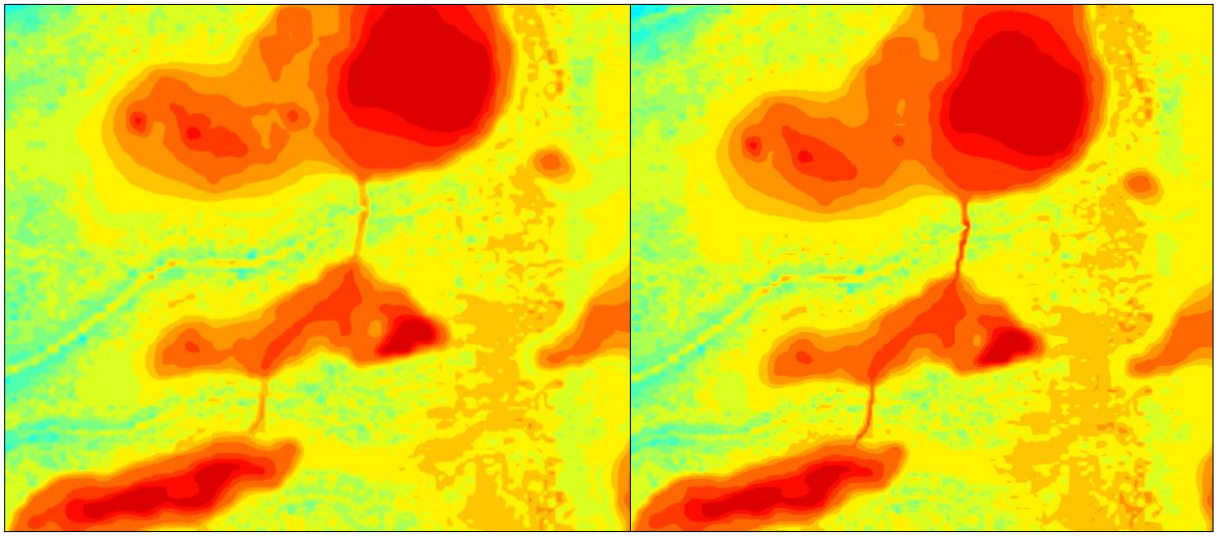

Figure 28. Connecting channels between the three lakes before (left) and after correction (right)

5.3 The FLOW-model

The parameters of the simulation are controlled through the Graphical User Interface (GUI) of Delft3D-FLOW (Figure 29).

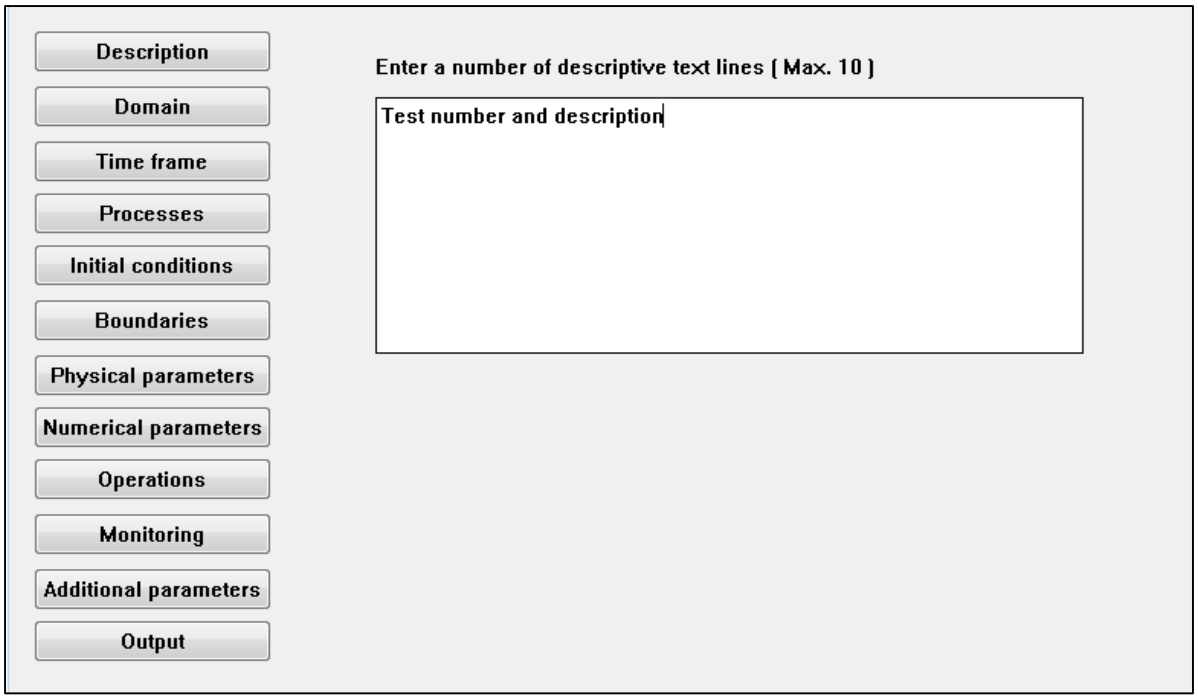

Figure 29. GUI of Delft3D-FLOW

Domain and time frame

The grid-file and the depth-file are required to set up the physical and numerical setting of the area. The boundaries of the model are defined by the grid (see chapter 5.1), which limits the computations. The number of dimensions is defined by the number of layers in the σ-coordinate system. One layer represents two dimensions whereas several numbers of layers represent three dimensions. The definition of layers can be defined by a parameter in the GUI. Due to low stratification in the area and no specific analysis of the vertical velocity distribution the application of a depth-averaged model is sufficient. Therefore, the number of layers has been set to one. In QUICKIN, depth-values are generated at the cell corners. As a result, the computation of the values in the cell centre must be defined based on the four corner values. When specifying the reference corner value, Deltares (2015) suggests the choice of the maximum value causing less computational time in locations with steeper bottom slopes. Due to the choice of Cartesian coordinates, only the latitude of the area has to be implemented to allow computation of the Coriolis force.

By defining the time frame, the relation between the time axis of the real world and of the simulation is specified. The time dependent input is defined by the date and time as [dd mm yyyy hh mm ss], whereas the time in the simulation is determined by its number of time-steps. The time-step is chosen as large as possible with regard to stability. In order to allow faster

computations, a stable restart-file with smaller time-steps can be created that can be re-used for further computations with larger time-steps. Additionally, the number of iterations when approximating the continuity equation plays a role for stability and computational effort. The default value is 2. The period of time that is necessary to simulate to allow investigation of the hydraulic changes in Fundu Mare Island was determined from the 9th of June 2015 to the middle of July. The simulation time depends on the temporal and spatial accuracy of the model.

Processes

Several processes can be specified that influence the hydrodynamic simulation, according to the requirements of the model. For this set-up no additional processes were defined. Wind shear stress is neglected due to lack of sufficient data. Temperature and sediments are excluded to simplify the model set-up with regard to limited time in this work. Secondary flow is only important for morphological calculations and can be applied for further investigations of sediment transport (Deltares, 2015). The more processes are selected, the more variables have to be chosen and defined. In this model only the basic parameters need to be described to provide input for the governing equations. Gravity $g = 9.81\, m/s^2$ and density $\rho = 1000$ kg/m^3 are default values. The horizontal eddy viscosity represents 2D-turbulences and has to be investigated within the calibration process.

Physical parameters

Furthermore, the roughness in the model needs to be specified and carefully calibrated. For the investigated area the vegetation distribution was taken into consideration to apply realistic roughness values. The data made available by Zinke (2015a) was pre-processed and implemented in the model.

The roughness-file with the Manning values can be directly implemented by the FLOW-GUI. During large-scale simulations, the tangential shear stress can be neglected at the closed boundaries (Deltares, 2015). Therefore, the free-slip condition for the wall roughness is specified.

Numerical parameters

Numerical parameters can be specified to determine the numerical approximations. For the wetting and drying process a threshold of 0.0002 m is specified. The cells are checked at grid cell centres and faces to define if the cell is set dry. The water levels in the velocity points are computed as mean values. The advection scheme for the momentum during spatial discretization is chosen by the user. Several methods are proposed by Delft3D. The “cyclic”-method is higher-order approximation of the advective term and does not impose a time-step restriction with good convergence behaviour. This method has been regarded as suitable for this work according to the user manual (Deltares, 2015).

Initial conditions and boundaries

The initial conditions were defined by a uniform water level over the whole domain. Due to stability issues, a higher water level than the downstream boundary was implemented. Thus, the model "runs out" until reaching the boundary conditions. In addition, a smoothing time of four hours has been applied during which the transition between initial and boundary conditions is linearly computed. The boundaries of the model were defined according to the available data. The inflow boundary was defined by a time-series of discharges and the outflow close to Brăila by the corresponding water levels.

Operations

Evaporation and precipitation were defined by implementation of discharge points in the centre of the lakes on the island to simulate the gain/loss due to atmospheric influences. In this way, evaporation is simulated through a flux depending on the inundated area. It has to be pointed out that only the evaporation on the island is taken into account. Evaporation in the main channels and west of the island is neglected. The total evaporation/precipitation is split into three discharge points which are located in the centres of the lakes. To allocate the total of evaporation/precipitation to the three discharges, a rough estimation of the lake surfaces was determined to be 1/2 (big lake), 1/4 (small lake) and 1/4 (northern lake) as can be seen in Figure 30. The interpolation type between the values can be defined as "linear" or "block"-interpolation. Here, "block"-interpolation was specified, defining the use of one value until the next value is defined.

Monitoring

In order to monitor the computations, several observation points and cross sections are defined in the model area. At these points, the computed quantities are saved as a time-series and can be visualised with the help of post-processing software. Figure 30 shows the observation points and cross sections. The points were set at the locations of the loggers, of the ADCP measurements (2-6), at the open boundaries and around the weir.

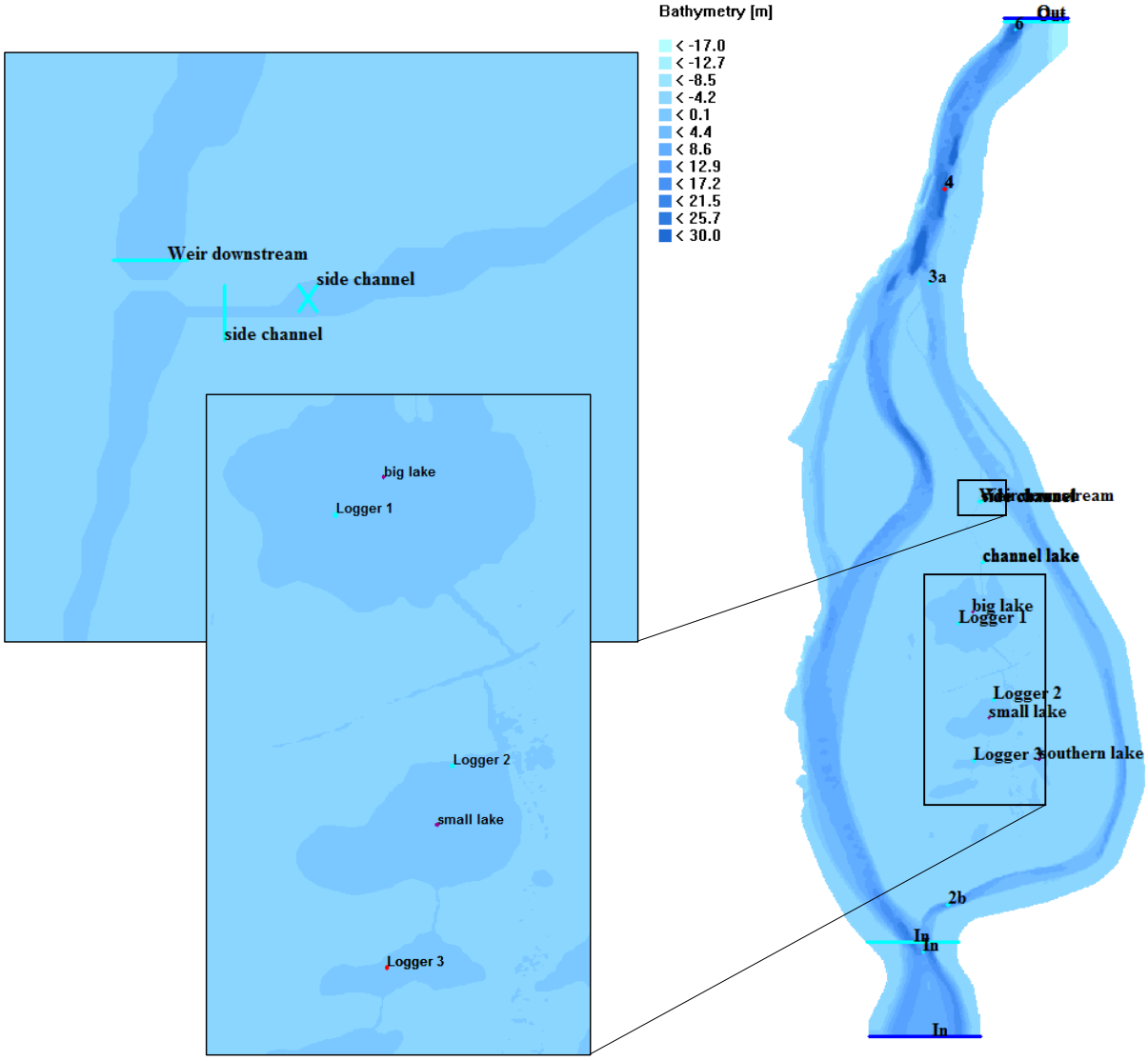

Figure 30. Monitoring of the flow parameters. Position of the observation points and cross sections in model

6 Results and analysis

6.1 Calibration

In order to determine the physical and numerical parameters of the model, the calibration of the model was carried out in a next step. The computed results were compared to the data presented in chapter 4.1 and the main parameters were evaluated. Different numerical and physical parameters were tested, including time-step, roughness, bathymetric data, and turbulent viscosity.

6.1.1 Time-step

The time-step is defined by the Courant number (see chapter 4.3.2). In order to save computational effort, the largest time-step possible is favourable. On the other hand, a maximum Courant number of 10 for most grid cells is suggested by Deltares (2015) to guarantee convergence of the advection term. With this in mind, a final time-step of 0.03 min = 1.8 s was evaluated that fulfils this criterion (cp. Figure 31). With the Courant number being dependent on the grid resolution and the water level, high numbers are computed for small grid sizes and high bottom depth. As a result, the Danube main channel and the lakes on the island show higher Courant numbers. Moreover, the observed "cross-pattern" is created due to the grid cells that were locally refined in these locations. Generally, the evaluated time-step is particularly small and causes high computational cost. This is especially due to the small cell sizes in some parts of the grid. At the same time, larger cell sizes are not suitable for the model due to small channel widths on the island of less than 10 metres. As the hydraulics in the channel are of major interest for the project, the grid requires high computational effort.

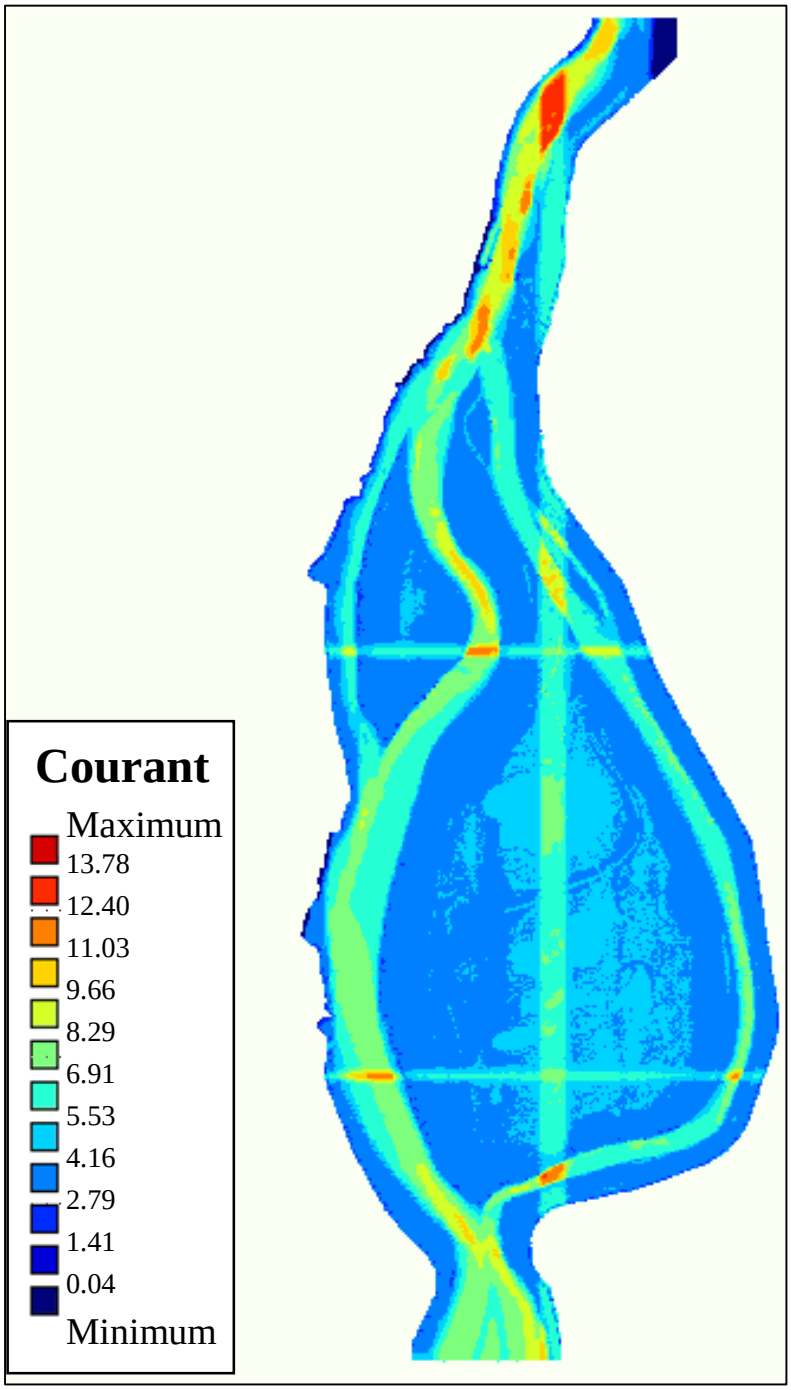

Figure 31. Courant number distributed over the whole domain with a time-step of 1.8 s

6.1.2 Roughness

In a next step, the roughness distribution in the channel had to be investigated. Therefore, first test runs were performed under steady conditions for a mean discharge in the Danube of 5810 m^3/s. For this discharge the main channel is entirely filled while the island is not inundated. The water level inclination for the whole area was defined as 15-30 cm for mean discharges according to literature (Habersack et al., 2014; Zinke et al., 2016). Much stronger inclination was computed which implied excessive roughness values in the main channel. As a result, the

roughness in the channel was lowered gradually from n=0.036 to n=0.01 until plausible water level inclination was reached. This value is extremely small for natural river beds and does not represent realistic conditions. Figure 32 shows the water level distribution in the main channel at the end of calculations over a period of 24 hours between the 14th and 15th of July 2015.

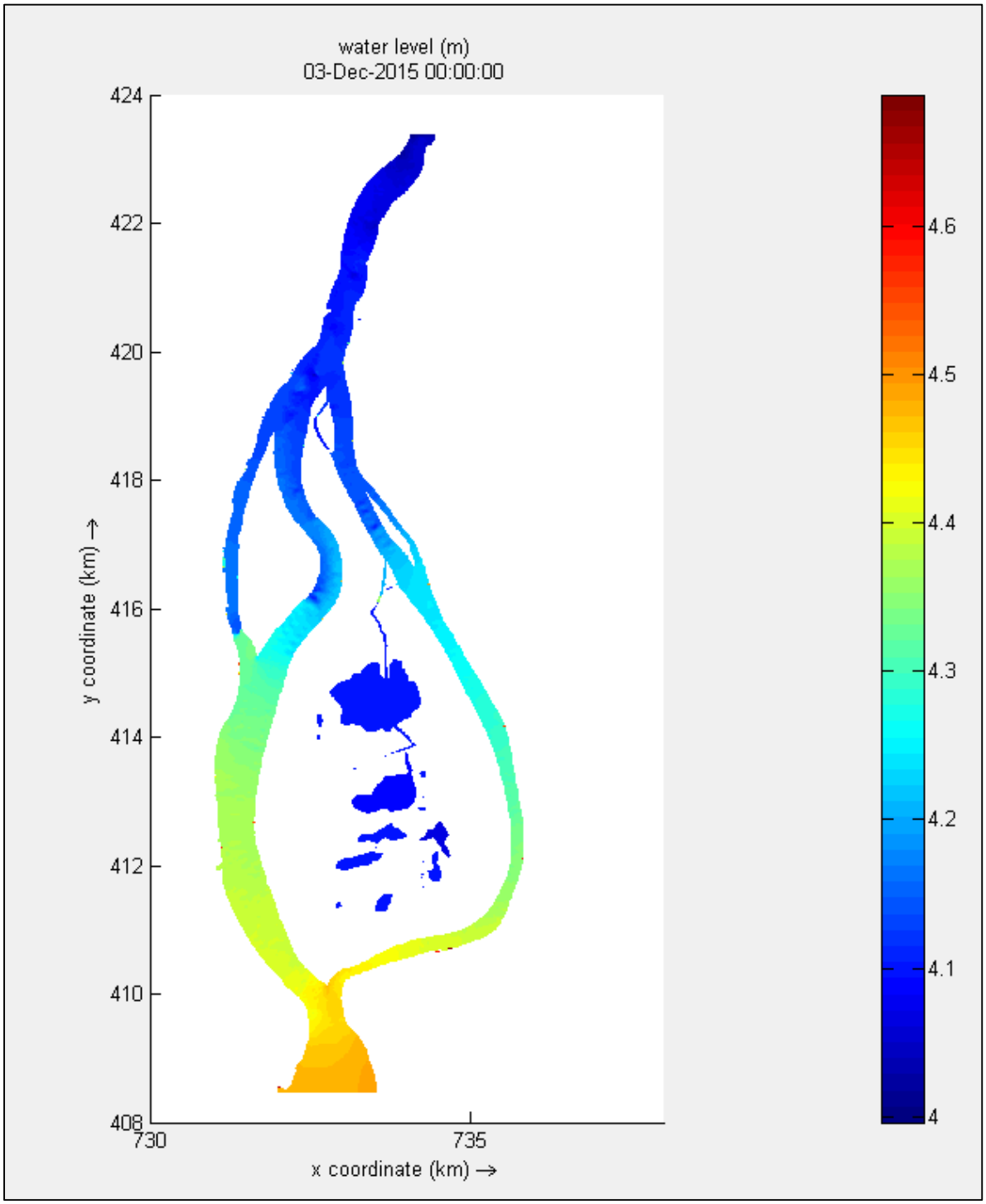

Figure 32. Water level declination over the whole island with Manning's values of 0.01 $s / m^{1/3}$ in the Danube channel. The colours represent the water levels in the Danube channel in metres.

In a next step the roughness on the island was evaluated, by comparing the computed water level values by the model to logger data. Field data measurements revealed water level changes in the lakes of 1-2 cm/day and a discharges in the Hogioaia channel of 650-700 l/s for the one-day-period between the 14th and the 15th of July 2015 (Zinke & Aberle, 2015). These values could not be obtained by the model. To further investigate the response of the model to the bed roughness on the island, low Manning values of 0.01 in the channels and between 0.015-0.15 on the island were implemented. For these values, a response of the hydraulics could be observed. The water levels in the logger points and the discharge in the Hogioaia-channel for the low Manning values are visualised in Figure 33. The water levels of logger 1, which is located closest to the Hogioaia-channel, shows adequate response with a drop of 1.5 cm/day. Logger 2 and 3 recorded a water level difference of less than 1.0 cm over the computed period. Thus, the modification of the roughness produced realistic values in comparison with the recorded logger data. However, the computed discharge in the Hogioaia-channel was below 600 l/s, which is lower than the values provided by the field data.

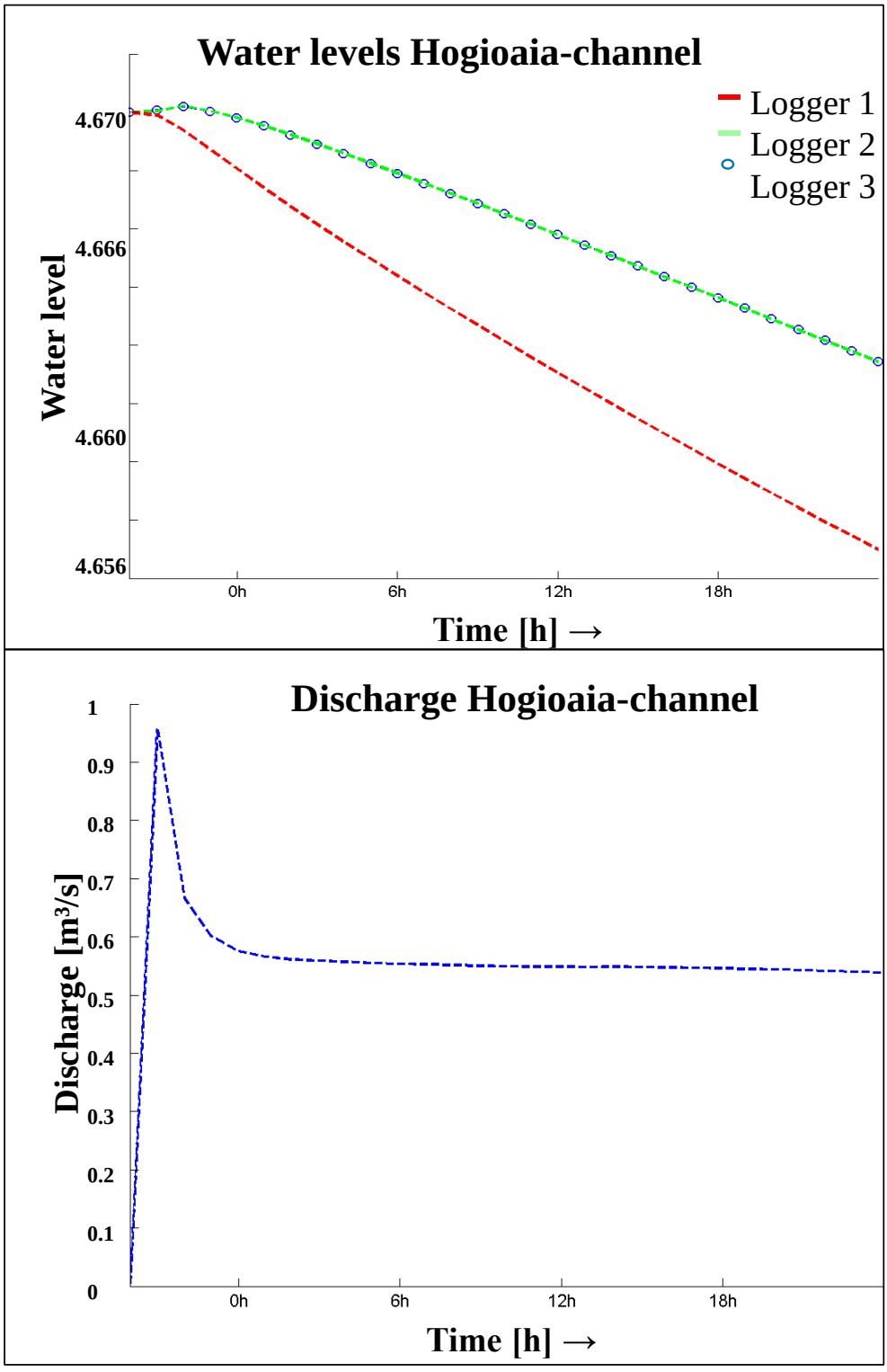

Figure 33. Computed water levels in the logger points and discharge in the Hogioaia-channel during the calibration between the 14th and 15th of July 2015 for small Manning values

In summary, a response to significant changes in roughness by the model could be observed. However, effects on the computational results were insufficient and the modification of the locally uncertain bathymetry was regarded as a suitable approach in the process.

6.1.3 Bathymetry

Due to the insufficient response of the model to roughness variations, the sensitivity with regard to bathymetric changes was investigated. During the model set-up the bathymetry was already optimized to substitute the alterations produced during the interpolation process. In this stage, the channels on the island were again widened and deepened to increase capacity and to reproduce the discharge data of 650 l/s in the Hogioaia-channel. Several combinations were tested but the data values for calibration were not obtained within a reasonable time-frame. It is likely that the grid resolution was too coarse to accurately represent the channels on the island. The implementation of cell sizes of 5 m did not reflect the original depth values. An increase of the channel width over several cells as shown in Figure 34 gave only small response with regard to discharge and water levels on the island. With this measure, the changes were not meeting the expectations, which indicates that higher changes in adjustment of the bathymetry and the numerical grid are required for calibration of the model.

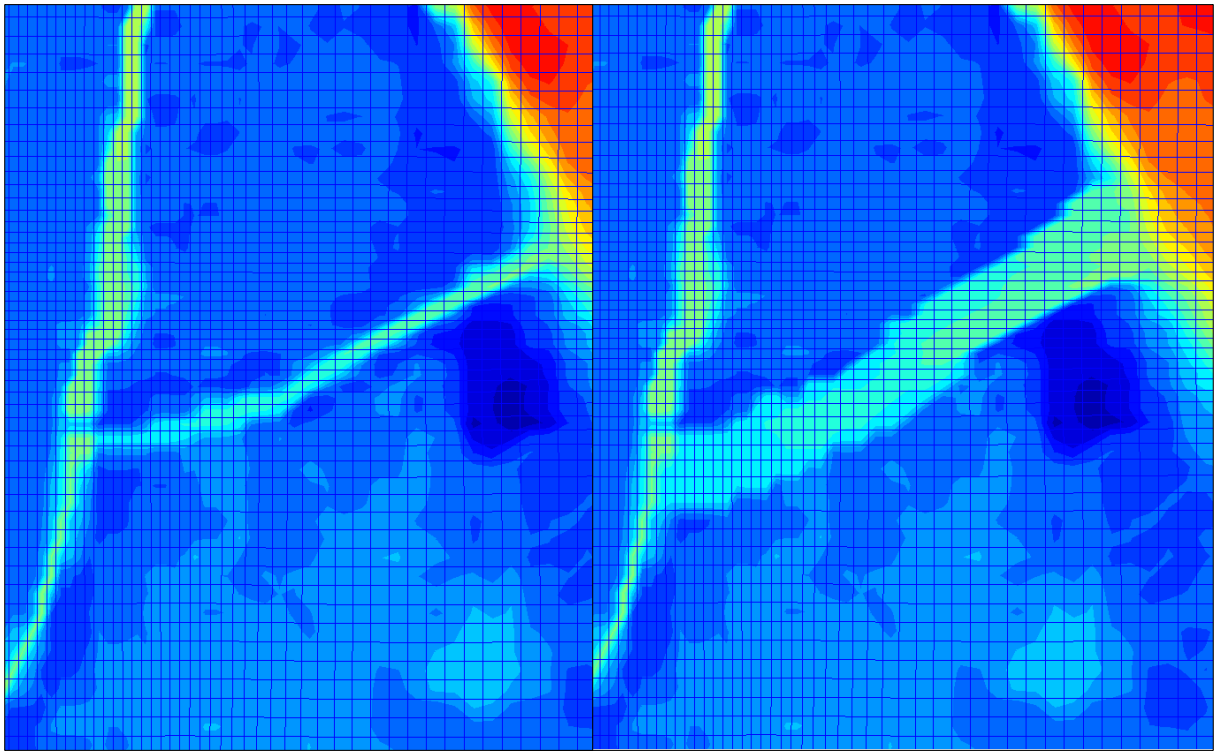

Figure 34. Channel width at the start of the calibration process in comparison with the extremely widened side channel

6.1.4 Eddy viscosity

The horizontal eddy viscosity/diffusivity are suggested by Deltares (2015) as 1-10 m²/s for fine grids of less than several tens of metres. The parameters are so-called calibration parameters and their impact has to be tested to determine the sensitivity of the model. During the calibration process, a value of 5 m²/s was implemented. Some sensitivity tests showed an impact of the eddy viscosity on the results but have not been analysed further due to insufficient calibration of the bathymetry and the roughness.

6.1.5 Summary

The response to changes in bathymetry was significant and shows high importance to improve the bathymetry data prior to further usage of the model. Another key point is the lack of the data of the LIFE-channel in the DEM, which had to be implemented manually within the calibration process. Its bathymetry was taken from maps and photos and includes even higher uncertainties in bed level elevation and geometric dimensions, respectively. However, the effect of the LIFE-channel is estimated as significant during high floods and has to be taken into consideration during computations. In general, it can be suggested that the lack of the LIFE-channel in the original DEM proves the inaccuracy of the bathymetric data. This is probably due to the interpolation within the GIS operator and the process of assigning the depth values to the grid points causing severe changes in the bathymetry. Furthermore, the representation of the channels by the numerical grid was inadequate due to insufficient grid resolution. The tools of RGFGRID were limited with regard to possibilities for local refinement which caused complications during improvement of the grid. A new grid creation would have created unreasonable time effort that was not feasible with regard to the time-frame of the thesis. In addition, it was found out that the period to be simulated, which was originally set to 5 weeks, was not manageable within the time-frame of this work.

In summary, the quality of the provided bathymetry data and the compromise between computational effort and grid resolution did not allow provision of a sufficiently calibrated numerical model of Fundu Mare Island within the given time frame. Due to these restrictions, the adherence of the project schedule was impossible. Thus, another method was selected to fulfil the given task of this work.

6.2 Restoration scenarios

In order to analyse the hydraulic alterations due to different restoration scenarios, a more simplified approach based on the methods described in chapter 2.2.2 has been applied, which can only represent steady conditions. The water levels in Fundu Mare Island were computed in MS Excel, depending on the different hydraulic implementations. All computations are based on the data presented in chapter 4.1. The calculations carried out in MS Excel can be found in Annex C. In order to obtain reasonable results, different assumptions and boundary conditions had to be defined. These were tested during further investigations to analyse plausibility and sensitivity of the results. The evaluated assumptions include the channel geometry, the time-series of water levels in the Danube and the computed water levels.

6.2.1 Approach and assumptions

The general approach to obtain results of the hydraulics in Fundu Mare Island is based on the equations described in chapter 2.2.2. The water balance was calculated with the help of mean monthly values of the precipitation/evaporation, the provided daily ground water loss and the surface runoff in the channels using the Poleni-formula (eq. 2.1) or the Manning's formula (eq. 2.4). The water volume on the island is determined by eq. 2.6. Based on the correlation presented left in Figure 19, the respective water levels are obtained. During all computations

back flowing water over the weir crest due to exceedingly high Danube water levels is neglected.

Generally, the implementation of hydraulic structures in the Hogioaia- and the LIFE-channel were investigated in order to increase the inundation duration on the island. To decrease the number of scenarios, the provisional weir in the Hogioaia channel is removed and the new structure is suggested to be implemented further upstream. The position is defined by the ADCP-measurements in the Hogioaia-channel described in chapter 4.1.2. One advantage of this location are the known channel dimensions at the determined position for water levels below 4.03 MNS. Moreover, the channel is blocked in one single location and no additional structure for damming of the side channel is required. Thus, only combinations including blockage of the Hogioaia-channel and the LIFE-channel have to be evaluated. On the other hand, the option of three different structures and the related higher flexibility can be evaluated during further investigation to optimize the results. A sketch of the location is presented in Figure 35.

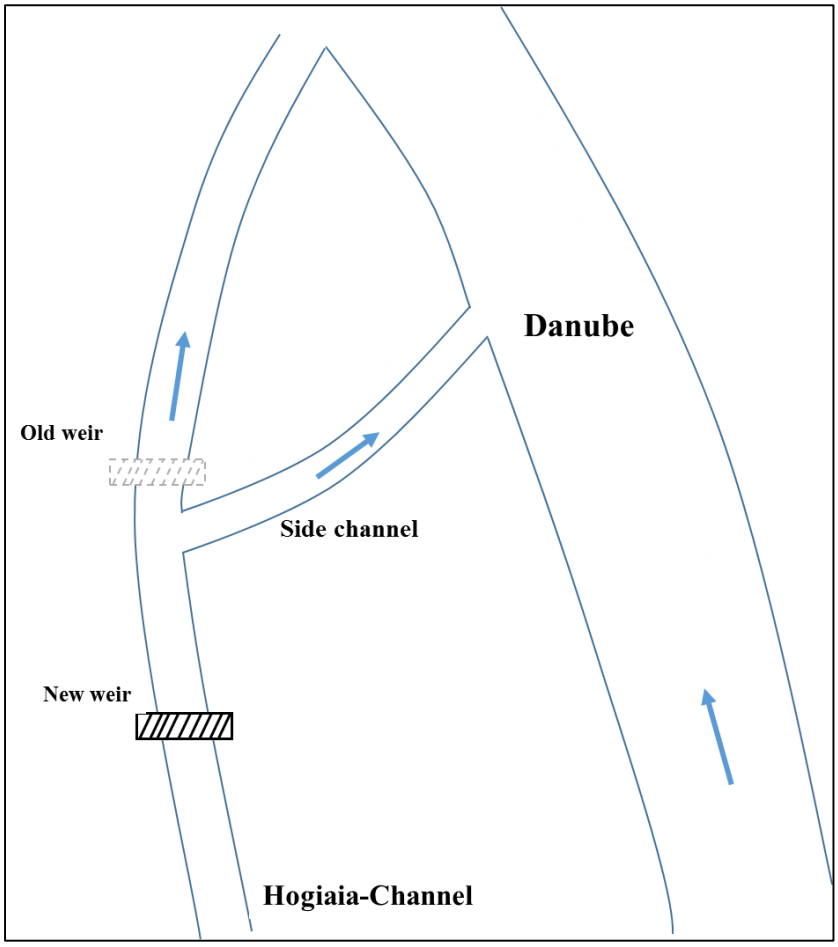

Figure 35. Position of the new hydraulic structure in the Hogioaia-channel

In a first step, the time-frame of the investigations had to be determined. Bearing in mind the hydrographs presented in chapter 4.1.2, the mean water level data between 2000 and 2009 were defined as representative due to an early and particularly high flood wave with a steep gradient in decline. The values indicate first changes of the flooding regime and in water retention on

the island, making it representative for the expected hydrological changes in the future. The mean daily values are visualised in Figure 36 (Zinke & Aberle, 2015). These water levels were determined to represent the time-series for calculations of the weir crest height of the different weir combinations.

Next, the period had to be defined over which the critical water level needs to be guaranteed. To determine the maximum capacity of the island to retain water, the water level that induces overtopping of the levees defines the initial conditions for the calculations. According to chapter 4.1.1, this value was determined to be 5.6 MNS in Brăila. A water level of 5.60 MNS was detected for the 11th of May in the hydrograph for the mean daily values in Brăila and selected as start date (red triangle in Figure 36). The distance between Brăila and the new weir structure is ca. 7.5 km. With regard to the water level inclination estimated to 1.6 cm/km over the island, a difference of 12 centimetres was added to the whole time-series to represent the actual water levels downstream the weir in the Hogioaia-channel. Due to the water level inclination, the initial water level in Fundu Mare Island is determined to be 5.72 MNS.

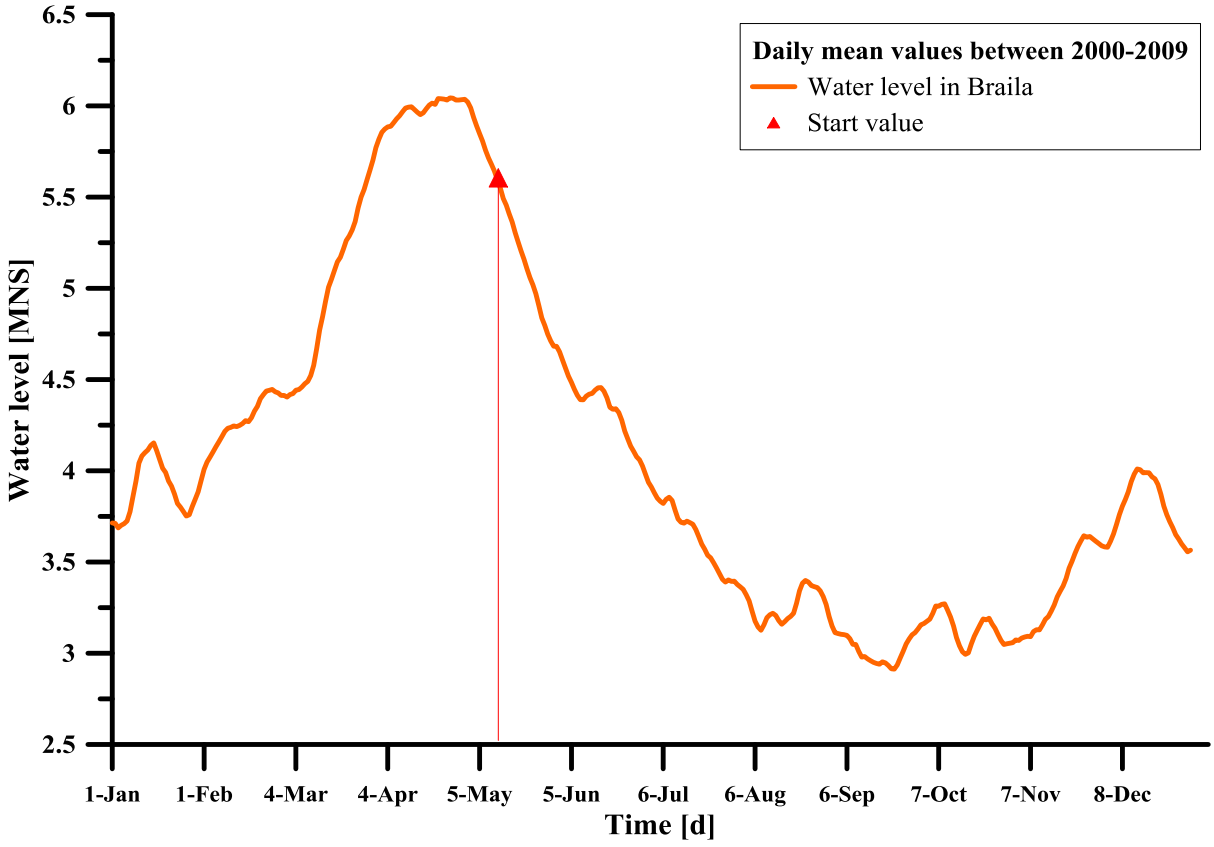

Figure 36. Selected hydrograph for the calculations. The values represent mean daily values of the years between 2000 and 2009 in Brăila. The red dot represents the start value of the computations the 11th of May.

To determine the minimum water level at the end of the computations, two different approaches were investigated. According to Zinke et al. (2016), the critical water level of 4.4-4.8 MNS in Brăila is required for inundation of the lakes. Consequently, the water level of 4.6 MNS was selected to guarantee inundation of large parts of the island. This scenario was seen as essential to guarantee sufficient inundation of the different vegetation zones. As a result, with the island

being flooded during the entire vegetation period, drying of the lakes with increasing growth of willow scrubs is prevented. The vegetation period in Fundu Mare Island was estimated to end in October (Zinke et al., 2016). Consequently, the investigated period was set between the 11th of May and the 31st of October. The objective of this scenario was to guarantee the water level of 4.6 MNS in Brăila until the 31st of October.

As a second approach, the water levels during the decade between 1970 and 1979 were seen as representative before an observation of increased willow scrub growth was recorded (Zinke et al., 2016). Peper et al. (2012) determined an inundation period of 150 days per year for the Upper Danube. This equals 41% exceedance of a specific water level over the entire year. The 41%-exceedance percentile of the mean daily values in Brăila was determined to be 4.52 MNS for the decade 1970 to 1979. This water level was defined as minimum water level during the investigated period. In order to ensure the 150 days of inundation, the relevant period was determined from the 11th of May until the 3rd of October. A possible inundation during winter is therefore neglected. In summary, this scenario guarantees a water level of 4.52 MNS in Brăila until the 3rd of October.

Figure 37 visualises the different water levels as a duration curve. The graph shows the mean daily values for the investigated decades. The green line defines the critical water level of 4.6 MNS, in the following referred to as Scenario 1 (S1). The red arrow represents the 41%-exceedance percentile of decade 1970-79, in the following referred to as Scenario 2 (S2). The 41%-exceedance percentile for the period between 2000 and 2009 is detected with 4.05 MNS (blue arrow), showing a water level difference compared to S1 of 0.55 m and to S2 of 0.47 m.

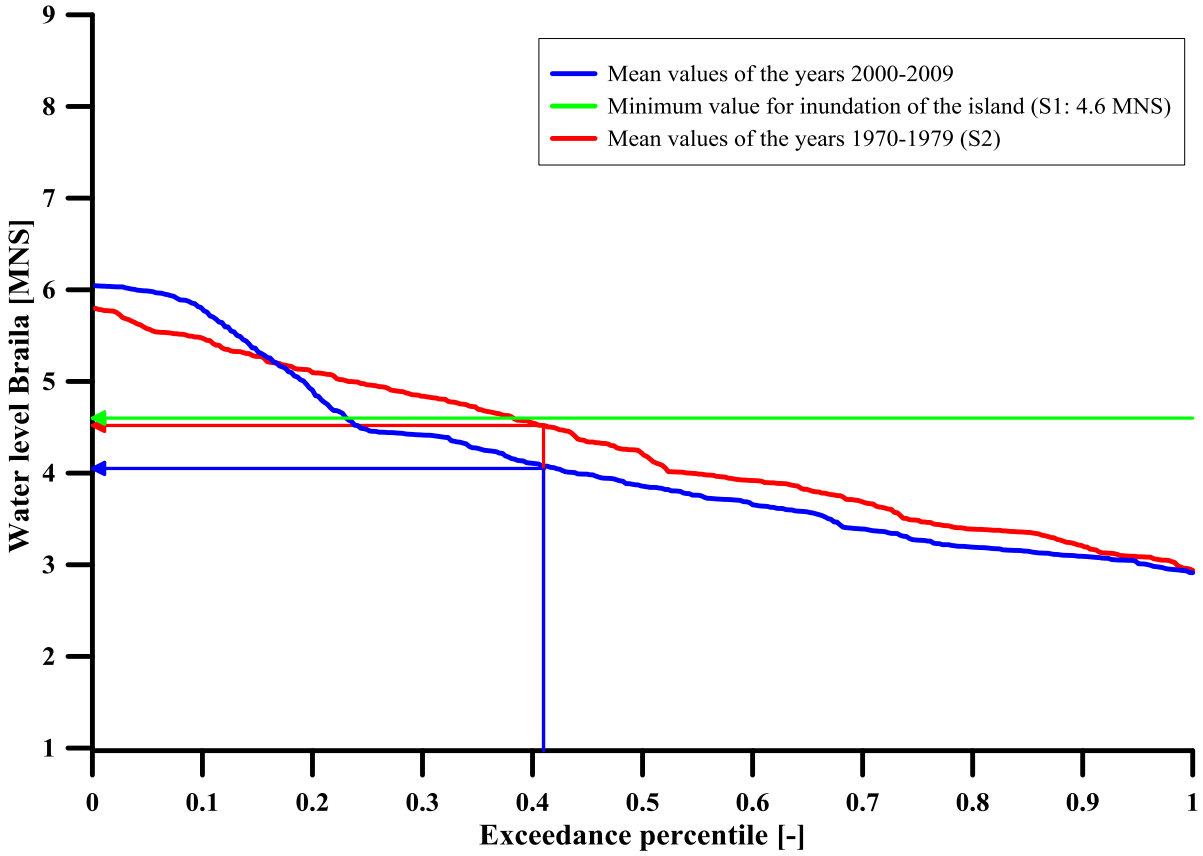

Figure 37. Determined minimum value for inundation of the island. 41%-exceedance percentile of the recorded water levels in Brăila from 2000-2009 (blue graph), 41%-exceedance percentile for the decade between 1970-1979 (red graph), critical water level of 4.6 MNS (green graph)

In order to determine the water levels in Fundu Mare Island, the water level gradient must be considered. A minimum water level in Fundu Mare Island of 4.72 MNS for S1 is determined. For S2 the required water level is 4.64 MNS. The objective of the calculations is to find hydraulic implementations that guarantee the two minimum water levels in Fundu Mare Island for the two different periods of time.

6.2.2 Geometric considerations

Due to uncertainties regarding the cross section of the channels for higher water levels, the dimensions of the weirs were determined to be rectangular (cp. Figure 38). The weir crest width L_W of the Hogioaia-channel was determined to 8 metres between the piers, which represents an intermediate value between the known minimum river width of 4.2 metres and the width of 10.4 metres for a water depth of 1.63 metres (cp. Figure 15). The width of the LIFE-channel was set to 2 metres. The maximum cross sectional area is defined by the initial water level of 5.72 MNS with the bed elevation 3.8 MNS subtracted. Consequently, the maximum cross sectional area is determined by a water depth in the LIFE-channel of 1.92 m. A straight weir design with an angle of 90° in the vertical is defined. During computations, the weir crest heights p for the two scenarios were evaluated.

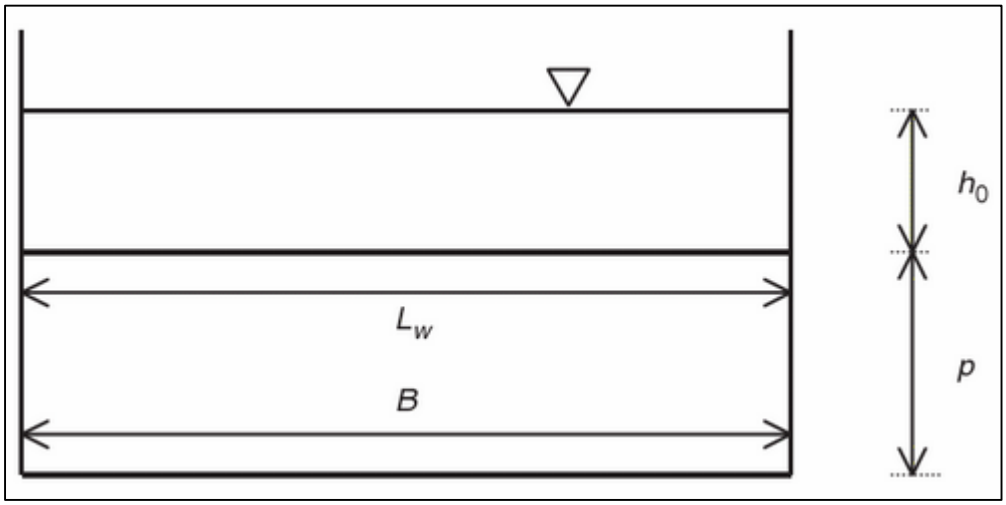

Figure 38. Dimensions of the channel cross section with h_0 the overfall height and p the weir height. The weir crest width equals the river width (Akan, 2006)

Manning's equation was applied to analyse the capacity of the channels (see eq. 2.4). According to Chow (1959), for straight natural rivers with weeds and stones n is determined to be $0.025\ s/m^{1/3}$. For winding rivers with the same properties n is $0.045\ s/m^{1/3}$. It is assumed that the overflow over the weir crest cannot exceed the channel capacity computed with the Manning's formula. Therefore, during the calculations the results of both formulas were compared and in case of a higher overflow rate, the Manning's formula restricts the weir overflow. As the bottom slope is unknown, the water level gradient was implemented for I_b.

To investigate the plausibility of the geometric assumptions of the Hogioaia-channel, the discharges over the weir crest were examined closely. Figure 39 shows the discharges in the Hogioaia-channel in combination with a closed LIFE-channel. The discharge over the different weir crest types is visualised. Additionally, the capacity of the channel calculated by Manning's formula is visualised in the same figure (orange graph). The increase of the overflow at the start of the calculations is explained by the impact of the factor σ_{id} representing the tailwater in the Poleni-formula. The dependency of σ_{id} on the ratio between up- and downstream water level significantly reduces the overflowing discharge for high water levels. A comparison of the discharges over the weir crest with the calculated capacity shows that the overflow for the different weir types remains below the maximum capacity of the channel. Only the discharge over the bag weir, which is not restricted by the influence of tailwater, is limited by the channel capacity.

It can be concluded that the calculated discharges over the weir crests are appropriate as they are not restricted by the Manning's formula. Consequently, it can be stated that the geometric assumptions are plausible. However, it has to be borne in mind that the channel geometry of the Hogioaia-channel is only known for discharges below 1.63 m. For high water levels the cross section may vary. In this case, the channel's capacity is overestimated for high discharges, leading to a smaller weir crest height in reality.

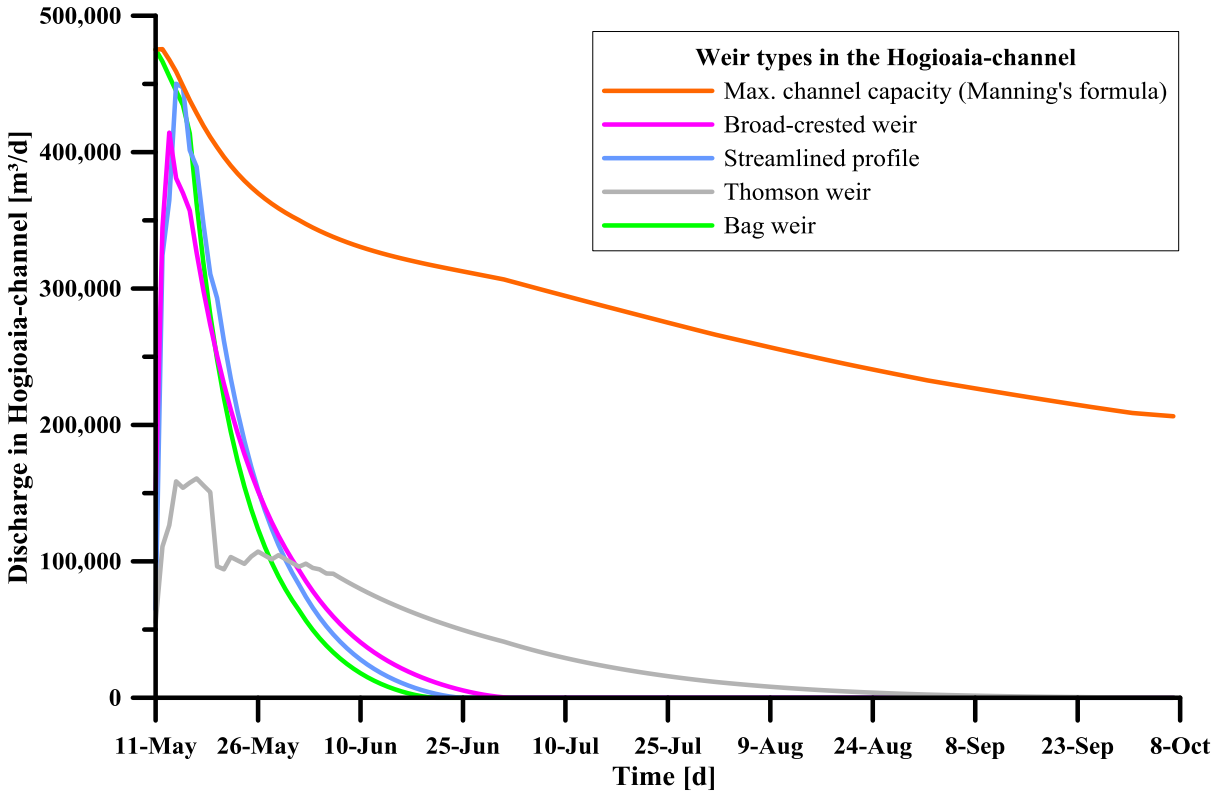

Figure 39. Validation of the geometric specifications with Manning's formula for the capacity of the Hogioaia-channel. Example with a closed LIFE-channel.

6.2.3 Investigation of the weir crest heights

In a first step, the two variations “non-dammed” and “fully dammed” for the Hogioaia- and the LIFE-channel, respectively, were compared to get an idea of the maximum dimensions of the water loss and water retention due to the discharge in the channels. Figure 40 shows the water levels in the Danube River compared to the water levels in Fundu Mare Island for mean daily values of 2000-2009 for the vegetation period after the spring flood. The water levels are determined by the storage volume on the island, which was obtained by the water balance approach presented in chapter 2.2.2.

For the majority of the days, the water levels on the island are higher than the Danube water level, indicating natural water retention. The red line shows the results for both channels fully dammed, which represents the water loss due to evaporation and leaching. This guarantees water levels of more than 5.0 MNS and therefore an exceedance of the required minimum water levels. The blue graph shows the estimated water levels on the island determined by the storage-water level relation from chapter 4.1.2. It is important to note that this relation is based on data recorded in 2015. It can be seen that the water levels on the island drop below the required minimum water levels down to 3.0 MNS in the beginning of August. To show the effect on the inundation of Fundu Mare Island by this relation, the percentage of dried surface on the island compared to the inundated area with the initial water level of 5.72 MNS is computed (light green graph). It can be stated that a drying of the lakes on the island occurs at the end of

September. Consequently, the damming of the channels is useful to control the water levels in Fundu Mare Island.

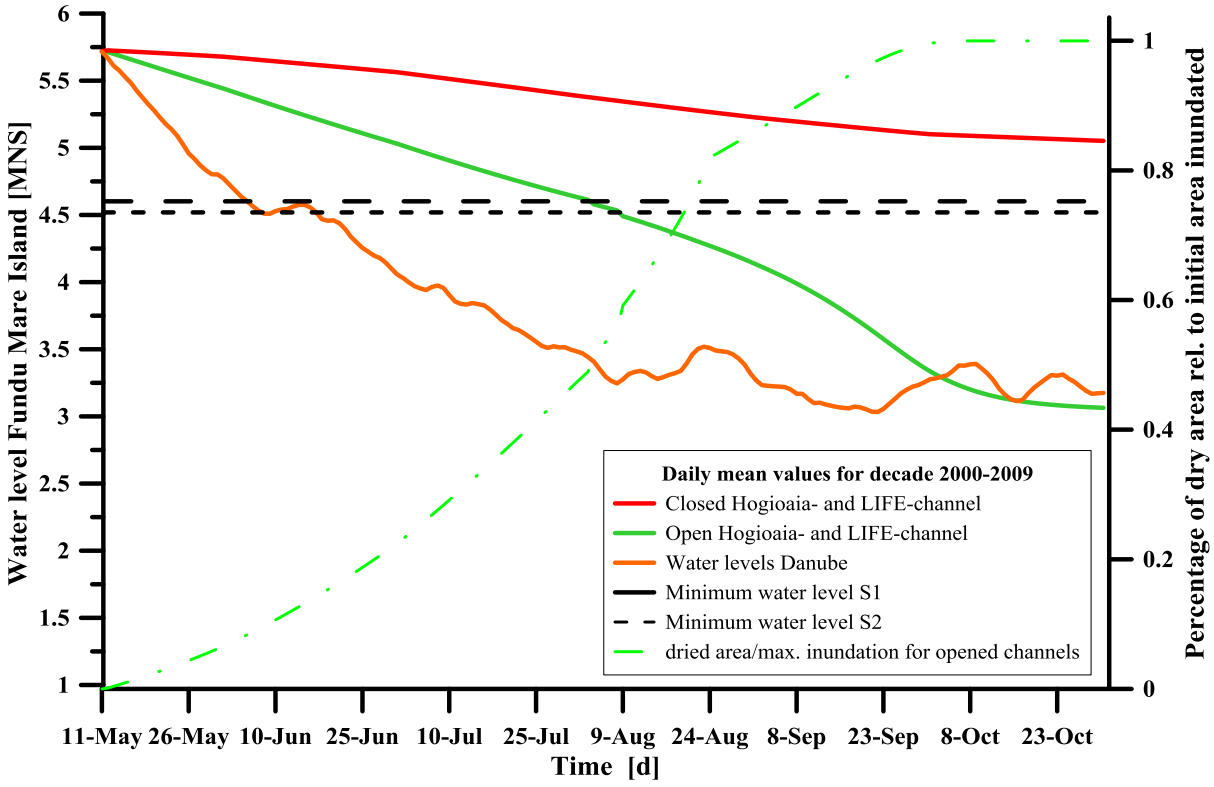

Figure 40. Comparison of fully dammed (red graph) and fully opened channels (green graphs) in Fundu Mare Island.

During the computations a broad-crested weir, a streamlined profile, a Thomson weir and a bag weir were analysed. Despite its definition as measurement weir, in this work the Thomson weir is representative for discharges over an inconstant overflow width. Due to the high variability of the bag weir, an investigation of its dimensions gives a high range of options that is outside the scope of this study. As a simplification, also for the bag weir a fixed minimum weir height is determined.

The Poleni-formula (eq. 2.1) was applied to determine the surface discharges of the different weir structures with the corresponding discharge coefficients. The broad-crested weir was defined by a coefficient of 0.5, the streamlined profile by 0.7, the Thomson weir by 0.64, and the bag weir by 0.8. The effect of the tailwater level on the backwater in the Danube was considered for the first 3 weir types. For the bag weir the tailwater height was neglected, due to lack of reliable approaches. The effect of the LIFE-channel was evaluated for three percentages of blockage with regard to the entire cross section: fully dammed (levee), 80%- dammed and 70%-dammed (broad-crested weir respectively). 10% of blockage is equal to 20 cm difference in weir crest height in the LIFE-channel. For the different combinations, the weir heights in the Hogioaia-channel were evaluated, which guarantee the minimum water levels.

The investigated combinations can be found in Table 1. The column numbers 1-4 describe the different weir types in the Hogioaia-channel. The rows 1-3 determine the percentage of

blockage of the LIFE-channel. The blockage in the LIFE-channel is calculated with the assumption of a broad-crested weir. Additionally, the implementation of a rock-filled slide in the LIFE-channel is tested to evaluate a more natural-oriented approach.

Table 1. Investigated combinations of hydraulic structures

Weir types Hogioaia: / **Blockage LIFE**	**1** Broad-crested weir	**2** Streamlined profile	**3** Thomson weir	**4** Bag weir
1 fully dammed	1-1	2-1	3-1	4-1
2 broad-crested weir (80% dammed)	1-2	2-2	3-2	4-2
3 broad-crested weir (70% dammed)	1-3	2-3	3-3	4-3

For the investigation of the weir crest heights, the determined scenarios were applied for the above combinations. First, the implementation of a minimum water level over the vegetation period after the spring flood was evaluated (S1). In a second step, the creation of the conditions of the decade between the years 1970 and 1979 for 150 days was achieved (S2). As a first step, for both scenarios the minimum required blockage of the LIFE-channel was determined and compared to the maximum cross section.

Scenario 1 (S1): Minimum water level over vegetation period

In order to analyse the minimum blockage of the LIFE-channel to guarantee the water level of 4.72 MNS, a fully blocked Hogioaia-channel was assumed. The minimum weir height was determined to 1.28 m, which is equal to 65% of blockage of the maximum cross section. For the bottom slide, a stone diameter of 0.86 m with 2 stones is required. In general, the implementation of two stones for a slide is not regarded as realistic and this option is neglected.

When comparing the different weir types, only minor changes in weir crest height could be observed (cp. Table 2).

Table 2. Results of the weir crest heights for Scenario 1

Weir types Hogioaia: / **Blockage LIFE**	**1** Broad-crested weir	**2** Streamlined profile	**3** Thomson weir	**4** Bag weir
1 fully dammed	2.90 m	2.93 m	2.41 m	2.95 m
2 broad-crested weir (80% dammed)	2.92 m	2.96 m	2.45 m	2.96 m
3 broad-crested weir (70% dammed)	3.05 m	3.10 m	2.62 m	3.13 m

For all weir types, a fully dammed and an 80%-dammed cross section show minor differences. Only for a smaller percentage of blockage (70%), the weir crest heights decrease notably by 10-20 cm. This indicates a non-linear correlation between the blockage of the LIFE-channel and the weir heights in the Hogioaia-channel. Increase of the opening of the LIFE-channel is not feasible, due to a minimum blockage of 65%. However, with regard to a decrease of weir height in the LIFE channel with 20 cm/10%, the decrease in the Hogioaia-channel is lower due to a larger width of the crest. Due to an increasing discharge coefficient between broad-crested weir, streamlined profile and bag weir, the weir crest heights between the types increase by a few centimetres. Significant changes between the different types are not observed. The Thomson weir is determined by a total weir height of the maximum water level of 5.72 MNS minus the bed elevation at 2.40 MNS. The angle of the triangle is 90 degrees. The weir height under the weir crest is between 2.40 m and 2.62 m. Different behaviour of the heights due to an inconstant weir crest width is not recorded.

To analyse the reasons for the small variations in height especially for higher weir crests, the water level changes of the different weir crest types are presented in Figure 41. The discharge in the channel shows variations only for high water levels. In fact, the discharge over the broad-crested weir and the streamlined profile becomes zero in the end of June for all LIFE-channel variations. Only the Thomson weir guarantees overflow until the end of September. This effect is represented by the trend changes of the graphs. As a result, a high effect of the evaporation and the ground water loss in the area is concluded, which can partly be compensated by the implementation of weirs. It is noticeable that the broad-crested weir, the streamlined profile and the bag weir show a strong effect on water level changes compared to the Thomson weir. This

can be explained by the inconstant width of the weir crest due to the triangular shape. With a more linear discharge over the Thomson weir's crest, the water levels are less controlled by the atmospheric influences and leaching towards the end of the vegetation period, which allows more control of the water levels by the weir.

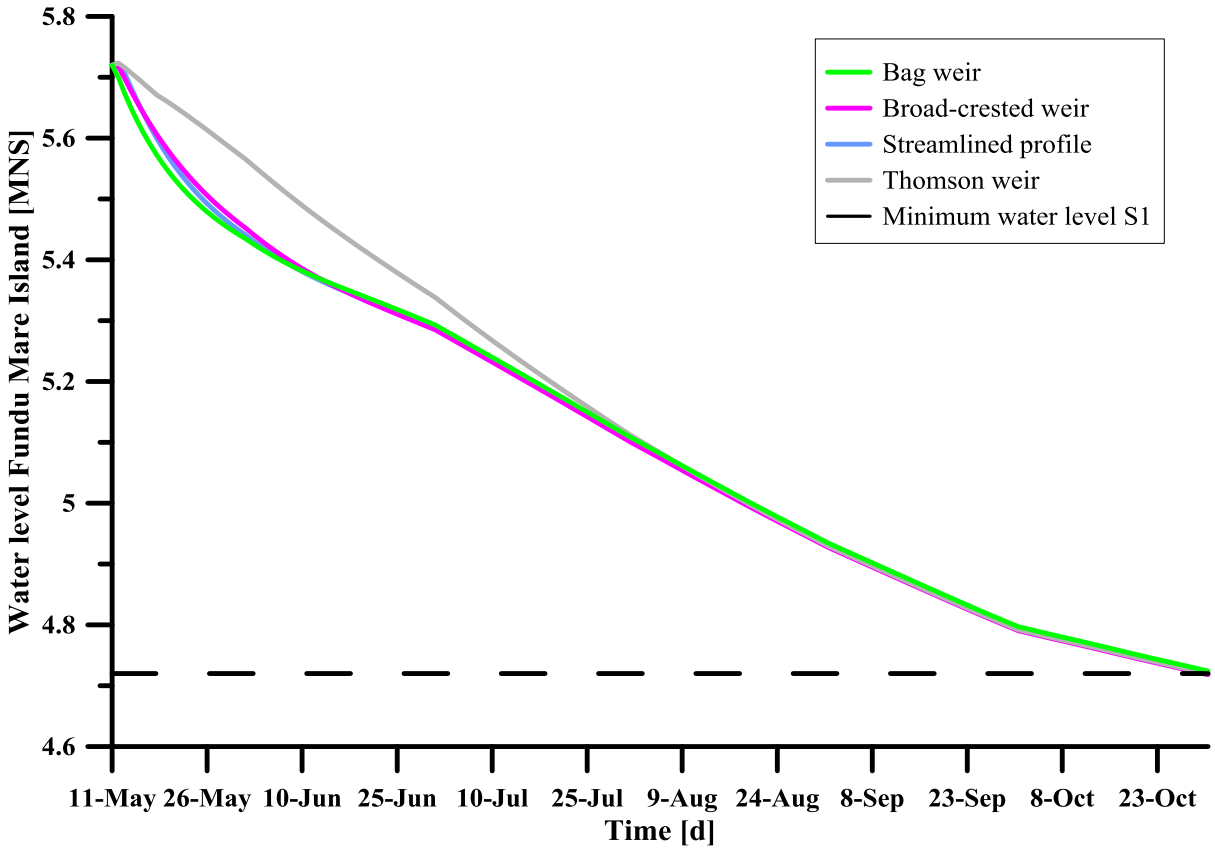

Figure 41. Comparison of the water level changes over the different weir types for a closed LIFE-channel for S1

To quantify the impact of evaporation and leaching, a comparison with surface runoff is displayed in Figure 42 by an example of a broad-crested weir. The total water loss induced by the surface runoff is smaller than the loss by evaporation and ground water. It has to be borne in mind that the evaporation is characterised by mean monthly values and depends on the inundated area. This causes the particular course of the graph (dark blue). Furthermore, after the end of June the surface runoff becomes zero. As a result, during the last months of the vegetation period the water levels are controlled by evaporation and leaching. Consequently, the graphs support the assumption that the evaporation has a strong influence on the water balance in the reach.

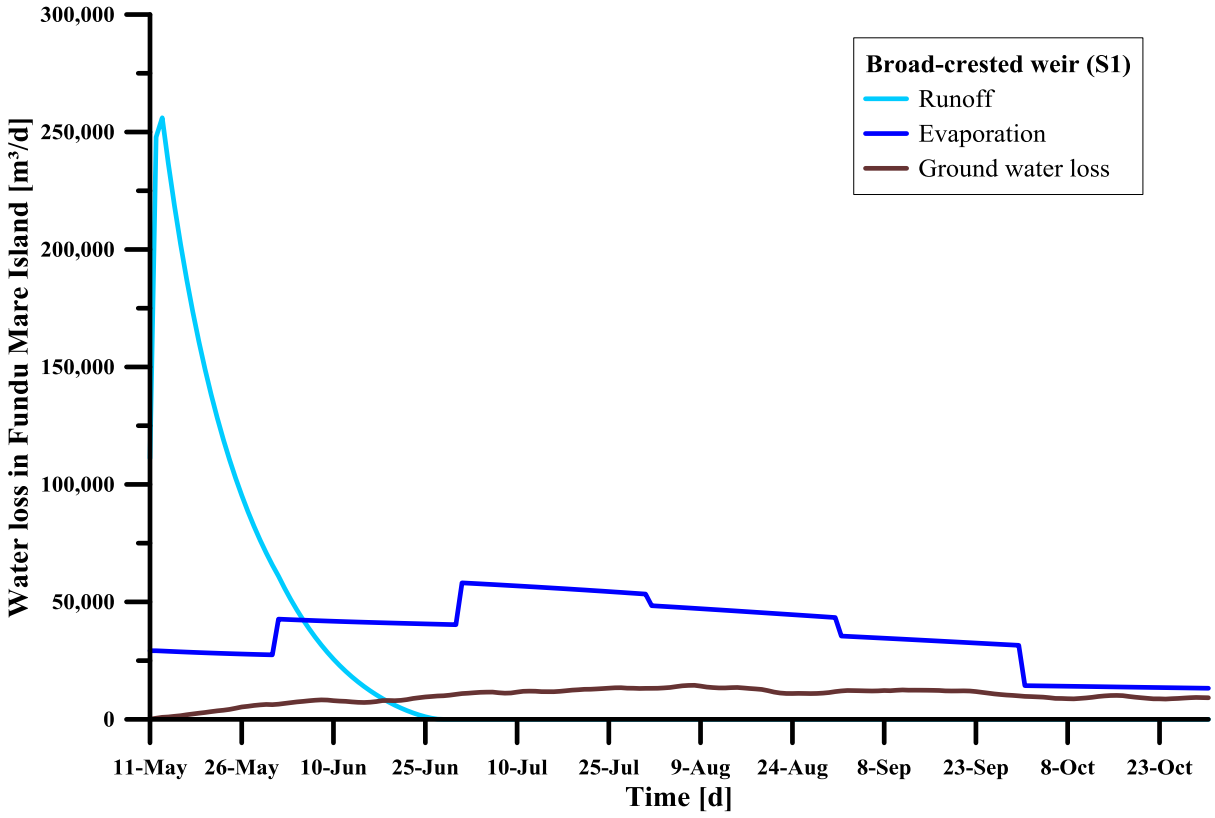

Figure 42. Comparison of the impacts of evaporation and ground water loss on the water levels in Fundu Mare Island for a closed LIFE-channel

Scenario 2 (S2): Minimum water level according to the years 1970-1979

S2 establishes a water level of 4.64 MNS for 150 days, which was found for the decade between 1970 and 1979. The minimum dam height for the LIFE-channel was determined to be 0.88 m, which represents a blockage of 45% of the maximum water depth. A bottom slide is applicable with a stone diameter of 0.31 m when at least 6 stones are installed. This is a realistic approach, but unfeasible with regard to theft and vandalism. The construction must guarantee fixed positioning of the stones. Furthermore, it has to be borne in mind that only one of many approaches was applied to determine the discharge on the slide. A validation by newer approaches is recommended to carefully analyse the feasibility of a bottom slide. Therefore, the construction of the bottom slide is neglected for the project.

The required weir heights for S2 are summarised in Table 3.

Table 3. Results of the weir crest heights for Scenario 2

Weir types Hogioaia: / **Blockage LIFE**	**1** Broad-crested weir	**2** Streamlined profile	**3** Thomson weir	**4** Bag weir
1 fully dammed	2.70 m	2.73 m	2.18 m	2.75 m
2 broad-crested weir (80% dammed)	2.71 m	2.74 m	2.19 m	2.75 m
3 broad-crested weir (70% dammed)	2.73 m	2.75 m	2.23 m	2.76 m

For S2, the variations show insignificant differences in weir crest height when the percentage of the blockage of the LIFE-channel decreases. For the different weir crest types, the heights vary insignificantly. It is indicated that the dependence of the discharge over the weirs in the Hogioaia-channel decreases with decreasing minimum water level. Due to a smaller required minimum water level, the weir crest heights are about 20-30 centimetres smaller compared to the results obtained in the first scenario.

Figure 43 displays the different weir types with the example of a closed LIFE-channel. Again, the surface flow in the channel shows variations only for high water levels. The discharge over the broad-crested weir, the bag weir and the streamlined profile becomes zero at the end of June for all LIFE-channel variations. The Thomson weir guarantees overflow until October. It is noticeable that the two scenarios do not show significant differences in water retention on the island. The influence of the evaporation and the leaching compared to the surface runoff is high in both scenarios.

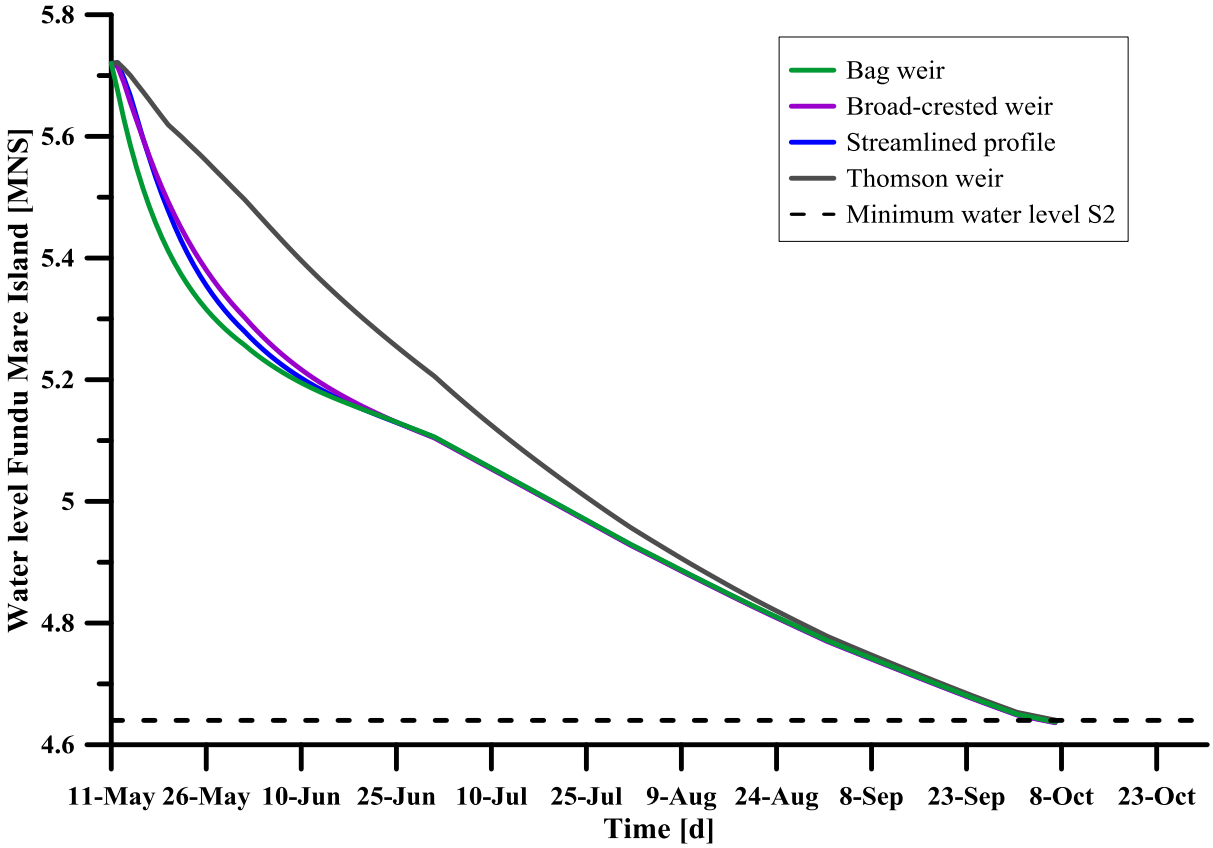

Figure 43. Comparison of the water level changes over the different weir types for a closed LIFE-channel for S2

Summary

In summary it can be stated that the differences in crest height between the weir types are minor. For high percentages in blockage of the cross sectional area within the LIFE-channel this percentage is not crucial for a difference in weir height in the Hogioaia-channel. With reduced blockage the weir crest heights increase by more than a decimetre.

The LIFE-channel

Damming of the LIFE-channel by different percentages shows small effects on the weir crest heights in the Hogioaia-channel, especially for small minimum water levels. As a result, to save installation and maintenance costs, a closing of the LIFE-channel is recommended. In that case, e.g. a levee can be constructed of sufficient dimensions equal to the surrounding levees to prevent water outflow during the investigated period. The whole surface flow will then be drained through the Hogioaia-channel and can be easily controlled by one weir installation.

The Hogioaia-channel

Overall, due to the small differences for the weir types, the selection of the weir type was made according to its properties. The installation of a Thomson weir is dismissed due to the requirement of a metal plate to guarantee the free and aerated overflow. This construction causes a high risk of deconstruction by theft or vandalism. Furthermore, the weir is generally used as a measurement weir. A Thomson weir made of other material can be considered, but

may imply different properties of discharge if e.g. aeration is not given. In general, it can be noted that a weir crest with inconstant overfall can be favourable in terms of higher discharge control. The streamlined profile is generally favourable in cases of drainage of high discharges due to its high discharge coefficient. For Fundu Mare Island the drainage of floods is a minor issue, whereas stabilisation of the water table is the main purpose. As a result, the weir crest heights are smaller for broad-crested weirs to achieve the same water level. That makes its installation less costly and favourable for the project. Moreover, the installation of a bag weir seems reasonable due to flexible regulation of the flow, possible navigation over the weir and low maintenance cost. In spite of its larger weir crest heights, the possibility of flow regulation gives many advantages especially with regard to variations of flow scenarios.

Due to the above reasons, the LIFE-channel is recommended to be closed. The broad-crested weir and the bag weir are selected for a more detailed study. In order to investigate the sensibility of the determined weirs, their functionality is tested for two extreme events, a dry and a rainy year.

6.2.4 Extreme conditions

To analyse the sensitivity of the evaluated weir heights, two yearly time-series from the investigated decade were implemented to test the weir's response under extreme conditions. The bag weir and the broad-crested weir were evaluated. A total blockage of the LIFE-channel was defined. The year 2003 was selected as an extremely dry year while 2005 represents a humid year. It has to be pointed out that the probability of the occurrence of such events is low. However, the events were selected to analyse the reaction on the water levels in Fundu Mare Island. The changes of the water levels were investigated in dependency of the water levels in the Danube. The parameter regarded as representative is the water level at the end of the vegetation period on the 31st of October. The effect on changes in vegetation is of main interest, having in mind 41%-exceedance percentile.

Figure 44 shows the effect of a dry year on the water levels in Fundu Mare Island. The initial water level of 5.66 MNS in Brăila is already observed in January, defining the beginning of the investigated period. The water level inclination is considered with 0.12 m. The bag weir (green graph) and the broad-crested weir (pink graph) were examined for the above scenarios and the determined weir crest heights. As a result, both scenarios cause a drop of the water levels below the required minimum water level, for S1 at the end of July and for S2 at the end of August. It is important to note that the surface discharge in the channels becomes zero at about the beginning of April. Consequently, the evaporation and the ground water loss induce the major water loss on the island between April and October. Due to the importance of evaporation and leaching, the weir scenarios give similar results. Consequently, it can be stated that for dry years, the water level during the vegetation period do not comply with the requirement of a minimum water level. The weir crest heights need to be increased.

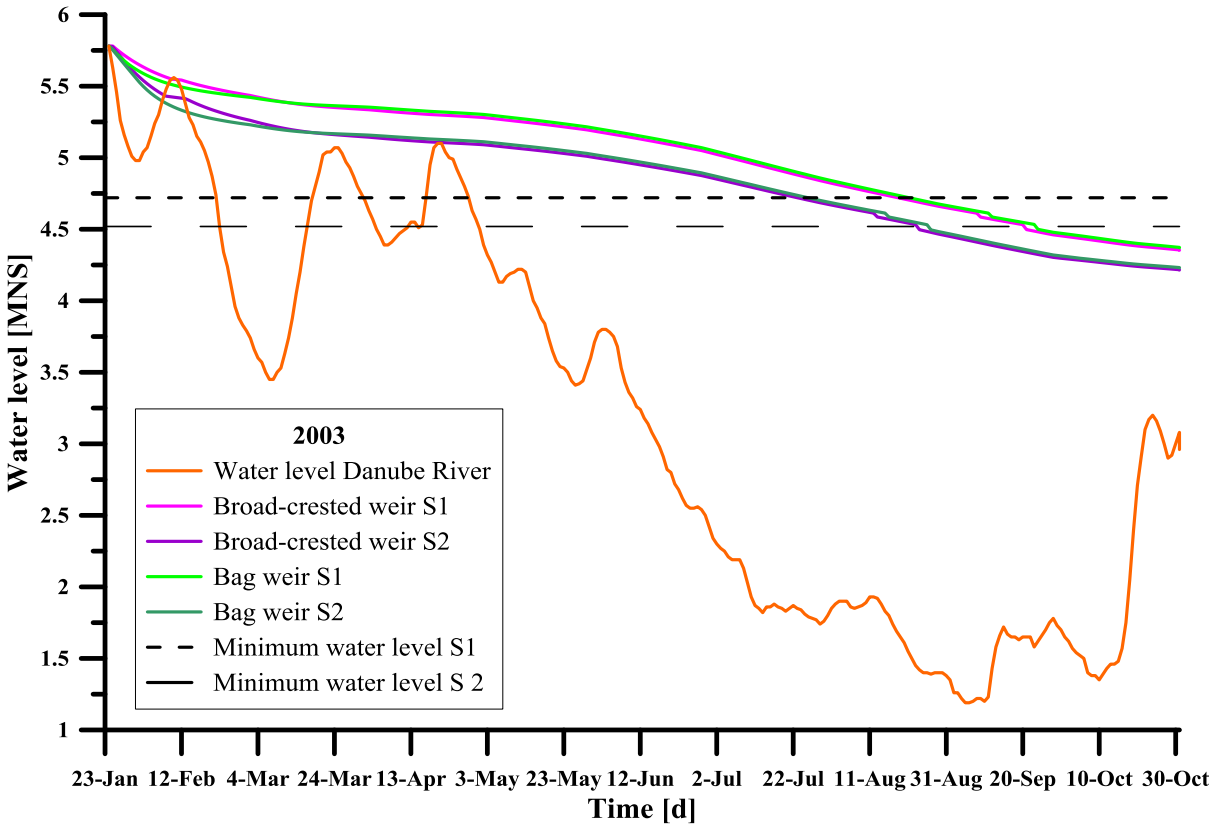

Figure 44. Water levels for the bag and broad-crested weir for both scenarios for daily values in 2003

In Figure 45 the inundation of the island with the water levels determined during the computations for 2003 is displayed for S1 and S2, respectively. Between the scenarios a difference of 15 cm is recorded. On the map small changes in inundation area on the island can be observed, indicating a high sensitivity to small water level changes for shallow water depths in the lakes. The lakes will fall dry when the water level falls below 3.32 MNS in the Danube close to the weir. This level is only 0.5-0.7 m below the calculated minimum water levels, indicating a risk of drying of the wetland. On the long term, a decrease in inundation area and days will cause an effect on biodiversity.

Figure 45. Inundation map of the dry year 2003. Left: S1, right: S2.

Figure 46 presents a humid year and the response of the water levels to the investigated weir heights. In this scenario the increase of the water levels and of the inundation period in Fundu Mare Island is studied. The opposed flow in direction of the island is neglected. For the water levels recorded in 2005, the initial water level at the start of the computations was detected on 23rd of June with 5.53 MNS in Brăila. The water level gradient of 0.12 m was added. Although this value had been exceeded in August and September, the investigation of a large part of the vegetation period was desirable and led to the decision for the examined period. The resulting water levels are significantly higher than the minimum water levels. With regard to a neglected backflow into the lakes, this result shows high sensitivity of the water levels in Fundu Mare Island to hydrological events.

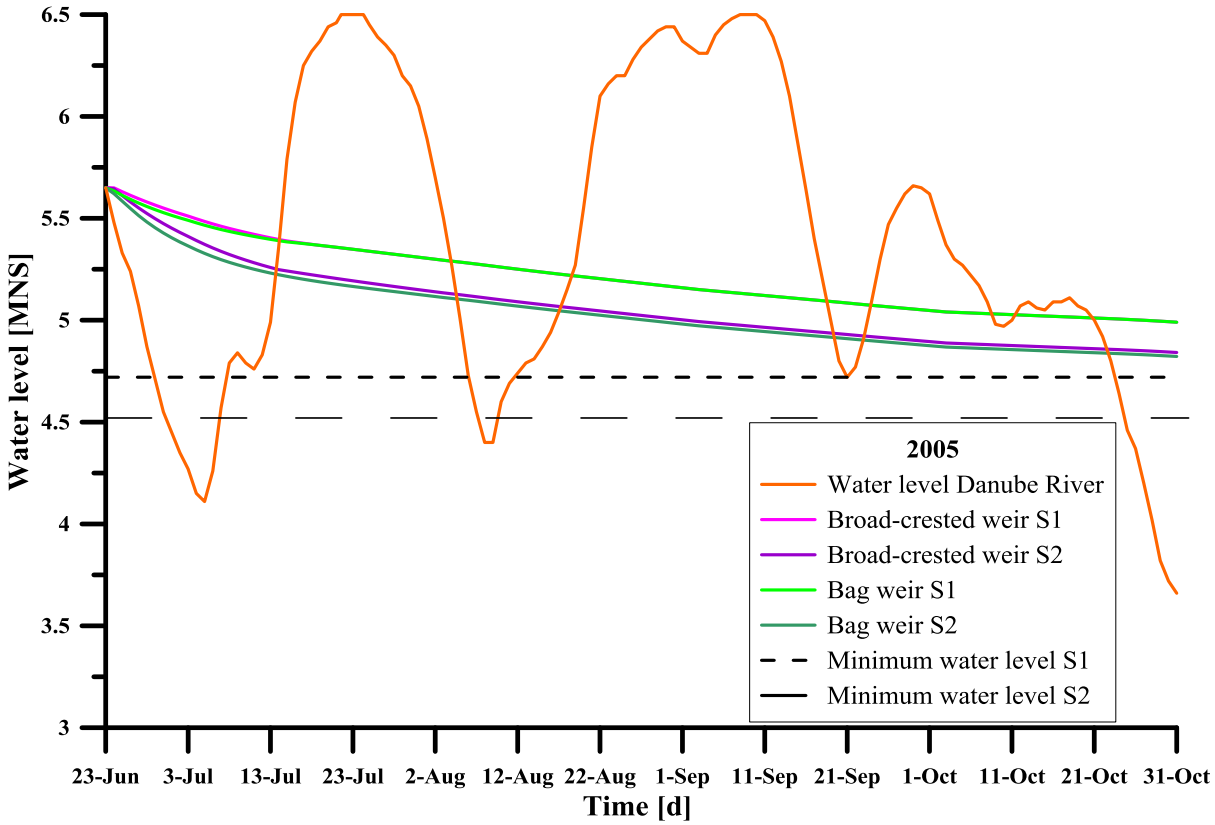

Figure 46. Water levels for the bag and broad-crested weir for both scenarios with the time-series of 2005

Figure 47 shows the respective inundation of the area at the end of the computations for 2005. Large areas are flooded for both scenarios, which leads to an inundation of an area including parts of the hardwood. Consequently, changes in vegetation can be provoked and the nesting areas for birds and animal species can be affected.

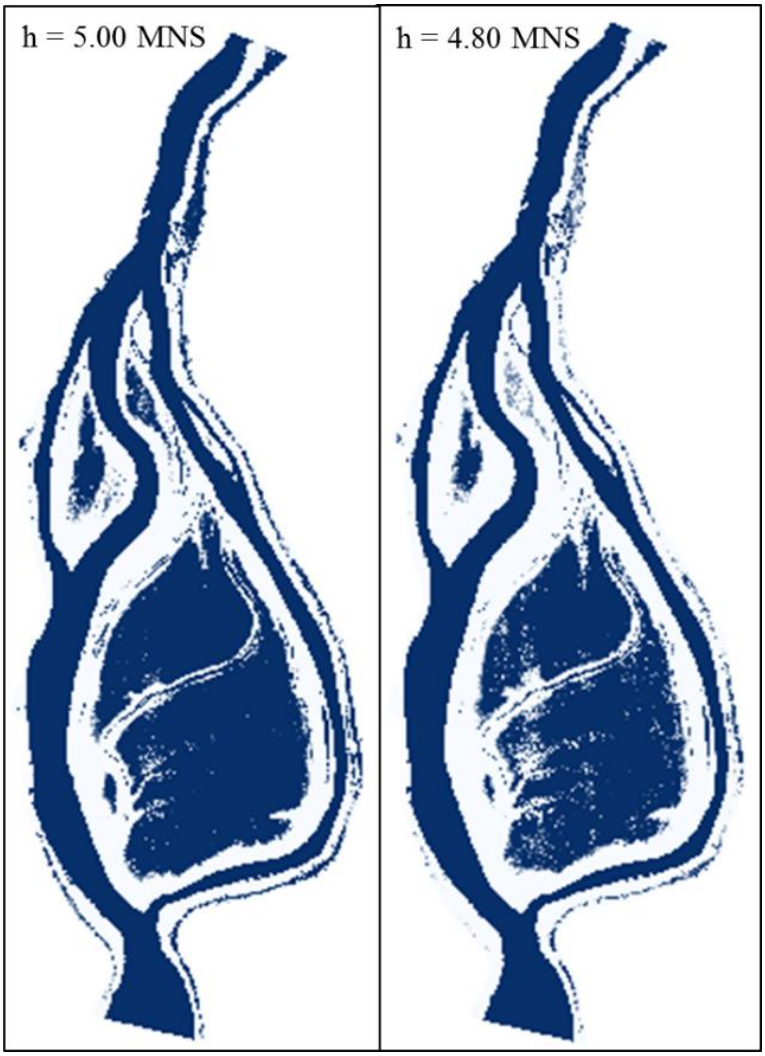

Figure 47. Inundation map for the rainy year 2005. Left: S1, right: S2.

In summary, the water levels in Fundu Mare Island can be positively affected by the installation of weir structures. The required water levels can be obtained and guarantee a sufficient period of inundation to stop the terrestrialization process. On the other hand, the investigations of the extreme events show a sensitivity to the type of flood occurring. Accordingly, long-term climatic changes can provoke negative consequences in case of an inappropriate design of the weirs. Consequently, biodiversity will be affected.

7 Discussion and recommendations

The discussion part is divided into three different sections. The first section discusses the results regarding the calibration of the numerical model. Part two evaluates the assumptions and results of the water balance approach and the last component analyses the findings from an ecological prospective. Correspondingly, evaluation of the restoration measures and recommendations with regard to future implementations are provided.

The results of the numerical model were insufficient with regard to the objectives of the project and the given time restrictions induced by this work. Originally, a period of five weeks between June and July 2015 was regarded as desirable to evaluate the water level changes in Fundu Mare Island. This period represents the time from shortly after the peak of the flood wave until its flattening and characterises the retention capacity of the island. Due to this period of time, the analysis of different restoration scenarios would have resulted in a significant duration of simulation time, which was defined by the computational power and the high spatial and temporal accuracy of the model. During calibration a simulation time of 28 hours required 15 hours of computational time. For a time-period of five weeks, a computational time of around 19 days is expected. Furthermore, unpredicted difficulties during software installation and application implied a significant time effort before a successful model set-up. In summary, these difficulties, the unexpected small time-step, and the complexity of the software gradually increased the time effort in model set-up and were not visible beforehand. One example of the problems encountered during creation of the model is a restricted local refinement of structured grids by the tools in Delft3D. When the grid resolution of the channels on the island gave insufficient results, the improvement of the grid in this area would have costed an unfeasible time effort and would have caused the creation of a significantly higher number of grid cells, leading to an increase in simulation time. A tool for the creation of unstructured grids in RGFGRID was not implemented at the time this work was written. Moreover, the bathymetric representation of the area was problematic. The available morphological model required manual improvement of the channel elevations on the island. The lack of the LIFE-channel in the bathymetry data shows poor representation of some small-scale structures on the island and required manual implementation of the channel's elevation data with strong uncertainties. Additionally, the interpolation process redistributing the depth values to the grid cells in combination with the manual assignment of depth values to non-defined grid cells altered the original morphological model. Especially with regard to small channel dimensions on the island and a grid resolution of 5 metres at these locations, a correct representation of the hydraulics in the channels could not be achieved. Consequently, with regard to the time schedule of this work and the poor data quality the realisation of the simulations was determined as not feasible.

However, to obtain the best results possible in this project, the maximum effort was made to create a representative model by making use of user service and providing suitable computational equipment. Delft3D is powerful software, which is suitable for the handling of the task in this work. However, more time is required to understand the complexity and variety of tools of the software package. It can be stated that the model reproduced the hydraulics in the main channel well and showed sufficient reaction to the roughness on the island. However,

the roughness implemented by the Manning coefficients was extremely low, and changes in bathymetry were required to reproduce the water level changes. Nevertheless, the calculated discharge did not match the one recorded during field works. As a result, to allow a full calibration of the model, the bathymetry data requires better quality and a more accurate reproduction of the small-scaled channels on the island, especially with regard to the LIFE-channel, is necessary. Furthermore, the grid requires higher resolution to represent the hydraulic conditions in the channels on the island and to give more accurate information about the effect on drainage of the lakes on the island. It has to be borne in mind that the time effort must be restricted when implementing a finer numerical grid. With regard to the special importance of the Hogioaia- and the LIFE-channel for the hydraulics, a reduction of the model area is suggested. The closed model boundaries could be defined e.g. at the outer shore of the Danube with the open boundaries closer to the island. Here, it has to be considered that the location of the evaluated area is preferably as far away from the boundaries as possible (Deltares, 2015). In order to give accurate results, a compromise between this requirement and the time effort must be found. Figure 48 gives an example of a possible model size for further numerical investigations. In general,

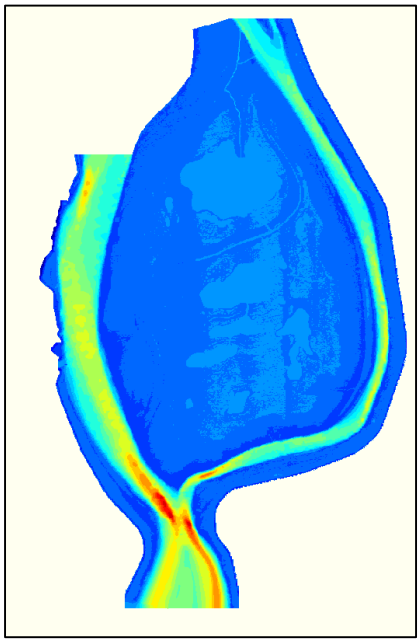

Figure 48. Suggestion of model size for further investigations

Contrary to the insufficient representation of the island by the numerical model, the simplified approach gave reasonable results with regard to the water level changes on the island. When evaluating the findings, the assumptions related to the water balance approach have to be borne in mind. One of the strongest simplifications of this method represents the limited description to stationary processes and the assumption of steady flow. Generally, a constant, horizontal water level at the beginning of the computations is assumed that is lowered by the three sinks: surface runoff, evaporation and leaching. Instationary processes as e.g. backflowing water from the Danube, turbulences, sediment transport, variations in bottom slope or density gradients cannot be described by this approach. Additionally, external factors, e.g. temperature variations,

solar radiation or wind are neglected. Moreover, the lakes are estimated as fully inundated when starting the calculations, neglecting possible variation of the water levels and the flood prior to the initial conditions. With regard to the high flood wave of the mean daily values between 2000 and 2009 this assumption is sufficient.

However, the tests under extreme conditions are based on time-series that show different behaviour. Nevertheless, the probability for these events to occur is rather small. Their investigation is carried out to give an example of the reaction of the hydraulics to extreme climatic changes. In these cases, a fully inundated island at the start of the calculations is an inappropriate assumption. Consequently, the initial water levels in 2003 are lower than assumed and the computed water levels are overestimated. Thus, the computed water levels give a buffer height to a drying of the lakes. With regard to future climate changes which can lead to reduced precipitation and higher temperature in the area, the risk of a drying of the lakes must be considered when setting up the weirs. Further investigation of an increase of the weir crest and its effects is suggested. For 2005, the same simplification was made. However, its effect is suggested to be outweighed by the neglected instationary processes. In reality, the lakes will be "filled up" when the water level in the Danube River exceeds the weir crest, which leads to an increased inundated area and to a water level rise on the island. It is important to note that the calculated final water level is extremely high compared to the critical water level. This effect leads to a much larger inundated area. With regard to the risk of an accumulation of rainy years due to climatic influences, a stronger impact on the vegetation zones by weir constructions must be considered.

The neglected instationary processes and external factors mentioned above affect the reliability of the calculated water levels. Turbulences and small waves due to wind alter flow velocity and direction locally. Depending on the wind direction, the water levels are affected by wind surge. Eddies have an impact on the flow pattern and the energy transport in the flow, which influence local velocities and bed forming processes. Sediment transport and the effect of bed forming processes are important in long-term simulations. The effect of morphological changes needs to be investigated in further research. Steady flow is not representative for natural river flow, which causes variations of the water levels that are not represented in the results.

When analysing the results of the different time-series, it is important to note that the water levels are mean daily values over a decade. The fluctuations of the water levels cause temporal variations on the island and in the channel that are neglected. The calculated weir crest heights are therefore not precise in comparison with realistic events. The same simplification was made for the precipitation and evaporation on the island, which is characterised by long-term mean monthly values. The ground water loss was estimated by a conductivity coefficient representative for the area and an estimated hydraulic gradient. From the results, a high impact of evaporation and leaching was concluded, showing the importance of the accuracy of these values for the results. To give more precise representation of these effects, the impact of the atmospheric values has to be evaluated. Here, temperature and wind need to be included. Additionally, the transpiration of the vegetation is neglected, which is assumed to have a high contribution to the evapotranspiration and must be analysed in future scenarios. These simplifications must be considered when determining the final weir crest height. To compensate the uncertainties, a safety margin for the weir crest is recommended.

The geometric assumptions of the weir dimensions give reasonable results in comparison with the Manning's formula. However, the Manning's formula is applied for an estimated cross section based on the ADCP-measurements. The water level gradient is assumed to represent the bottom slope. This requirement is a simplification that is not given in in natural channel flow, but for a rough estimation of the channel capacity this approach is sufficient. Moreover, a constant vertical slope at the foothills is estimated. This assumption leads to an overestimation of the capacity of the channel. As a result, in reality the discharge in the Hogioaia-channel can be restricted by the channel capacity instead of by the Poleni-formula. Consequently, higher water levels on the island are possible. To investigate the effect of the channel capacity on the water level, the cross section of the Hogioaia-channel needs to be defined more accurately. Additionally, the dimensions of the weir can be varied to allow quantification of their effect on the water levels.

Despite these assumptions it can be stated that the control of the water levels is possible. The results of the simplified model can be used to give suggestions for a future implementation of weirs in the Hogioaia- and the LIFE-channel. In general, the critical water level in S1 is higher and established over a longer period than in S2. As a consequence, the computed weir heights differ of around 20 centimetres. When determining the weir crest height, the results of S1 guarantee higher reliability with regard to the uncertainties.

It was demonstrated that the different weir combinations give small differences in weir height for both scenarios. This can be explained by the strong impact of the evaporation and the leaching that results in similar results for the combinations. In general, the weir heights are plausible. In order to save maintenance and cost, the closing of the LIFE-channel by a levee is suggested to establish conditions that are controlled by only one weir. The height of the levee is defined by the surrounding levees, guaranteeing flooding in spring and water retention in summer and autumn. For the material, local sediments are recommended to limit visual and ecological impact. The selection of the weir type in the Hogioaia-channel is based on the different properties. For the project, a broad-crested weir or a bag weir were selected as final designs, due to simple installation and maintenance as well as low visual impact. The broad-crested weir can be applied for several weir crest designs and combined with movable structures. Installation and operation are simple and less costly. On the other hand, navigation and fish passage are limited to periods with high water levels. This can be compensated by the application of an optional fish pass that guarantees passage of boats and fish. However, the minimum water level in the pass must be guaranteed by the water levels on the island. The bag weir requires control by educated personnel and is therefore more costly in terms of operation and maintenance. The protection of possible metal structures and pumps need to be guaranteed to prevent theft. However, this weir allows a flexible control of the water levels. This is especially important with regard to the uncertainties of hydrological events and future climate change, to allow navigation and facilitate fish passage.

Drying of the wetland and increased growth of ruderal plants and willow encroachment alter the biologic conditions and affect biodiversity. However, damming of the water in the lakes by weirs and levees creates ecological impact. The connectivity between the river channel and the lakes is important for nutrient and water exchange and for migrating aquatic species (see chapter 2.1). Damming can reduce water quality in the lakes in accordance with rising temperature and

reduced oxygen content. Information obtained from the experts A. Foldvik and J.O. Gjershaug, biologists at NINA, during a project meeting on the 10th of February 2016, allow a brief discussion of the impact of the determined measures on ichthyo-fauna and avifauna. Typical fish species found in this area come into the lakes with the flood in spring, and spawn between May and July on vegetation and substrate in shallow water. If their migration back into the Danube is prevented by damming, competition and water quality changes increase biological pressure. A complete drying of the lakes in case of dry years leads to mortality of complete generations of fish and can, on the long-term, cause extinction. Bird species come into the area for nesting and feeding in spring and leave the island in August. Their habitat is endangered by reduced fish reproduction, due to a decrease in food availability. As a result, the connectivity between the lakes and the Danube must be guaranteed for a certain period to allow fish to enter the lakes and to migrate back into the Danube. For migration, fish is not sensitive to a specific time period throughout the year. With regard to the breeding period of the birds, the time for providing connectivity is suggested to be in August, which decreases the required 150 days of inundation. On the other hand, the inundation during winter is not accounted for in this approach, which requires further investigation to evaluate the total number of inundation days per year. However, by providing connectivity between the island and the Danube in August, spawning and nesting are guaranteed. It is important to prevent drainage of the island to ensure sufficient rest water in the lakes. One consideration is the provision of hibernation areas for aquatic species that requires a prevention of freezing of the lakes during winter. The enhancement of biodiversity in Fundu Mare Island has a high priority with regard to habitat degradation in the Danube River. Habitat loss induced by the construction measures carried out in the 20th century minimised the remaining suitable river structures to few biotopes in the Romanian Danube. Especially for sensitive fish species, the loss of Fundu Mare Island would cause a high risk of extinction.

Generally speaking, an increase of the water levels in Fundu Mare Island is possible by the two suggested weir types. With regard to the hydrological uncertainty, climate change and ecological requirements the implementation of a fixed weir structure is insufficient and the selection of the bag weir as a flexible weir structure is therefore recommended. However, further research needs to be carried out to investigate the weir dimensions and to analyse sufficient water storage in the island in comparison with the above requirements.

8 Conclusion

Due to increased observation of willow encroachment in the wetland area Fundu Mare Island, this work aimed at an investigation of a number of restoration scenarios to allow conservation of biodiversity. The hydraulics of the area were studied to obtain information about the inundation time and area of the lakes. The implementation of a two-dimensional numerical model was examined. Within this work a wide range of fields within hydraulic engineering were covered, which led to a comprehensive investigation of the problem definition. Due to the time restrictions of the thesis and unforeseen problems during model calibration, a deeper analysis of the restoration measures was not feasible. As a compromise, a general investigation by the application of a simplified water balance to the problem was chosen. Through this approach, the restoration effects by implementation of different weir types could be tested. For further investigations, a precise analysis of the weir dimensions, including effects of instationary processes and external sources is recommended prior to implementation of specific measures.

Delft3D was determined as suitable to fulfil the task of this thesis and a high effort was made to implement a two-dimensional model. Although the model showed good reaction to adjustment in roughness, changes in bathymetry were required to obtain results for the channels on the island. Despite this, the results did not match the field data. Due to time restrictions in this work and insufficient data quality of the morphology, calibration of the numerical model was not feasible. In case of further usage of the model, higher resolution of bathymetry data and of the numerical grid is recommended to allow correct representation of small-scale structures in Fundu Mare Island. Moreover, a reduction of the numerical domain in size must be implemented to allow calculations within the time-frame of the project. The application of high performance computers is regarded as useful to reduce time effort.

The simplified approach based on water balance represents steady processes and provides adequate results with regard to the water levels in Fundu Mare Island. In general, it can be concluded that the water levels on the island can be positively influenced by the implementation of weirs. The inundation time can be increased and the terrestrialization process is halted. Drying of the lakes and willow encroachment can be prevented. The enhancement of biodiversity in the wetland is therefore feasible. However, this method is based on simplifications, and careful evaluation of the weir dimensions prior to actual implementation is therefore required. Evaporation, ground water loss and unsteady processes need to be taken into account during further investigation. The analysis of different hydrological events showed strong sensitivity of the water levels in Fundu Mare Island to the water level in the Danube. To meet uncertainties with regard to the assumptions made, a security margin or a flexible weir structure is suggested to compensate impacts of future climatic changes.

The demands of fish in the area can be met by seasonal opening of the Hogioaia-channel to enhance water exchange and allow migration into the Danube. In order to allow connectivity between main channel and island, the opening of the weir is recommended to be applied in August. This will allow spawning of fish as well as guarantee feed for bird species during their

nesting period. However, further research needs to be carried out to analyse if a sufficient discharge during opening can be provided by the water volume stored in the lakes of Fundu Mare Island. One consideration is that the rest water volume in the lakes must be sufficiently large to prevent entire freezing of the lakes during winter, in order to ensure habitat for hibernation of aquatic species.

Among the examined weir types, the flexible bag weir was determined as appropriate. It has to be considered that the installation of the bag weir involves high cost and maintenance as well as trained staff to allow correct operation of the flexible weir crest. The feasibility of the implementation of this weir structure needs to be evaluated further before setting up a restoration plan. Additionally, to determine the weir's dimensions, the flexibility of the weir crest and the corresponding impact on the water levels need to be carefully evaluated prior to construction. However, to meet the requirements regarding security, hydrological uncertainty and ecological demands, the installation of the bag weir is especially recommended.

To find a compromise between the simplified water balance approach and the complex two-dimensional model, an analysis with the help of a one-dimensional model is suggested to calculate the water levels on the island. However, a close examination of the evapotranspiration and the ground water loss needs to be carried out in addition.

References

Aberle, J., and Kulisch, H. (2009). "Hydraulik und numerische Simulation." *DWA Themen*, DWA, Hennef, 50-67.

Acreman, M., Fisher, J., Stratford, C., Mould, D., and Mountford, J. (2007). "Hydrological science and wetland restoration: some case studies from Europe." *Hydrology and Earth System Sciences Discussions*, 11(1), 158-169.

Akan, O. A. (2006). *Open Channel Hydraulics*, Butterworth-Heinemann, Jordan Hill, GBR.

Allaire, G. (2007). *Numerical Analysis and Optimization: An Introduction to Mathematical Modelling and Numerical Simulation*, Oxford University Press, Cary, New York, USA.

Amoros, C., Rostan, J.-C., Pautou, G., and Bravard, J.-P. (1987). "The reversible process concept applied to the environmental management of large river systems." *Environmental Management*, 11(5), 607-617.

Andrei, A. (2011). "Small Wetland of Brăila Natural Park Administration" *After-LIFE Conservation Plan*, Brăila, Romania.

Andrewartha, H. G., and Birch, L. C. (1964). The distribution and abundance of animals, University of Chicago Press.

Andronache, I. (2009). "Regimul hidrologic al Dunarii in sectorul Baltii Brailei, inainte si dupa indiguire." *Geography, Geoecology – experiences of scientific research*, Int. Conf. Dnepropetrovsk, 10-18.

Arthington, A. H., and Pusey, B. J. (2003). "Flow restoration and protection in Australian rivers." *River research and applications*, 19(5-6), 377-395.

Bailey, R. H. (1992). "Restoration of Aquatic Ecosystems." *Journal of Ecology*, 81(2), 387-389.

BmB (2010). "Conservation, restoration and durable management in Small Island of Brăila." (September, 2015).

Bodescu, F., and Iordache, V. (2010) "Modelling hydrological processes to evaluate alternatives for ecologic reconstruction in the Danube floodplain near Brăila, Romania." *Proc., 38th IAD Conference.*

Bollrich, G. (2007). *Technische Hydromechanik 1, Grundlagen, 6., durchgesehene und korrigierte Auflage*, Huss.

Bondar, C. (1996). "Aspects hydrologiques dans L'étude de cas du Delta du Danube." Danube Delta-Black Sea Systems under Global Changes Impact, 1, 48-52.

Broomans, P., Vuik, C., Mynett, A., and Mooiman, J. (2004). "Numerical accuracy in the solution of the shallow-water equations." *GH Jirka & WSJ Uittewaal (Eds.)*, Shallow flows, 527-533.

Buijse, A. D., Coops, H., Staras, M., Jans, L., Van Geest, G., Grift, R., Ibelings, B. W., Oosterberg, W., and Roozen, F. C. (2002). "Restoration strategies for river floodplains along large lowland rivers in Europe." *Freshwater biology*, 47(4), 889-907.

Bullock, A., and Acreman, M. (2003). "The role of wetlands in the hydrological cycle." *Hydrology and Earth System Sciences Discussions*, 7(3), 358-389.

Burkett, V., and Kusler, J. (2000). "Climate change: Potential impacts and interactions in wetlands of the United States." *JAWRA Journal of the American Water Resources Association*, 36(2), 313-320.

Busch, K.-F., Luckner, L., and Tiemer, K. (1993). *Geohydraulik*, Gebrüder Borntraeger.

Chow, V. T. (1959). Open-Channel Hydraulics, McGraw-Hill, New York, USA.

Cioaca, E., Bondar, C., and Borcia, C. "Hydrographical network of the Danube Delta Biosphere Reserve - modelling the morphological dynamics." *Proc., 38th IAD Conference*.

Connor, K. J., and Gabor, S. (2006). "Breeding waterbird wetland habitat availability and response to water-level management in Saint John River floodplain wetlands, New Brunswick." *Hydrobiologia*, 567(1), 169-181.

Coops, H., Vulink, J. T., and Van Nes, E. H. (2004). "Managed water levels and the expansion of emergent vegetation along a lakeshore." *Limnologica-Ecology and Management of Inland Waters*, 34(1), 57-64.

Copp, G. H. (1989). "The habitat diversity and fish reproductive function of floodplain ecosystems." *Environmental Biology of Fishes*, 26(1), 1-27.

Cowardin, L. M., Carter, V., Golet, F. C., and LaRoe, E. T. (1979). *Classification of wetlands & deepwater habitats of the US*, DIANE Publishing.

Day, J. W., Barras, J., Clairain, E., Johnston, J., Justic, D., Kemp, G. P., Ko, J.-Y., Lane, R., Mitsch, W. J., and Steyer, G. (2005). "Implications of global climatic change and energy cost and availability for the restoration of the Mississippi delta." *Ecological Engineering*, 24(4), 253-265.

Deleersnijder, E., and Beckers, J.-M. (1992). "On the use of the σ-coordinate system in regions of large bathymetric variations." *Journal of Marine Systems*, 3(4), 381-390.

Deltares (2014a). "Delft3D, Functional Specifications." D. Systems, ed.Delft.

Deltares (2014b). "RGFGRID Generation and manipulation of curvilinear grids for Delft3D-FLOW and Delft3D-WAVE." D. Systems, ed.Delft.

Deltares (2014c). "Generation and manipulation of grid-related parameters such as bathymetry, initial conditions and roughness." D. Systems, ed.Delft.

Deltares (2015). "Delft3D-Flow." D. Systems, ed.Delft.

Desgranges, J.-L., Ingram, J., Drolet, B., Morin, J., Savage, C., and Borcard, D. (2006). "Modelling wetland bird response to water level changes in the Lake Ontario–St. Lawrence River hydrosystem." *Environmental Monitoring and Assessment*, 113(1-3), 329-365.

Dittrich, A., Aberle, J., and Koll, K. (2007). "Berechnungsverfahren naturnah gestalteter Fließgewässer." *Flussbau*, Weiterbildendes Studium "Wasser und Umwelt" Bauhaus-Universität Weimar, Weimar, 67-96.

Dudgeon, D., Arthington, A. H., Gessner, M. O., Kawabata, Z. I., Knowler, D. J., Lévêque, C., Naiman, R. J., Prieur-Richard, A. H., Soto, D., and Stiassny, M. L. (2006). "Freshwater biodiversity: importance, threats, status and conservation challenges." *Biological reviews*, 81(2), 163-182.

Earth, G. (2014). "Digital photo of Fundu Mare Island." (13th of January, 2014).

Ebert, S., Hulea, O., and Strobel, D. (2009). "Floodplain restoration along the lower Danube: a climate change adaptation case study." *Climate and Development*, 1(3), 212-219.

ECRR (2014). http://www.ecrr.org. (06. November, 2015).

Edmonds, D., Slingerland, R., Best, J., Parsons, D., and Smith, N. (2010). "Response of river-dominated delta channel networks to permanent changes in river discharge." *Geophysical Research Letters*, 37(12).

Ehrenfeld, J. G. (2000). "Defining the limits of restoration: the need for realistic goals." *Restoration ecology*, 8(1), 2-9.

Elias, E., Walstra, D., Roelvink, J., Stive, M., and Klein, M. "Hydrodynamic validation of Delft3D with field measurements at Egmond." *Proc., Coastal Engineering Conference*, ASCE American Society of Civil Engineers, 2714-2727.

ERDF (2013). "Sustainable Transport and Tourism along the Danube."

Erwin, K. L. (2009). "Wetlands and global climate change: the role of wetland restoration in a changing world." *Wetlands Ecology and management*, 17(1), 71-84.

EU (2013). "Interpretation Manual of European Union Habitats." *Nature ENV B.3*.

Ferziger, J. H., and Perić, M. (2002). *Computational methods for fluid dynamics*, Springer Berlin.

Gebhardt, M. (2006). "Hydraulische und statische Bemessung von Schlauchwehren." PhD-thesis, University of Karlsruhe, Karlsruhe.

Geleynse, N., Storms, J. E., Walstra, D.-J. R., Jagers, H. A., Wang, Z. B., and Stive, M. J. (2011). "Controls on river delta formation; insights from numerical modelling." *Earth and Planetary Science Letters*, 302(1), 217-226.

Giardino, A., Van der Werf, J., and Van Ormondt, M. (2010). "Simulating Coastal Morphodynamics with Delft3D: case study Egmond aan Zee." PhD-thesis. Delft University of Technology.

Giesecke, J., Heimerl, S., and Mosonyi, E. (2014). *Wasserkraftanlagen: Planung, Bau und Betrieb*, Springer-Verlag.

Glaeser, J., and Wulf, M. (2009). "Effects of water regime and habitat continuity on the plant species composition of floodplain forests." *Journal of Vegetation Science*, 20(1), 37-48.

Gore, J. A., and Shields, F. D. (1995). "Can large rivers be restored?" *BioScience*, 142-152.

Griebel, M., Dornseifer, T., and Neunhoeffer, T. (1997). *Numerical simulation in fluid dynamics: a practical introduction*, Siam.

Grift, R. E. (2001). "How fish benefit from floodplain restoration along the lower River Rhine."PhD-thesis, Netherlands Institute for Fisheries Research, Wageningen.

Habersack, H., Hein, T., Stanica, A., Liska, I., Mair, R., Jäger, E., Hauer, C., and Bradley, C. (2016). "Challenges of river basin management: Current status of, and prospects for, the River Danube from a river engineering perspective." *Science of The Total Environment*, 543, 828-845.

Habersack, H., Tritthart, M., P., G., and Glock, K. (2014). "3D numerical modelling Romanian Danube between Calarasi and Brăila." University of Natural Resources and Life Sciences Vienna, Austria.

Henry, C. P., and Amoros, C. (1995). "Restoration ecology of riverine wetlands: I. A scientific base." *Environmental Management*, 19(6), 891-902.

Hoekstra, J. M., Molnar, J. L., Jennings, M., Revenga, C., Spalding, M., Boucher, T., Robertson, J., Heibel, T., and Ellison, K. (2010). *The atlas of global conservation: changes, challenges and opportunities to make a difference*, University of California Press Berkeley, California, USA.

Hooijer, A. (2002). "Hydrological Studies in the Danube Delta, Part A." *Technical Report Q3230*, WL Deltares Hydraulics.

Iordache, V., Bodescu, F., and Dumitru, M. (2005). "Elements sustaining the lobby for the restoration of Big Island of Brăila, Danube floodplain." *Arch. Hydrobiol. Suppl*, 155, 677-692.

IPOC. (1997). "The regional impacts of climate change: an assessment of vulnerability. "Geneva.

IUCN (2012). "Protected Areas Category V." http://www.iucn.org/about/work/programmes/gpap_home/gpap_quality/gpap_pacategories/gpap_category5/. (15. December, 2015).

Jang, C.-L., and Shimizu, Y. (2005). "Numerical simulation of relatively wide, shallow channels with erodible banks." *Journal of Hydraulic Engineering*, 131(7), 565-575.

Junk, W. J., Bayley, P. B., and Sparks, R. E. "The flood pulse concept in river-floodplain systems." *Proc., Proceeding of the international large rivers symposium, Canadian special publication in fisheries and aquatic sciences. NRC, Ottawa, ON*, 110-127.

Kaminski, M. R., Baldassarre, G. A., and Pearse, A. T. (2006). "Waterbird responses to hydrological management of wetlands reserve program habitats in New York." Wildlife Society Bulletin, 34(4), 921-926.

Kang, H., and Choi, S.-U. (2005). "3D numerical simulation of compound open-channel flow with vegetated floodplains by Reynolds stress model." *KSCE Journal of Civil Engineering*, 9(1), 7-11.

Knight, D., and Shiono, K. (1996). "River channel and floodplain hydraulics." *Floodplain processes*, 5, 139-181.

Kolmogorov, A. N. "Equations of turbulent motion in an incompressible fluid." *Proc., Dokl. Akad. Nauk SSSR*, 299-303.

Lesser, G., Roelvink, J., Van Kester, J., and Stelling, G. (2004). "Development and validation of a three-dimensional morphological model." *Coastal engineering*, 51(8), 883-915.

LUBW (2005). "Durchgängigkeit für Tiere in Fließgewässern. Teil 1." *Landesamt für Umwelt, Messungen, und Naturschutz Baden-Württemberg*. (February, 2016).

Malmqvist, B., and Rundle, S. (2002). "Threats to the running water ecosystems of the world." *Environmental conservation*, 29(02), 134-153.

Nguyen, V. T. (2015). "3D numerical simulation of free surface flows over hydraulic structures in natural channels and rivers." *Applied Mathematical Modelling*.

Nichersu, I. (2016). "ADCP data of the Danube Delta National Institute." P. Zinke, ed.Tulcea.

Nicholas, A., and Mitchell, C. (2003). "Numerical simulation of overbank processes in topographically complex floodplain environments." *Hydrological Processes*, 17(4), 727-746.

NMAR (2015). "Flooding maps of the Danube."

Novak, P., Moffat, A., Nalluri, C., and Narayanan, R. (2007). *Hydraulic structures*, CRC Press.

Ntiamoa-Baidu, Y., Piersma, T., Wiersma, P., Poot, M., Battley, P., and Gordon, C. (1998). "Water depth selection, daily feeding routines and diets of waterbirds in coastal lagoons in Ghana." *Ibis*, 140(1), 89-103.

Olson, D. M., and Dinerstein, E. (1998). "The Global 200: a representation approach to conserving the Earth's most biologically valuable ecoregions." *Conservation Biology*, 12(3), 502-515.

Patt, H., and Gonsowski, P. (2010). *Wasserbau: Grundlagen, Gestaltung von wasserbaulichen Bauwerken und Anlagen*, Springer-Verlag.

Peper, J. H., P; Schleuter, M (2012). "Vegetation der Donauaue zwischen Straubing und Vilshofen. Standortpotenzial für die Auenvegetation des Ist-Zustands und der Ausbauvarianten." *BfG-Bericht 1773*, Bundesanstalt für Gewässerkunde, Koblenz, 117.

Pott, R., and Remy, D. (2000). "Ökosysteme Mitteleuropas aus geobotanischer Sicht: Gewässer des Binnenlandes." *Ulmer. Stuttgart*.

Prandtl, L., and Wieghardt, K. (1947). *Über ein neues Formelsystem für die ausgebildete Turbulenz*, Vandenhoeck & Ruprecht.

Rameshwaran, P., and Naden, P. S. (2003). "Three-dimensional numerical simulation of compound channel flows." *Journal of hydraulic engineering*, 129(8), 645-652.

Rock, A. D., Zhang, R., and Wilkinson, D. (2008). "Velocity variations in cross-hole sonic logging surveys." Federal Highway Administration

Schäfer, M. (2006). *Computational Engineering — Introduction to Numerical Methods*, Springer.

Schiemer, F., Baumgartner, C., and Tockner, K. (1999). "Restoration of floodplain rivers: The 'Danube restoration project'." Regulated Rivers: Research & Management, 15(1), 231-244.

Schneider-Binder, E. (2011). "Aquatic macrophytes and their use as ecological status indicators in restoration projects in the Danube Delta (Romania)." *Romanian Journal of Aquatic Ecology*, 1(1), 45-62.

Schwarz, U. (2008). "Assessment of the balance and management of sediments of the Danube." *Slovenian National Commitee for IHP Unesco, Ljubljana*.

Simons, J. H., Bakker, C., Schropp, M. H., Jans, L. H., Kok, F. R., and Grift, R. E. (2001). "Man-made secondary channels along the River Rhine (The Netherlands); results of post-project monitoring." *Regulated Rivers: Research & Management*, 17(4-5), 473-491.

Somes, N. L., Bishop, W. A., and Wong, T. H. (1999). "Numerical simulation of wetland hydrodynamics." *Environment International*, 25(6), 773-779.

Stagl, J. C., and Hattermann, F. F. (2015). "Impacts of Climate Change on the Hydrological Regime of the Danube River and Its Tributaries Using an Ensemble of Climate Scenarios." *Water*, 7(11), 6139-6172.

Stanford, J. A., Ward, J., Liss, W. J., Frissell, C. A., Williams, R. N., Lichatowich, J. A., and Coutant, C. C. (1996). "A general protocol for restoration of regulated rivers." *US Department of Energy Publications*, 43.

Statzner, B., Gore, J. A., and Resh, V. H. (1988). "Hydraulic stream ecology: observed patterns and potential applications." *Journal of the North American Benthological Society*, 307-360.

Stelling, G. S. (1983). "On the construction of computational methods for shallow water flow problems." TU Delft, Delft University of Technology.

Stelling, G. S., and Leendertse, J. J. "Approximation of convective processes by cyclic AOI methods." *Proc., Estuarine and Coastal Modeling (1991)*, ASCE, 771-782.

Stelling, G. S., and Van Kester, J. A. T. M. (1994). "On the approximation of horizontal gradients in sigma co-ordinates for bathymetry with steep bottom slopes." *International Journal for Numerical Methods in Fluids*, 18(10), 915-935.

Strobl, T., and Zunic, F. (2006). *Wasserbau*, Springer.

Teklemariam, E., Korbaylo, B. W., Groeneveld, J. L., and Fuchs, D. M. "Computational fluid dynamics: Diverse applications in hydropower project's design and analysis." *Proc., CWRA 55th Annual Conference, Winnipeg, Manitoba, CA*, 1-20.

Temmerman, S., Bouma, T., Govers, G., Wang, Z., De Vries, M., and Herman, P. (2005). "Impact of vegetation on flow routing and sedimentation patterns: Three-dimensional modeling for a tidal marsh." *Journal of Geophysical Research: Earth Surface (2003–2012)*, 110(F4).

Tockner, K., Pennetzdorfer, D., Reiner, N., Schiemer, F., and Ward, J. (1999). "Hydrological connectivity, and the exchange of organic matter and nutrients in a dynamic river–floodplain system (Danube, Austria)." *Freshwater Biology*, 41(3), 521-535.

Tritthart, M., and Gutknecht, D. (2007). "Three-dimensional simulation of free-surface flows using polyhedral finite volumes." *Engineering Applications of Computational Fluid Mechanics*, 1(1), 1-14.

Vadineanu, A. (2001). "Lower Danube Wetlands System (LDWS)." *Observatorio Medioambiental*, 4, 373-402.

Vadineanu, A., Adamescu, M., Vadineanu, R., Cristofor, S., and Negrei, C. (2003). "Past and Future Management of Lower Danube Wetlands System: A Bioeconomic Appraisal." *The Journal of Interdisciplinary Economics*, 14, 415–447.

Via donau, (2015). "Donaukarte 2014." <http://www.viadonau.org/newsroom/publikationen/wasserstrassenkarten/ >. (12th of November, 2015).

Vischer, D., and Huber, A. (2013). *Wasserbau: Hydrologische Grundlagen, Elemente des Wasserbaus, Nutz-und Schutzbauten an Binnengewässern*, Springer-Verlag.

Ward, J. V., and Stanford, J. (1983). "The serial discontinuity concept of lotic ecosystems." *Dynamics of lotic ecosystems*, 10, 29-42.

Zedler, J. B. (2000). "Progress in wetland restoration ecology." *Trends in Ecology & Evolution*, 15(10), 402-407.

Zalewski, M. (2011). "Hydroecology and Ecohydrology: Past, Present and Future." Vadose Zone Journal, 10(2), 773-777.

Zinke, P. (2015a). "Processing of data and production of the model morphology for RFM." SINTEF Energy Research, Trondheim, Unpublished project note, EEA Grant Project Restoration Fundu Mare Island.

Zinke, P. (2015b). "Production of the roughness file for the 2D modelling of Fundu Mare." SINTEF Energy Research, Trondheim, Unpublished project note, EEA Grant Project Restoration Fundu Mare Island

Zinke, P., and Aberle, J. (2015). "Data, photos and notes of the field measurements in Fundu Mare Island in July 2015." SINTEF Energy Research & Norwegian University of Science and Technology, Trondheim, Unpublished project note, EEA Grant Project Restoration Fundu Mare Island.

Zinke, P., Aberle, J., and Nedelcuț, F. (2016). “Vegetation changes at “Fundu Mare Island” in the Inner Danube Delta near Brăila (Romania).”, Unpublished project note.

Annex A

He investigated software packages are summarised below. An overview on the specifications, according to the requirements of the project is given.

Table 4. Investigated software packages

Name	Open source	2D/3D	Sediment transport	Usability	Ground water flow	Remarks	Webpage
OpenFOAM	X	3D	applicable	Programming knowledge required (PKR)	-	-	http://openfoam.com/
Gerris	X	3D	No	PKR	No	Only Linux, Unix	http://gfs.sourceforge.net/wiki/index.php/Introduction
RSim-3D	-	3D	In combination with iSed	-	-	Poor visualisation, Download not found	Tritthart (2007)
TELEMAC-3D	X	3D	X	PKR	X	Sigma-grid	http://wiki.opentelemac.org/doku.php?id=user_manual_telemac-3d
NaSt3DGP	X	3D	No	PKR	No	Interface to Matlab/VTK	http://wissrech.iam.uni-bonn.de/research/projects/NaSt3DGP/documentation/userguide.pdf
GEMSS	No	3D/2D	X	-	No	GIS compatibility, training (online?)	http://gemss.com/

Continuation from previous page

LISFLOOD-FP 2d	-	2D	In combination with CAESAR	-	No	Accurate data required; ARC-View/Flood view	http://www.bristol.ac.uk/media-library/sites/geography/migrated/documents/lisflood-manual-v2.6.2.pdf
FLO-2D	-	2D	No	-	-	Only basic package for free	http://www.flo-2d.com/flo-2d-basic/
CCHE2D	no	2D	X	-	No	Only Windows XP or older, GIS compatibility	www.ncche.olemiss.edu/cche2d
River 2D Morphology	No	2D	X	-	No	Different packages	http://www.river2d.ualberta.ca/
PIHM	No	2D	X	-	X	Output: ASCII	http://www.pihm.psu.edu/pihm_home.html
HEC-RAS 2D	Only for strong cases	2D	Bed load	Software still under development and has several issues	No	Only beta version available	http://www.hec.usace.army.mil/misc/files/ras/Combined_1D_and_2D_Modeling_with_HEC-RAS.pdf
Telemac2D	X	2D	X	Good	No	First steps	http://www.opentelemac.org/index.php/presentation?id=17)
FEATFLOW2	X	2D	No	PKR	No	Paraview output; no turbulence model/free surface	http://www.featflow.de/en/software/featflow.html
CAESAR	optional	2D	X	PKR	-	Only sediment transport	http://sourceforge.net/p/caesar-lisflood/wiki/Background/

Table 5 gives a comparison of the two software packages SSIIM and Delft3D. The main properties of the software are summarised.

Table 5. Specification of Delft3D and SSIIM

Name of software	**SSIIM**	**Delft3D**
Author/Start of development	Nils Reidar Olsen/ 1990/91	Deltares/ 1988
Web page	http://folk.ntnu.no/nilsol/ssiim/	http://oss.deltares.nl/web/delft3d/home
Applications	Sediment transport in rivers, reservoirs and around hydraulic structures	Currents, waves, effluents, sediment transport, water quality, particle tracking
Spatial discretization	Finite Volumes	Finite Differences
Grid types	Structured and unstructured, non-orthogonal	Orthogonal curvilinear grid; structured and unstructured
Modules	Pre-processor, solver, post-processor	Pre-processor, solver, post-processor
Turbulence closure	k-ω-, k-ε turbulence model	k-ε, k-L, algebraic and constant coefficient, LES
Remarks		σ-coordinate transformation to smoothly represent the bottom topography

Annex B

In Annex B a more detailed view on the grid creation is given. The process of the grid smoothening and the orthogonalisation is presented to allow more understanding of the changes made within the model set-up.

The smoothening process represents the ratio between neighbouring cell sizes and requires a number around 1.2 maximum. The ration is tested for both axis-directions respectively. Figure 49 gives an example of a part of the grid before the smoothening process in x-axis direction was performed.

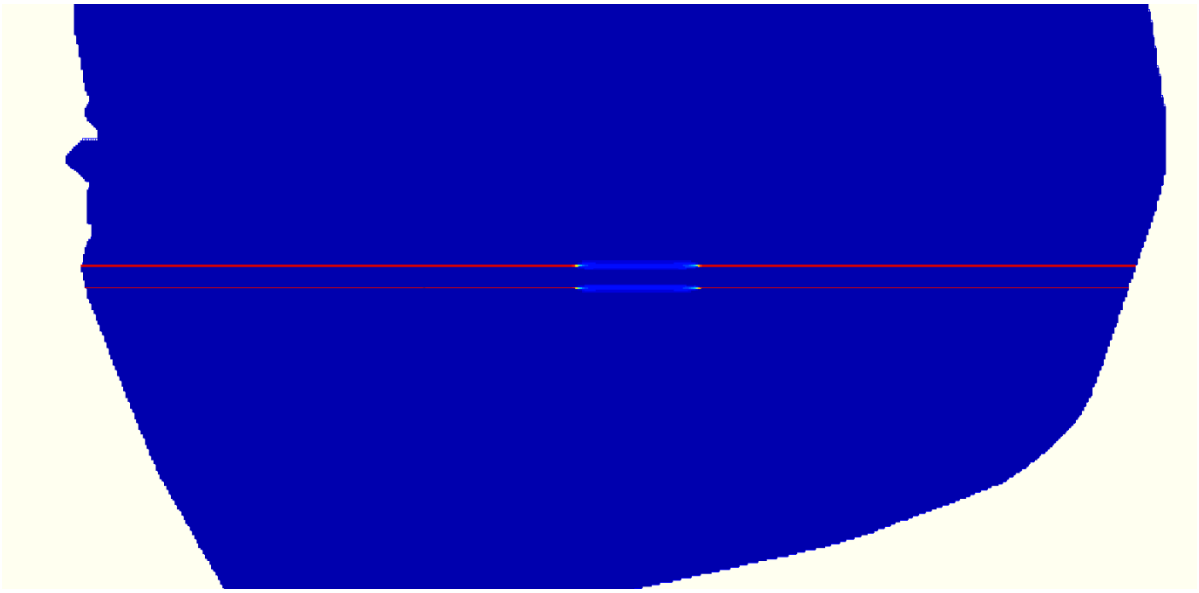

Figure 49. Cells before the smoothening process in x-axis direction. The red cells represent much higher ratios of around 2. The smoothening tool reduces this ratio.

The performed smoothening process is shown in Figure 50. The ratios are sufficient in y-axis direction.

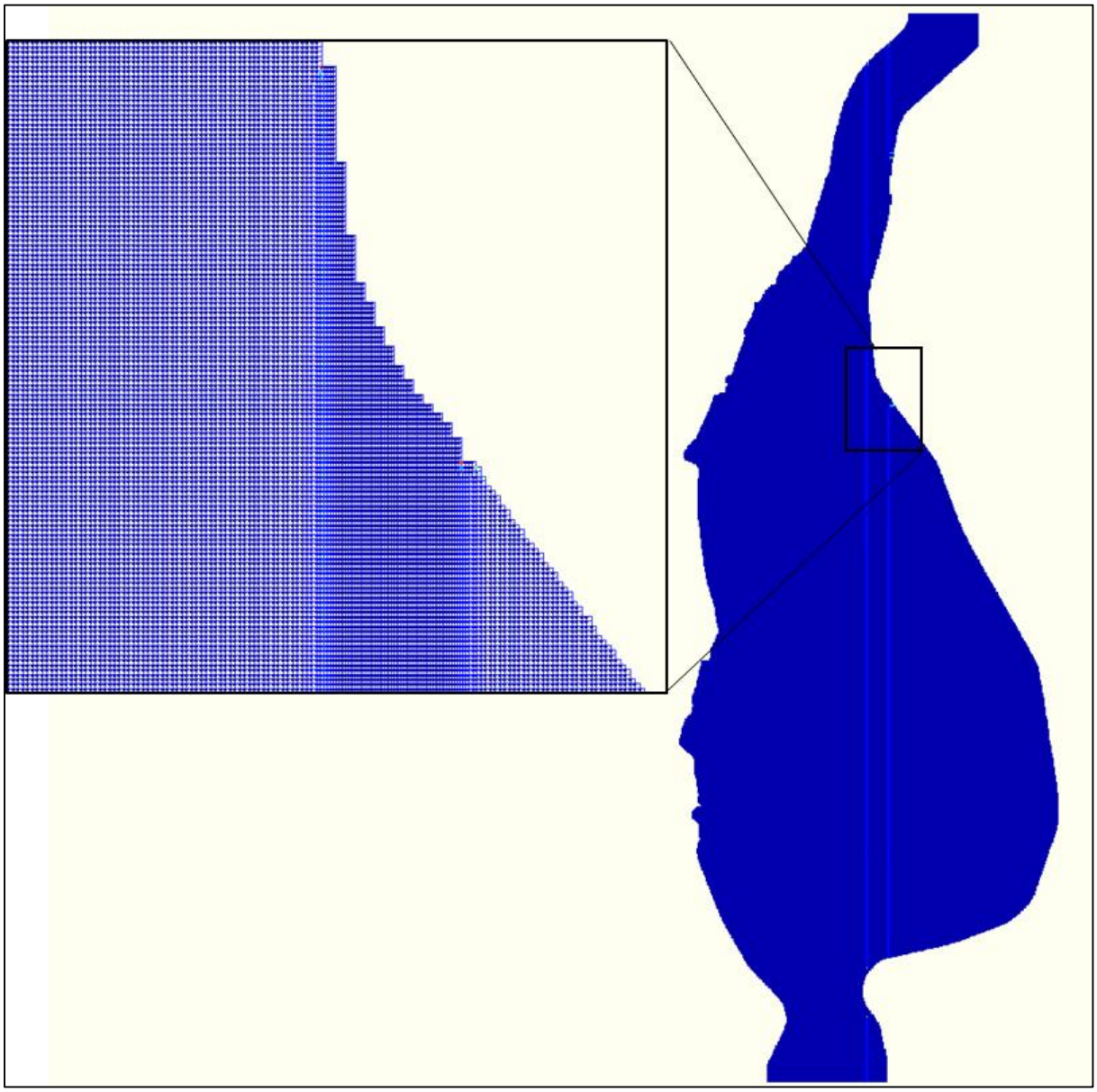

Figure 50. Smoothened grid in y-direction. The different blue colours represent the ratios to the neighbouring cells. Aside from some exceptions the required ratio is given.

Furthermore, orthogonality is required, which is implied by a rectangular grid. Figure 51 shows the entire domain with values close to zero.

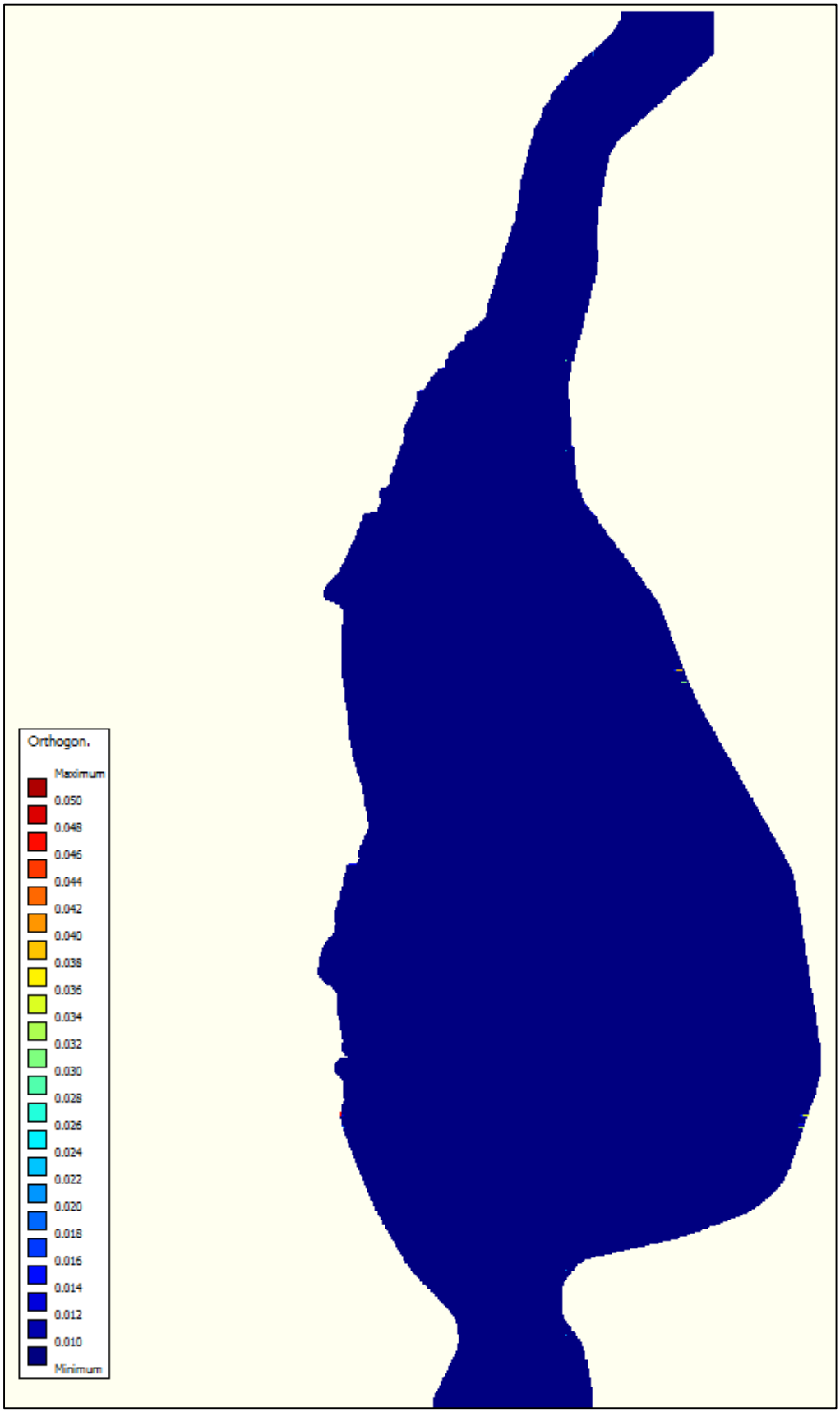

Figure 51. Orthogonality of the grid over the entire domain.

Annex C

The MS Excel calculations are presented in this annex. The first sheets give an example of the calculations of the water levels on the island. The broad-crested weir was selected as an example for the water balance approach. S2 was selected. Due to the long time period, not all values are visualised. Roughly one third of the days is presented.

First the calculations for the minimum damming of the LIFE-channel are presented

		min. damming LIFE		LIFE-channel	Cd=	0.50	
					hweir=	0.88	
	Braila	Hogioaia	Volume lakes	Hneu,island	Lw=	2	
	2000-2009	m³/d	m³	m	Q Surface	h0	Manning
11. Mai	5.72	0	15169616.89	5.72	73401.558	1.04	73401.56
12. Mai	5.67	0	15066951.41	5.72	73418.4209	1.04	73418.42
13. Mai	5.61	0	14963810.05	5.71	72928.7593	1.03	72928.76
14. Mai	5.58	0	14860687.96	5.71	72439.4877	1.03	72439.49
19. Mai	5.33	0	14347412.38	5.67	70008.5708	0.99	70008.57
20. Mai	5.28	0	14245044.29	5.66	69524.6038	0.98	69524.60
21. Mai	5.23	0	14142824.37	5.65	69041.6186	0.97	69041.62
22. Mai	5.18	0	14040693.73	5.65	68559.3352	0.97	68559.34
23. Mai	5.14	0	13938693.76	5.64	68077.9473	0.96	68077.95
24. Mai	5.09	0	13836905.27	5.63	67597.8346	0.95	67597.83
12. Jun	4.54	0	11776564.76	5.48	57940.4857	0.80	57940.49
13. Jun	4.56	0	11666776.26	5.47	57429.3104	0.79	57429.31
14. Jun	4.58	0	11557882.31	5.46	56922.6725	0.78	56922.67
15. Jun	4.58	0	11449830.25	5.45	56420.3241	0.77	56420.32
16. Jun	4.56	0	11342501.80	5.44	55921.7131	0.76	55921.71
17. Jun	4.52	0	11235695.29	5.43	55425.9022	0.75	55425.90
18. Jun	4.47	0	11129259.06	5.42	54932.1893	0.74	54932.19
19. Jun	4.46	0	11023043.68	5.42	54439.8847	0.74	54439.88
20. Jun	4.46	0	10917436.25	5.41	53950.7848	0.73	53950.78
21. Jun	4.44	0	10812565.76	5.40	53465.4867	0.72	53465.49
22. Jun	4.40	0	10708205.05	5.39	52982.9395	0.71	52982.94
23. Jun	4.34	0	10604158.25	5.38	52502.2402	0.70	52502.24
24. Jun	4.30	0	10500269.58	5.37	52022.6739	0.69	52022.67
25. Jun	4.26	0	10396699.95	5.37	51544.9885	0.69	51544.99
26. Jun	4.23	0	10293460.40	5.36	51069.2391	0.68	51069.24
17. Jul	3.80	0	7971017.42	5.16	40497.0845	0.48	40497.08
18. Jul	3.76	0	7864203.37	5.15	40017.999	0.47	40018.00
19. Jul	3.72	0	7757944.80	5.14	39542.1467	0.46	39542.15
20. Jul	3.69	0	7652227.67	5.13	39069.4703	0.45	39069.47
21. Jul	3.66	0	7547163.02	5.12	38600.4704	0.44	38600.47
22. Jul	3.64	0	7442710.47	5.11	38134.9702	0.43	38134.97
23. Jul	3.62	0	7339028.10	5.10	37673.676	0.42	37673.68
24. Jul	3.59	0	7236008.30	5.09	37216.1102	0.41	37216.11
25. Jul	3.56	0	7133635.59	5.08	36762.2063	0.40	36762.21
26. Jul	3.53	0	7031894.90	5.07	36311.8997	0.39	36311.90
27. Jul	3.51	0	6930787.66	5.06	35865.1992	0.38	35865.20
28. Jul	3.52	0	6830443.39	5.05	35422.6776	0.37	35422.68
29. Jul	3.51	0	6731075.88	5.04	34985.2737	0.36	34985.27
16. Aug	3.29	0	5133933.51	4.89	24729.117	0.21	28080.64
17. Aug	3.31	0	5055985.16	4.88	23377.822	0.20	27750.50
18. Aug	3.32	0	4979908.47	4.88	22079.7606	0.20	27428.99
19. Aug	3.34	0	4905607.50	4.87	20832.4706	0.19	27115.65
20. Aug	3.39	0	4833059.24	4.86	19634.7654	0.18	26810.35
21. Aug	3.46	0	4762468.83	4.85	18489.133	0.17	26513.91
22. Aug	3.50	0	4693861.30	4.85	17394.9597	0.17	26226.39
23. Aug	3.52	0	4626994.59	4.84	16347.4347	0.16	25946.75
24. Aug	3.51	0	4561629.19	4.83	15342.0382	0.15	25673.94
25. Aug	3.49	0	4497554.85	4.83	14374.9438	0.15	25407.05
09. Sep	3.17	0	3705208.02	4.74	4225.3533	0.06	22153.78
10. Sep	3.13	0	3661419.61	4.74	3784.05174	0.06	21976.68
11. Sep	3.10	0	3618074.56	4.74	3362.78843	0.06	21801.67

12. Sep	3.10	0	3575196.55	4.73	2962.03016	0.05	21628.84
13. Sep	3.09	0	3532971.28	4.73	2583.67506	0.05	21458.92
14. Sep	3.08	0	3491277.40	4.72	2226.81048	0.04	21291.43
15. Sep	3.07	0	3450110.33	4.72	1891.71058	0.04	21126.32
16. Sep	3.06	0	3409452.99	4.71	1578.65005	0.03	20963.52
17. Sep	3.06	0	3369299.86	4.71	1288.13121	0.03	20803.02
18. Sep	3.07	0	3329638.73	4.71	1020.78405	0.03	20644.74
19. Sep	3.07	0	3290544.56	4.70	778.010591	0.02	20488.97
20. Sep	3.05	0	3251878.93	4.70	560.24032	0.02	20335.17
21. Sep	3.04	0	3213569.27	4.69	369.107073	0.01	20183.04
22. Sep	3.03	0	3175565.57	4.69	207.589774	0.01	20032.36
23. Sep	3.06	0	3137930.37	4.68	81.4983442	0.00	19883.39
24. Sep	3.09	0	3100769.95	4.68	4.47822438	0.00	19736.54
25. Sep	3.13	0	3064117.29	4.68	0	0.00	19591.93
26. Sep	3.17	0	3027889.87	4.67	0	0.00	19449.24
27. Sep	3.20	0	2992096.32	4.67	0	0.00	19308.47
28. Sep	3.22	0	2956659.86	4.67	0	0.00	19169.34
29. Sep	3.23	0	2921555.41	4.66	0	0.00	19031.73
30. Sep	3.25	0	2886719.57	4.66	0	0.00	18895.40
01. Okt	3.28	0	2852194.96	4.65	0	0.00	18760.50
02. Okt	3.28	0	2832461.16	4.65	0	0.00	18683.49
03. Okt	3.30	0	2812836.32	4.65	0	0.00	18606.98
04. Okt	3.31	0	2793347.19	4.65	0	0.00	18531.07
05. Okt	3.34	0	2773992.98	4.65	0	0.00	18455.75
06. Okt	3.38	0	2754881.27	4.64	0	0.00	18381.44
07. Okt	3.38	0	2736053.47	4.64	0	0.00	18308.31

Next, the calculations for the bottom slide are provided.

bottom slide		LIFE-channel	lambda:	0.6	
			hslide:	0.31	6
Hogioaia	Volume lakes	Hneu,island	Lw=	2	
m³/d	m³	m	Q Surface	h0	Manning
0	15169616.89	5.72	43781.44437	1.61	73401.56
0	15096571.52	5.72	43877.34698	1.61	73559.10
0	15022938.22	5.72	43664.44251	1.61	73209.43
0	14949013.79	5.71	43450.62565	1.60	72858.54
0	14577111.37	5.69	42373.85073	1.58	71095.55
0	14502102.34	5.68	42156.45051	1.57	70740.44
0	14426938.82	5.67	41938.52551	1.56	70384.74
0	14351562.79	5.67	41719.90647	1.56	70028.20
0	14276016.76	5.66	41500.71578	1.55	69671.00
0	14200383.01	5.66	41281.19134	1.55	69313.55
0	12577912.41	5.54	36552.79776	1.43	61682.49
0	12488022.15	5.53	36289.77672	1.42	61261.81
0	12398731.56	5.52	36028.40654	1.41	60844.16
0	12309990.08	5.52	35768.5426	1.41	60429.31
0	12221680.06	5.51	35509.84348	1.40	60016.69
0	12133598.29	5.50	35251.71647	1.39	59605.37
0	12045591.74	5.50	34993.71526	1.39	59194.63
0	11957509.03	5.49	34735.39773	1.38	58783.77
0	11869746.71	5.48	34477.92902	1.37	58374.63
0	11782438.89	5.48	34221.70569	1.37	57967.85
0	11695355.48	5.47	33966.05543	1.36	57562.34
0	11608297.44	5.46	33710.39638	1.35	57157.19
0	11521105.98	5.46	33454.2642	1.35	56751.65
0	11433946.73	5.45	33198.14764	1.34	56346.51
0	11346832.08	5.44	32942.08555	1.33	55941.82
0	9285391.68	5.27	26868.28817	1.16	46447.37
0	9187604.59	5.26	26579.95811	1.15	46001.49
0	9090080.45	5.26	26292.43755	1.15	45557.28
0	8992805.76	5.25	26005.69465	1.14	45114.69
0	8895899.30	5.24	25720.08761	1.13	44674.25
0	8799320.11	5.23	25435.50374	1.12	44235.79
0	8703237.63	5.22	25152.45031	1.11	43800.09
0	8607539.90	5.21	24870.60548	1.10	43366.63
0	8512212.36	5.21	24589.93444	1.10	42935.36
0	8417240.72	5.20	24310.4034	1.09	42506.21
0	8322628.26	5.19	24032.03025	1.08	42079.21
0	8228515.33	5.18	23755.23603	1.07	41654.99
0	8135133.59	5.17	23480.70944	1.06	41234.60
0	6607105.22	5.03	19014.45133	0.92	34440.73
0	6527923.46	5.03	18784.87758	0.92	34093.60
0	6449449.17	5.02	18557.59448	0.91	33750.12
0	6371639.80	5.01	18332.4815	0.90	33410.08
0	6294531.10	5.00	18109.64448	0.89	33073.65
0	6218412.24	5.00	17889.91977	0.89	32742.06
0	6143374.19	4.99	17673.56829	0.88	32415.71
0	6069208.04	4.98	17459.98633	0.87	32093.67
0	5995701.69	4.98	17248.56352	0.87	31775.02
0	5922670.25	4.97	17038.7704	0.86	31458.95
0	4930263.50	4.87	14218.58461	0.76	27219.56
0	4870357.45	4.86	14050.46518	0.75	26967.23
0	4810637.33	4.86	13883.14313	0.75	26716.12

0	4751154.29	4.85	13716.76497	0.74	26466.45
0	4692143.30	4.85	13551.98903	0.74	26219.20
0	4633493.08	4.84	13388.50474	0.73	25973.90
0	4575223.72	4.83	13226.36874	0.72	25730.63
0	4517341.31	4.83	13065.59838	0.72	25489.41
0	4459865.16	4.82	12906.24739	0.71	25250.32
0	4402807.42	4.82	12748.34917	0.71	25013.41
0	4346279.31	4.81	12592.21015	0.70	24779.12
0	4290151.99	4.81	12437.47311	0.70	24546.93
0	4234371.80	4.80	12283.99007	0.69	24316.60
0	4178912.44	4.79	12131.68919	0.68	24088.02
0	4123877.83	4.79	11980.85561	0.68	23861.63
0	4069427.21	4.78	11831.92323	0.67	23638.06
0	4015651.66	4.78	11685.13648	0.67	23417.67
0	3962538.00	4.77	11540.45375	0.66	23200.42
0	3910098.55	4.77	11397.90281	0.66	22986.33
0	3858244.47	4.76	11257.23691	0.65	22775.03
0	3806945.36	4.76	11118.36908	0.65	22566.38
0	3756127.94	4.75	10981.09721	0.64	22360.09
0	3705838.14	4.75	10845.54175	0.64	22156.33
0	3672307.52	4.74	10755.32382	0.63	22020.69
0	3639021.99	4.74	10665.89641	0.63	21886.21
0	3606010.40	4.73	10577.33541	0.62	21753.02
0	3573270.70	4.73	10489.63352	0.62	21621.09
0	3540921.78	4.73	10403.10676	0.62	21490.90
0	3509008.10	4.72	10317.87054	0.61	21362.62

The calculations for both the open channels are shown.

	Danube	Open channels	bed level		bed level LIFE:	3.80		
	2000-2009		Hoigaia [m]:	2.4	GW loss			
Date	hm	Surface inund.	CWB = P+ET	ET/P	1200	Surface Q	hneu	V for hneu
	m	m²	mm/d	[m³/d	m³/d	m³/d	m	m³
11. Mai	5.72	14044885.78	2.08	29213	51	165681.84	5.72	15169616.89
12. Mai	5.67	14028062.13	2.08	29178	441	164919.70	5.71	14974671.12
13. Mai	5.61	13990454.88	2.08	29100	885	163248.56	5.70	14780131.64
20. Mai	5.28	13705866.16	2.08	28508	3203	151874.76	5.60	13457073.17
21. Mai	5.23	13662010.99	2.08	28417	3570	150295.11	5.59	13273487.20
22. Mai	5.18	13617313.27	2.08	28324	3895	148726.28	5.58	13091205.12
29. Mai	4.83	13280020.76	2.08	27622	6211	138047.56	5.48	11851621.93
30. Mai	4.80	13228250.45	2.08	27515	6335	136565.56	5.47	11679741.14
31. Mai	4.80	13175613.86	2.08	27405	6192	135095.94	5.45	11509325.99
07. Jun	4.53	12749622.33	3.24	41309	7535	124390.92	5.35	10268572.94
08. Jun	4.51	12683639.93	3.24	41095	7585	122896.06	5.34	10095337.79
09. Jun	4.51	12616583.39	3.24	40878	7425	121415.60	5.33	9923761.52
17. Jun	4.52	12046426.5	3.24	39030	6031	110173.97	5.22	8619831.30
18. Jun	4.47	11970789.46	3.24	38785	6325	108837.60	5.20	8464595.60
19. Jun	4.46	11894009.94	3.24	38537	6263	107512.94	5.19	8310647.91
26. Jun	4.23	11328640.1	3.24	36705	7082	98626.85	5.10	7275472.47
27. Jun	4.20	11243699.94	3.24	36430	7166	97408.01	5.08	7133058.40
28. Jun	4.18	11157777.47	3.24	36151	7144	96202.30	5.07	6992054.47
05. Jul	3.95	10486090.33	4.68	49075	7708	87608.56	4.97	5982677.55
06. Jul	3.94	10381333.9	4.68	48585	7617	86385.55	4.96	5838285.68
07. Jul	3.96	10275614.81	4.68	48090	7267	85179.63	4.95	5695698.48
14. Jul	3.84	9511496.74	4.68	44514	6905	77213.16	4.85	4747544.12
15. Jul	3.84	9399132.052	4.68	43988	6790	76140.36	4.84	4618911.94
16. Jul	3.83	9286103.08	4.68	43459	6682	75083.95	4.83	4491993.92
23. Jul	3.62	8475795.245	4.68	39667	6852	68109.86	4.74	3647043.65
24. Jul	3.59	8357694.123	4.68	39114	6858	67172.42	4.73	3532414.79
25. Jul	3.56	8239104.388	4.68	38559	6874	66249.34	4.71	3419269.89
01. Aug	3.48	7400527.166	4.26	31526	6127	60196.04	4.63	2669861.98
02. Aug	3.47	7283896.864	4.26	31029	6048	59414.06	4.62	2572012.66
03. Aug	3.44	7167195.528	4.26	30532	6046	58644.97	4.61	2475521.60
10. Aug	3.32	5570367.585	4.26	23730	4661	49292.69	4.48	1859218.83
11. Aug	3.33	5400214.604	4.26	23005	4405	48408.33	4.46	1781535.04
12. Aug	3.34	5225154.471	4.26	22259	4180	47518.14	4.45	1705717.28
19. Aug	3.34	3845922.291	4.26	16384	2795	41131.24	4.35	1227456.19
20. Aug	3.39	3626262.471	4.26	15448	2451	40206.28	4.33	1167146.63
06. Sep	3.22	1581665.966	3.5	5536	928	24294.85	4.03	421754.40
07. Sep	3.20	1506582.891	3.5	5273	881	23308.52	4.01	390995.33
08. Sep	3.17	1431192.5	3.5	5009	846	22314.91	3.99	361533.19
15. Sep	3.07	903790.2713	3.5	3163	485	15246.66	3.82	192120.45
16. Sep	3.06	830479.8577	3.5	2907	433	14242.48	3.79	173225.05
17. Sep	3.06	758353.7295	3.5	2654	382	13247.40	3.76	155642.79
24. Sep	3.09	314406.131	3.5	1100	102	6878.77	3.54	67388.89
25. Sep	3.13	264147.3615	3.5	925	73	6112.99	3.51	59307.68
26. Sep	3.17	218210.9507	3.5	764	49	5398.28	3.48	52197.52
03. Okt	3.30	21773.82514	1.6	35	0	1999.51	3.29	23435.43
04. Okt	3.31	8815.651481	1.6	14	0	1724.41	3.27	21401.08
05. Okt	3.34	2400	1.6	4	0	1486.73	3.25	19662.56
06. Okt	3.38	2400	1.6	4	0	1281.74	3.23	18171.99
07. Okt	3.38	2400	1.6	4	0	1104.76	3.22	16886.41

Next, the closed variation is presented.

Q=0		distance Danube-island [m]			
		1200			
Surface inundated	ET/P	GW loss [m³/d]	Surface Q [m³/d]	V for Q=0	hneu
m²	m³/d	1200		m³	m
14044885.78	29213.36	50.56	165681.84	15169616.89	5.72
14059312.96	29243.37	442.39	166342.79	15140352.97	5.73
14053765.28	29231.83	888.88	166087.82	15110667.20	5.72
14012459.59	29145.92	3274.66	164220.99	14893330.82	5.71
14006192.21	29132.88	3659.92	163942.49	14860910.24	5.71
13999824.51	29119.63	4004.72	163660.79	14828117.43	5.70
13952440.24	29021.08	6525.26	161603.24	14588627.94	5.69
13945272.92	29006.17	6678.20	161297.82	14553081.60	5.68
13938042.24	28991.13	6550.36	160991.19	14517397.23	5.68
13865134.32	44923.04	8194.75	157980.96	14167137.26	5.66
13853763.27	44886.19	8284.99	157524.35	14114019.48	5.65
13842295.73	44849.04	8146.30	157067.26	14060848.30	5.65
13749627.43	44548.79	6884.06	153492.91	13645178.86	5.62
13737777.91	44510.40	7258.31	153050.50	13593746.00	5.61
13725763.32	44471.47	7226.99	152605.18	13541977.29	5.61
13638824.36	44189.79	8526.70	149476.23	13178335.61	5.58
13625841.66	44147.73	8684.62	149022.50	13125619.12	5.58
13612731.55	44105.25	8715.33	148567.74	13072786.77	5.57
13496558.85	63163.90	9921.43	144680.99	12621390.89	5.54
13477026.24	63072.48	9888.39	144051.46	12548305.57	5.54
13457319.28	62980.25	9517.09	143422.95	12475344.70	5.53
13314580.77	62312.24	9666.19	139057.94	11968823.78	5.49
13293426.43	62213.24	9602.88	138437.44	11896845.35	5.49
13272096.23	62113.41	9550.19	137818.29	11825029.24	5.48
13116136.49	61383.52	10603.78	133478.28	11321776.09	5.44
13092866.43	61274.61	10744.25	132857.31	11249788.79	5.43
13069337.08	61164.50	10903.72	132236.03	11177769.92	5.43
12898254.46	54946.56	10678.71	127906.92	10676023.24	5.39
12874920.46	54847.16	10689.64	127340.63	10610397.97	5.38
12851389.39	54746.92	10840.10	126775.10	10544861.17	5.38
12679511.94	54014.72	10610.33	122803.82	10084647.45	5.34
12654416.48	53907.81	10321.17	122246.18	10020022.40	5.33
12629233.32	53800.53	10103.80	121691.98	9955793.42	5.33
12448466.87	53030.47	9045.85	117863.77	9512042.38	5.29
12422206.65	52918.60	8397.15	117328.38	9449966.06	5.29
11983387.12	41941.85	7033.86	109057.98	8490199.76	5.20
11959247.72	41857.37	6990.02	108636.45	8441224.05	5.20
11934993.23	41772.48	7052.63	108216.10	8392376.66	5.20
11761988.65	41166.96	6317.92	105306.35	8054025.71	5.17
11736993.63	41079.48	6121.01	104898.28	8006540.83	5.16
11711969.93	40991.89	5901.89	104492.73	7959340.35	5.16
11536844.20	40378.95	3743.90	101734.95	7638114.73	5.13
11512117.99	40292.41	3166.15	101356.47	7593991.87	5.12
11487602.21	40206.61	2568.51	100983.77	7550533.31	5.12
11345868.38	18153.39	0.00	98877.43	7304736.36	5.10
11335190.08	18136.30	0.00	98721.98	7286582.97	5.10
11324492.48	18119.19	0.00	98566.70	7268446.66	5.09
11313775.63	18102.04	0.00	98411.57	7250327.48	5.09
11303039.52	18084.86	0.00	98256.61	7232225.44	5.09

The next sheets show the results for the broad-crested weir with a LIFE-channel 100% closed, 70%-closed, and 80%-closed:

broad-crested weir		Hogioaia channel:	Cd=	0.50			
LIFE:100% closed			hweir=	2.70			
Sigma	**h_u/h**	**Manning**	**h0**	**Lw**	**Surface inund.**	**ET/P**	**GW loss**
-	-	m^3/s	m	m	m^2	m^3/d	m^3/d
0.30	0.99	475226.70	0.62	8	14044885.78	29213.362	50.5615888
0.70	0.93	473631.74	0.61	8	14031152.07	29184.796	453.144983
0.90	0.87	465406.14	0.59	8	13958101.52	29032.851	765.347043
1.00	0.00	407647.46	0.39	8	13320322.42	27706.271	2044.7097
1.00	0.00	401485.95	0.37	8	13236875.44	27532.701	2319.16346
1.00	0.00	395776.27	0.35	8	13156416.66	27365.347	2566.18153
1.00	0.00	365444.74	0.24	8	12672868.81	26359.567	4619.67086
1.00	0.00	362157.88	0.23	8	12614216.66	26237.571	4748.87063
1.00	0.00	359072.43	0.21	8	12557941.45	26120.518	4630.7554
1.00	0.00	340246.85	0.14	8	12187359.71	39487.045	6206.63228
1.00	0.00	338056.87	0.13	8	12141021.68	39336.91	6317.41955
1.00	0.00	335975.34	0.12	8	12096317.46	39192.069	6231.18759
1.00	0.00	322556.66	0.07	8	11791943.69	38205.898	5524.27233
1.00	0.00	321180.83	0.07	8	11759081.47	38099.424	5901.81031
1.00	0.00	319848.11	0.06	8	11726942.97	37995.295	5932.72484
1.00	0.00	311599.22	0.03	8	11521129.94	37328.461	7455.30344
1.00	0.00	310529.40	0.02	8	11493543.5	37239.081	7649.01114
1.00	0.00	309480.25	0.02	8	11466285.05	37150.764	7735.23808
1.00	0.00	301032.93	0.00	8	11239209.64	52599.501	9132.42841
1.00	0.00	299688.17	0.00	8	11201775.97	52424.312	9152.89449
1.00	0.00	298347.21	0.00	8	11164086	52247.922	8891.48346
1.00	0.00	289083.36	0.00	8	10893512.61	50981.639	9305.59938
1.00	0.00	287774.12	0.00	8	10853789.03	50795.733	9289.83885
1.00	0.00	286469.76	0.00	8	10813835.84	50608.752	9281.58113
1.00	0.00	277390.46	0.00	8	10524949.53	49256.764	10330.3369
1.00	0.00	276101.21	0.00	8	10482348.61	49057.392	10464.1839
1.00	0.00	274813.95	0.00	8	10439409.06	48856.434	10611.2409
1.00	0.00	265920.04	0.00	8	10131318.39	43159.416	10531.1955
1.00	0.00	264763.37	0.00	8	10089737.62	42982.282	10551.4302
1.00	0.00	263610.64	0.00	8	10047940.6	42804.227	10679.4646
1.00	0.00	255561.60	0.00	8	9745836.067	41517.262	10982.0931
1.00	0.00	254435.79	0.00	8	9702107.374	41330.977	10784.4085
1.00	0.00	253318.81	0.00	8	9658353.744	41144.587	10643.8593
1.00	0.00	245658.55	0.00	8	9348113.161	39822.962	10058.6521
1.00	0.00	244594.26	0.00	8	9303562.62	39633.177	9608.30342
1.00	0.00	228280.27	0.00	8	8572991.953	30005.472	9449.7487
1.00	0.00	227447.32	0.00	8	8533151.43	29866.03	9490.9624
1.00	0.00	226616.92	0.00	8	8493173.304	29726.107	9610.7466
1.00	0.00	220870.57	0.00	8	8209255.477	28732.394	9703.83455
1.00	0.00	220063.43	0.00	8	8168334.222	28589.17	9666.67534
1.00	0.00	219260.57	0.00	8	8127369.161	28445.792	9617.72467
1.00	0.00	213771.87	0.00	8	7840193.071	27440.676	8927.15923
1.00	0.00	213012.39	0.00	8	7799454.489	27298.091	8650.95115
1.00	0.00	212262.12	0.00	8	7758965.454	27156.379	8360.87538
1.00	0.00	207819.12	0.00	8	7514113.341	12022.581	7300.77961
1.00	0.00	207417.55	0.00	8	7491546.857	11986.475	7202.752
1.00	0.00	207018.91	0.00	8	7469072.096	11950.515	6997.78558
1.00	0.00	206625.42	0.00	8	7446815.85	11914.905	6751.36099
1.00	0.00	206237.92	0.00	8	7424828.849	11879.726	6725.85827

		LIFE-channel:	broad-crested weir		Hogioaia channel:	Cd=	0.50
			LIFE:70% closed			hweir=	2.73
Surface Q	Volume lakes	Hneu,island	Sigma	h_u/h	Manning	h0	Lw
m^3/d	m^3	m	-	-	m^3/s	m	m
149465.4332	15169616.89	5.72	0.30	0.99	475226.70	0.59	8
344420.6113	14990887.53	5.71	0.70	0.93	472253.05	0.58	8
414297.5801	14616828.98	5.69	0.90	0.88	463057.39	0.55	8
250663.4982	11988491.61	5.49	1.00	0.00	402255.26	0.34	8
230002.6228	11708077.13	5.47	1.00	0.00	396017.92	0.32	8
211230.9133	11448222.64	5.45	1.00	0.00	390328.65	0.30	8
118714.6306	10067479.41	5.34	1.00	0.00	361561.76	0.19	8
109555.228	9917785.54	5.33	1.00	0.00	358588.41	0.18	8
101139.877	9777243.87	5.31	1.00	0.00	355821.97	0.17	8
54215.32146	8919142.85	5.24	1.00	0.00	339203.70	0.11	8
49327.46624	8819233.85	5.23	1.00	0.00	337306.54	0.10	8
44809.99582	8724252.05	5.22	1.00	0.00	335509.00	0.09	8
19170.56608	8111385.93	5.17	1.00	0.00	323995.25	0.05	8
16941.4559	8048485.19	5.17	1.00	0.00	322807.45	0.04	8
14866.52921	7987542.50	5.16	1.00	0.00	321650.13	0.04	8
4216.359349	7610039.22	5.13	1.00	0.00	314253.96	0.01	8
3175.304133	7561039.09	5.12	1.00	0.00	313255.71	0.00	8
2252.970939	7512975.70	5.12	1.00	0.00	312264.40	0.00	8
0	7125614.53	5.08	1.00	0.00	303846.52	0.00	8
0	7063882.60	5.08	1.00	0.00	302489.56	0.00	8
0	7002305.40	5.07	1.00	0.00	301136.34	0.00	8
0	6576337.68	5.03	1.00	0.00	291785.18	0.00	8
0	6516050.44	5.02	1.00	0.00	290463.24	0.00	8
0	6455964.87	5.02	1.00	0.00	289146.12	0.00	8
0	6037052.49	4.98	1.00	0.00	279975.45	0.00	8
0	5977465.39	4.97	1.00	0.00	278672.84	0.00	8
0	5917943.82	4.97	1.00	0.00	277372.17	0.00	8
0	5505918.54	4.93	1.00	0.00	268382.83	0.00	8
0	5452227.93	4.92	1.00	0.00	267213.25	0.00	8
0	5398694.21	4.92	1.00	0.00	266047.58	0.00	8
0	5024138.59	4.88	1.00	0.00	257905.98	0.00	8
0	4971639.24	4.87	1.00	0.00	256766.88	0.00	8
0	4919523.85	4.87	1.00	0.00	255636.63	0.00	8
0	4561322.26	4.83	1.00	0.00	247883.09	0.00	8
0	4511440.65	4.83	1.00	0.00	246805.51	0.00	8
0	3742891.38	4.75	1.00	0.00	230276.45	0.00	8
0	3703436.16	4.74	1.00	0.00	229431.89	0.00	8
0	3664079.17	4.74	1.00	0.00	228589.87	0.00	8
0	3391092.61	4.71	1.00	0.00	222761.77	0.00	8
0	3352656.39	4.71	1.00	0.00	221942.96	0.00	8
0	3314400.54	4.70	1.00	0.00	221128.43	0.00	8
0	3052228.91	4.68	1.00	0.00	215558.72	0.00	8
0	3015861.08	4.67	1.00	0.00	214787.84	0.00	8
0	2979912.03	4.67	1.00	0.00	214026.26	0.00	8
0	2766559.79	4.64	1.00	0.00	209514.40	0.00	8
0	2747236.43	4.64	1.00	0.00	209106.18	0.00	8
0	2728047.20	4.64	1.00	0.00	208700.92	0.00	8
0	2709098.90	4.64	1.00	0.00	208300.86	0.00	8
0	2690432.63	4.64	1.00	0.00	207906.88	0.00	8

		distance Danube-island [m]			LIFE-channel	Cd=
		1200				hweir=
Surface inund.	ET/P	GW loss	Surface Q	Volume lakes	Hneu,island	Lw=
m²	m³/d	m³/d	m³/d	m³	m	Q Surface
14044885.78	29213.3624	50.5615888	138749.443	15169616.89	5.72	73401.56
14019169.74	29159.8731	407.7832062	315878.7494	14928201.96	5.71	72759.78
13936538.02	28987.9991	687.1447664	375133.8551	14509995.78	5.68	70777.80
13247482.96	27554.7646	1851.17157	205080.8445	11743088.98	5.47	49381.69
13159884.7	27372.5602	2120.280541	185408.567	11459220.51	5.45	44031.58
13076720.77	27199.5792	2365.523086	167897.2816	11200287.53	5.43	39291.74
12603436.9	26215.1488	4461.146573	86944.07994	9890634.18	5.32	17818.86
12549004.69	26101.9298	4601.763822	79441.81439	9755194.95	5.31	15888.58
12497350.36	25994.4887	4496.729404	72635.47263	9629160.87	5.30	14152.04
12165375.89	39415.8179	6159.480279	35825.70787	8871556.24	5.24	5156.99
12124982.02	39284.9417	6283.204121	32140.20636	8784998.24	5.23	4319.98
12086212.73	39159.3292	6209.900906	28762.75638	8702969.91	5.22	3571.52
11825965.53	38316.1283	5589.849793	10231.35354	8177142.13	5.18	154.90
11797899.42	38225.1941	5977.417991	8684.698776	8122849.90	5.17	20.42
11770326.69	38135.8585	6016.847315	7258.317606	8069942.18	5.17	0.00
11588685.46	37547.3409	7590.524435	561.5018809	7731590.19	5.14	0.00
11563432.26	37465.5205	7789.473877	135.0721135	7685890.82	5.13	0.00
11538176.62	37383.6922	7879.65701	0	7640500.75	5.13	0.00
11316372	52960.6209	9291.751759	0	7254712.65	5.09	0.00
11279351.76	52787.3662	9312.425671	0	7192460.28	5.09	0.00
11242073.08	52612.902	9049.254987	0	7130360.48	5.08	0.00
10974306.09	51359.7525	9466.769412	0	6700680.13	5.04	0.00
10934973.14	51175.6743	9450.960634	0	6639853.61	5.04	0.00
10895407.29	50990.5061	9442.708507	0	6579226.97	5.03	0.00
10609160.67	49650.8719	10500.32031	0	6156446.79	4.99	0.00
10566925.16	49453.2098	10635.38365	0	6096295.60	4.98	0.00
10524347.75	49253.9475	10783.78322	0	6036207.00	4.98	0.00
10218671.15	43531.5391	10704.14683	0	5620153.15	4.94	0.00
10177386.58	43355.6668	10724.68846	0	5565917.46	4.93	0.00
10135881.38	43178.8547	10853.97615	0	5511837.11	4.93	0.00
9835716.345	41900.1516	11160.41938	0	5133373.19	4.89	0.00
9792242.584	41714.9534	10961.06557	0	5080312.62	4.89	0.00
9748737.367	41529.6212	10819.35466	0	5027636.60	4.88	0.00
9440073.045	40214.7112	10229.41014	0	4665491.03	4.84	0.00
9395721.888	40025.7752	9774.706196	0	4615046.91	4.84	0.00
8667421.893	30335.9766	9615.591202	0	3837356.38	4.76	0.00
8627649.237	30196.7723	9657.311958	0	3797404.81	4.75	0.00
8587734.17	30057.0696	9778.48406	0	3757550.73	4.75	0.00
8304119.92	29064.4197	9873.114543	0	3481061.40	4.72	0.00
8263221.339	28921.2747	9835.60075	0	3442123.87	4.72	0.00
8222273.618	28777.9577	9786.154369	0	3403366.99	4.71	0.00
7935068.277	27772.739	9087.771719	0	3137704.41	4.68	0.00
7894303.8	27630.0633	8808.24325	0	3100843.90	4.68	0.00
7853783.449	27488.2421	8514.645066	0	3064405.60	4.68	0.00
7608577.446	12173.7239	7441.190991	0	2848062.64	4.65	0.00
7585948.808	12137.5181	7341.863366	0	2828447.72	4.65	0.00
7563410.416	12101.4567	7134.240925	0	2808968.34	4.65	0.00
7541089.141	12065.7426	6884.623956	0	2789732.64	4.65	0.00
7519035.789	12030.4573	6858.718276	0	2770782.28	4.64	0.00

0.58		broad-crested weir		Hogioaia channel:	Cd=	0.50		
1.37		LIFE:80% closed			hweir=	2.71		
2		Sigma	h_u/h	Manning	h0	Lw	Surface inund.	ET/P
h0	Manning	-	-	m^3/s	m	m	m^2	m^3/d
0.55	73401.56	0.30	0.99	475226.70	0.61	8	14044885.78	29213.362
0.54	72759.78	0.70	0.93	472549.03	0.60	8	14021750.86	29165.242
0.51	70777.80	0.90	0.88	463454.34	0.57	8	13940204.88	28995.626
0.30	57784.58	1.00	0.00	404721.28	0.37	8	13281120.18	27624.73
0.28	56463.97	1.00	0.00	398777.40	0.35	8	13199091.28	27454.11
0.26	55261.62	1.00	0.00	393315.91	0.33	8	13120784.24	27291.231
0.15	49217.04	1.00	0.00	364814.01	0.23	8	12661716.11	26336.37
0.14	48595.82	1.00	0.00	361728.74	0.21	8	12606460.9	26221.439
0.13	48018.46	1.00	0.00	358827.38	0.20	8	12553420.58	26111.115
0.07	44563.69	1.00	0.00	340915.96	0.13	8	12201377.04	39532.462
0.06	44170.82	1.00	0.00	338815.93	0.13	8	12157162.82	39389.208
0.05	43798.88	1.00	0.00	336816.81	0.12	8	12114467.58	39250.875
0.01	41423.65	1.00	0.00	323853.72	0.07	8	11822633.62	38305.333
0.00	41179.34	1.00	0.00	322515.66	0.06	8	11790968.9	38202.739
0.00	40941.44	1.00	0.00	321217.44	0.06	8	11759959.89	38102.27
0.00	39424.24	1.00	0.00	313133.93	0.02	8	11560339.15	37455.499
0.00	39219.90	1.00	0.00	312078.20	0.02	8	11533413.09	37368.258
0.00	39017.08	1.00	0.00	311040.90	0.01	8	11506759.15	37281.9
0.00	37299.13	1.00	0.00	302593.37	0.00	8	11282196.6	52800.68
0.00	37022.93	1.00	0.00	301241.82	0.00	8	11244991.96	52626.562
0.00	36747.70	1.00	0.00	299894.03	0.00	8	11207529.81	52451.24
0.00	34851.64	1.00	0.00	290581.59	0.00	8	10938510.09	51192.227
0.00	34584.45	1.00	0.00	289265.29	0.00	8	10899002.65	51007.332
0.00	34318.45	1.00	0.00	287953.83	0.00	8	10859263.74	50821.354
0.00	32472.53	1.00	0.00	278823.69	0.00	8	10571836.86	49476.196
0.00	32211.23	1.00	0.00	277527.01	0.00	8	10529437.83	49277.769
0.00	31950.55	1.00	0.00	276232.29	0.00	8	10486698.32	49077.748
0.00	30155.38	1.00	0.00	267285.30	0.00	8	10179940.05	43366.545
0.00	29922.67	1.00	0.00	266121.46	0.00	8	10138522.59	43190.106
0.00	29690.95	1.00	0.00	264961.52	0.00	8	10096886.42	43012.736
0.00	28078.26	1.00	0.00	256861.03	0.00	8	9795849.784	41730.32
0.00	27853.46	1.00	0.00	255727.83	0.00	8	9752261.278	41544.633
0.00	27630.62	1.00	0.00	254603.47	0.00	8	9708644.199	41358.824
0.00	26107.68	1.00	0.00	246891.36	0.00	8	9399268.676	40040.885
0.00	25896.84	1.00	0.00	245819.70	0.00	8	9354827.334	39851.564
0.00	22690.02	1.00	0.00	229386.23	0.00	8	8625491.375	30189.22
0.00	22527.62	1.00	0.00	228546.83	0.00	8	8585687.06	30049.905
0.00	22365.86	1.00	0.00	227709.98	0.00	8	8545742.464	29910.099
0.00	21250.43	1.00	0.00	221918.24	0.00	8	8261982.587	28916.939
0.00	21094.32	1.00	0.00	221104.62	0.00	8	8221072.384	28773.753
0.00	20939.18	1.00	0.00	220295.28	0.00	8	8180115.412	28630.404
0.00	19882.50	1.00	0.00	214761.61	0.00	8	7892912.276	27625.193
0.00	19736.83	1.00	0.00	213995.80	0.00	8	7852157.785	27482.552
0.00	19593.07	1.00	0.00	213239.26	0.00	8	7811649.842	27340.774
0.00	18744.37	1.00	0.00	208758.05	0.00	8	7566592.122	12106.547
0.00	18667.84	1.00	0.00	208352.79	0.00	8	7543990.311	12070.384
0.00	18591.91	1.00	0.00	207950.48	0.00	8	7521479.408	12034.367
0.00	18517.00	1.00	0.00	207553.35	0.00	8	7499186.253	11998.698
0.00	18443.26	1.00	0.00	207162.25	0.00	8	7477161.622	11963.459

distance Danube-island [m]			LIFE-channel	Cd=	0.50	
1200				hweir=	1.57	
GW loss	Surface Q	Volume lakes	Hneu,island	Lw=	2	
m³/d	m³/d	m³	m	Q Surface	h0	Manning
50.5615888	145863.9545	15169616.89	5.72	52829.2021	0.35	73401.56
417.5219635	333141.0221	14941659.81	5.71	50884.3694	0.34	72823.64
700.3620356	397114.817	14528051.65	5.68	44416.159	0.31	70863.27
1939.661311	231403.7048	11855319.48	5.48	9542.92681	0.11	58307.40
2220.626172	211921.9127	11584808.45	5.46	6965.49231	0.09	57047.91
2475.534439	194385.3277	11336246.31	5.44	4831.44139	0.07	55892.66
4593.924442	109585.8737	10038755.86	5.34	0	0.00	49897.33
4731.187252	101206.2545	9898239.69	5.32	0	0.00	49251.95
4620.651815	93494.22509	9766080.81	5.31	0	0.00	48645.72
6236.868295	50029.47014	8949664.02	5.24	0	0.00	44918.55
6352.023665	45472.67403	8853865.22	5.24	0	0.00	44483.36
6269.589313	41256.91904	8762651.32	5.23	0	0.00	44069.45
5583.398376	17273.20479	8170673.41	5.18	0	0.00	41394.53
5963.856952	15186.0864	8109511.47	5.17	0	0.00	41119.35
5996.650806	13244.01294	8050158.79	5.17	0	0.00	40852.52
7533.501571	3351.592542	7680315.04	5.13	0	0.00	39194.98
7728.838553	2409.401418	7631974.44	5.13	0	0.00	38979.00
7816.226009	1589.084257	7584467.95	5.12	0	0.00	38766.91
9220.849834	0	7197223.36	5.09	0	0.00	37044.05
9241.43007	0	7135201.83	5.08	0	0.00	36769.14
8979.037175	0	7073333.83	5.08	0	0.00	36495.21
9395.034763	0	6645300.45	5.04	0	0.00	34608.36
9379.245719	0	6584713.19	5.03	0	0.00	34342.51
9370.989479	0	6524326.61	5.03	0	0.00	34077.85
10424.66466	0	6103262.68	4.99	0	0.00	32241.48
10559.18704	0	6043361.81	4.98	0	0.00	31981.57
10706.9897	0	5983524.86	4.97	0	0.00	31722.28
10627.15902	0	5569259.08	4.93	0	0.00	29937.00
10647.56288	0	5515265.38	4.93	0	0.00	29705.63
10776.29313	0	5461427.71	4.92	0	0.00	29475.23
11081.03238	0	5084699.11	4.89	0	0.00	27872.03
10882.41722	0	5031887.76	4.88	0	0.00	27648.59
10741.21996	0	4979460.71	4.88	0	0.00	27427.10
10153.36584	0	4619066.84	4.84	0	0.00	25913.63
9700.592972	0	4568872.59	4.83	0	0.00	25704.14
9541.704847	0	3795244.11	4.75	0	0.00	22518.85
9583.199364	0	3755513.19	4.75	0	0.00	22357.60
9703.754052	0	3715880.08	4.75	0	0.00	22196.99
9797.691646	0	3440948.07	4.72	0	0.00	21089.61
9760.334245	0	3402233.44	4.71	0	0.00	20934.65
9711.106961	0	3363699.35	4.71	0	0.00	20780.65
9016.190216	0	3099589.24	4.68	0	0.00	19731.88
8738.136236	0	3062947.86	4.68	0	0.00	19587.32
8446.102426	0	3026727.17	4.67	0	0.00	19444.66
7378.581159	0	2811714.76	4.65	0	0.00	18602.61
7279.831187	0	2792229.63	4.65	0	0.00	18526.72
7073.389132	0	2772879.41	4.65	0	0.00	18451.42
6825.191002	0	2753771.66	4.64	0	0.00	18377.13
6799.464341	0	2734947.77	4.64	0	0.00	18304.02

The following sheets represent the extreme events. Scenario 1 was selected as an example. First, the year 2003 is summarised. One third of the computed days is shown.

Scenario 1 Sohlhöhe Hoigaia	2.4	2003	Cd=	0.80			Distance Danube-lakes [m]:			
Closed LIFE-channel		Bag weir	hweir=	3.02			1200			
		ET	Manning	h0	Lw	Surface inundated	ET/P	GW loss	Surface Q	Volumen lakes	H,island
Date	2003	mm/d	m³/s	m	m	m²	m³/d	m³/d	m³/d	m³	m
23. Jan	5.77	-1.2	896436.00	0.35	8	14172818.97	-17007.38	0	338106.8935	15875119.05	5.77
24. Jan	5.66	-1.2	887944.23	0.33	8	14134350.04	-16961.22	962.2625	315975.6037	15554019.53	5.75
25. Jan	5.51	-1.2	876433.37	0.31	8	14080354.22	-16896.43	2265.604	286593.2357	15254042.89	5.73
26. Jan	5.34	-1.2	865996.67	0.29	8	14029474.79	-16835.37	3780.175	260604.1148	14982080.47	5.71
27. Jan	5.14	-1.2	856495.48	0.28	8	13981493.68	-16777.79	5602.969	237518.1717	14734531.55	5.70
28. Jan	5.04	-1.2	847806.54	0.26	8	13936170.42	-16723.4	6425.294	216913.7217	14508188.21	5.68
29. Jan	4.96	-1.2	839873.19	0.25	8	13893538.78	-16672.25	7056.756	198549.3513	14301572.59	5.67
30. Jan	4.89	-1.2	832617.09	0.23	8	13853466.56	-16624.16	7597.869	182147.9286	14112638.73	5.65
31. Jan	4.86	-1.2	825966.68	0.22	8	13815805.25	-16578.97	7750.028	167464.5118	13939517.10	5.64
01. Feb	4.86	-1	819871.29	0.21	8	13780480.37	-13780.48	7614.861	154314.1144	13780881.52	5.63
18. Feb	4.93	-1	765207.01	0.10	8	13425787.36	-13425.79	5711.701	52312.59846	12360189.32	5.52
19. Feb	4.85	-1	763488.50	0.10	8	13413432.78	-13413.43	6446.005	49672.89455	12315590.81	5.52
20. Feb	4.75	-1	761842.78	0.09	8	13401527.18	-13401.53	7373.528	47184.89878	12272885.34	5.51
21. Feb	4.62	-1	760256.59	0.09	8	13389982.97	-13389.98	8589.946	44824.68356	12231728.45	5.51
22. Feb	4.39	-1	758713.91	0.09	8	13378689.72	-13378.69	10768.51	42565.5664	12191703.80	5.51
23. Feb	4.22	-1	757173.77	0.08	8	13367350.04	-13367.35	12365.88	40346.74419	12151748.42	5.50
24. Feb	4.12	-1	755657.02	0.08	8	13356118.68	-13356.12	13287.9	38198.15411	12112403.14	5.50
25. Feb	3.98	-1	754187.00	0.08	8	13345172.49	-13345.17	14593.87	36151.1593	12074273.21	5.50
26. Feb	3.84	-1	752745.01	0.08	8	13334376.45	-13334.38	15898.36	34177.84346	12036873.35	5.50
27. Feb	3.76	-1	751328.27	0.07	8	13323712.7	-13323.71	16625.77	32273.2975	12000131.52	5.49
25. Mrz	4.95	0.63	718720.21	0.01	8	13061932.22	8229.017	4482.757	886.7451911	11155262.83	5.43
26. Mrz	4.91	0.63	718194.89	0.01	8	13057446.32	8226.191	4847.075	679.083828	11141664.31	5.43
27. Mrz	4.85	0.63	717663.62	0.00	8	13052900.49	8223.327	5398.959	488.6773925	11127911.96	5.42
28. Mrz	4.81	0.63	717118.48	0.00	8	13048226.49	8220.383	5762.231	316.2669	11113801.00	5.42
29. Mrz	4.75	0.63	716566.06	0.00	8	13043480.28	8217.393	6312.887	169.1256662	11099502.12	5.42
30. Mrz	4.68	0.63	715998.15	0.00	8	13038590.64	8214.312	6956.638	54.04066527	11084802.71	5.42
31. Mrz	4.63	0.63	715409.92	0.00	8	13033514.93	8211.114	7411.713	0	11069577.72	5.42
01. Apr	4.58	1.15	714806.30	0.00	8	13028294.68	14982.54	7866.04	0	11053954.89	5.42
02. Apr	4.51	1.15	713923.46	0.00	8	13020638.2	14973.73	8500.512	0	11031106.32	5.42
03. Apr	4.45	1.15	713016.41	0.00	8	13012745.03	14964.66	9039.891	0	11007632.07	5.41
19. Apr	4.95	1.15	698081.67	0.00	8	12878806.83	14810.63	4021.494	0	10621283.73	5.38
20. Apr	4.98	1.15	697353.41	0.00	8	12872079.52	14802.89	3727.181	0	10602451.61	5.38
21. Apr	4.98	1.15	696636.80	0.00	8	12865441.69	14795.26	3711.309	0	10583921.53	5.38
24. Apr	4.87	1.15	694435.04	0.00	8	12844933.58	14771.67	4679.867	0	10526992.18	5.38
25. Apr	4.8	1.15	693682.69	0.00	8	12837886.45	14763.57	5309.679	0	10507540.64	5.37
26. Apr	4.74	1.15	692906.27	0.00	8	12830592.64	14755.18	5845.824	0	10487467.39	5.37
27. Apr	4.68	1.15	692109.41	0.00	8	12823084.36	14746.55	6380.841	0	10466866.38	5.37
28. Apr	4.61	1.15	691292.15	0.00	8	12815360.25	14737.66	7006.974	0	10445739.00	5.37
13. Mai	4.08	2.08	671205.01	0.00	8	12617744.18	26244.91	11325.22	0	9926694.46	5.33
14. Mai	3.98	2.08	669750.39	0.00	8	12602836.17	26213.9	12190.88	0	9889124.33	5.32
15. Mai	3.88	2.08	668263.37	0.00	8	12587510.04	26182.02	13053.35	0	9850719.55	5.32
16. Mai	3.83	2.08	666744.10	0.00	8	12571761.17	26149.26	13459.97	0	9811484.18	5.32
17. Mai	3.76	2.08	665210.27	0.00	8	12555768.06	26116	14045.74	0	9771874.95	5.31
18. Mai	3.72	2.08	663654.96	0.00	8	12539454.67	26082.07	14358.28	0	9731713.22	5.31
19. Mai	3.62	2.08	662088.77	0.00	8	12522928.58	26047.69	15210.46	0	9691272.87	5.31
20. Mai	3.53	2.08	660490.83	0.00	8	12505964.72	26012.41	15969.07	0	9650014.72	5.30
21. Mai	3.46	2.08	658864.78	0.00	8	12488595.38	25976.28	16544.59	0	9608033.25	5.30
22. Mai	3.42	2.08	657217.75	0.00	8	12470891.03	25939.45	16848.16	0	9565512.38	5.30
04. Jun	3.66	3.24	632270.48	0.00	8	12188533.43	39490.85	13879.16	0	8921693.11	5.24
05. Jun	3.63	3.24	630201.84	0.00	8	12163876.54	39410.96	14073.5	0	8868323.10	5.24
06. Jun	3.56	3.24	628128.69	0.00	8	12138967.12	39330.25	14616.08	0	8814838.64	5.23
07. Jun	3.41	3.24	626037.58	0.00	8	12113638.44	39248.19	15853.11	0	8760892.30	5.23
08. Jun	3.31	3.24	623901.65	0.00	8	12087554.05	39163.68	16647.67	0	8705791.00	5.22

09. Jun	**3.24**	**3.24**	621738.14	0.00	8	12060911.75	39077.35	17176.7	0	8649979.66	5.22
10. Jun	**3.2**	**3.24**	619557.42	0.00	8	12033830.3	38989.61	17442.25	0	8593725.60	5.21
18. Jun	**2.79**	**3.24**	601803.81	0.00	8	11804598.86	38246.9	20252.4	0	8135769.16	5.17
19. Jun	**2.7**	**3.24**	599536.02	0.00	8	11774158.66	38148.27	20919.11	0	8077269.87	5.17
20. Jun	**2.68**	**3.24**	597246.24	0.00	8	11743148.69	38047.8	20988.68	0	8018202.48	5.16
21. Jun	**2.6**	**3.24**	594957.72	0.00	8	11711877.17	37946.48	21563	0	7959166.00	5.16
22. Jun	**2.56**	**3.24**	592650.93	0.00	8	11680071.47	37843.43	21796.11	0	7899656.52	5.15
08. Jul	**2.07**	**4.68**	548593.13	0.00	8	11013799.6	51544.58	23614.23	0	6762323.89	5.05
09. Jul	**2.01**	**4.68**	545684.79	0.00	8	10965597.98	51319	23929.12	0	6687165.08	5.04
10. Jul	**1.91**	**4.68**	542773.54	0.00	8	10916786.39	51090.56	24553.16	0	6611916.96	5.03
11. Jul	**1.81**	**4.68**	539847.58	0.00	8	10867154.38	50858.28	25168.32	0	6536273.24	5.03
12. Jul	**1.75**	**4.68**	536907.43	0.00	8	10816694.99	50622.13	25462.9	0	6460246.63	5.02
13. Jul	**1.73**	**4.68**	533965.68	0.00	8	10765611.85	50383.06	25441.9	0	6384161.60	5.01
14. Jul	**1.7**	**4.68**	531034.68	0.00	8	10714114.37	50142.06	25496.15	0	6308336.63	5.01
15. Jul	**1.74**	**4.68**	528111.61	0.00	8	10662151.2	49898.87	25010.19	0	6232698.43	5.00
16. Jul	**1.74**	**4.68**	525217.47	0.00	8	10610098.99	49655.26	24833.5	0	6157789.37	4.99
17. Jul	**1.76**	**4.68**	522340.33	0.00	8	10557750.01	49410.27	24504.77	0	6083300.61	4.98
02. Aug	**1.76**	**4.26**	479287.44	0.00	8	9697132.325	41309.78	21743.35	0	4965692.67	4.87
03. Aug	**1.78**	**4.26**	476866.28	0.00	8	9644104.351	41083.88	21441.72	0	4902639.54	4.87
04. Aug	**1.78**	**4.26**	474466.35	0.00	8	9591018.377	40857.74	21280.34	0	4840113.94	4.86
05. Aug	**1.78**	**4.26**	472082.27	0.00	8	9537761.866	40630.87	21119.23	0	4777975.86	4.86
06. Aug	**1.74**	**4.26**	469714.08	0.00	8	9484339.94	40403.29	21231.54	0	4716225.77	4.85
07. Aug	**1.73**	**4.26**	467351.32	0.00	8	9430518.153	40174.01	21136.63	0	4654590.94	4.84
08. Aug	**1.74**	**4.26**	465002.01	0.00	8	9376479.716	39943.8	20906.04	0	4593280.30	4.84
09. Aug	**1.75**	**4.26**	462671.39	0.00	8	9322350.078	39713.21	20676.73	0	4532430.46	4.83
10. Aug	**1.77**	**4.26**	460359.44	0.00	8	9268135.24	39482.26	20381.97	0	4472040.52	4.82
11. Aug	**1.81**	**4.26**	458068.65	0.00	8	9213901.946	39251.22	19956.79	0	4412176.30	4.82
27. Aug	**1.27**	**4.26**	422787.22	0.00	8	8309564.863	35398.75	20652.08	0	3486262.54	4.72
28. Aug	**1.28**	**3.5**	420661.53	0.00	8	8250661.24	28877.31	20410.94	0	3430211.71	4.72
29. Aug	**1.28**	**3.5**	418793.37	0.00	8	8198451.877	28694.58	20250.84	0	3380923.45	4.71
30. Aug	**1.28**	**3.5**	416939.19	0.00	8	8146220.763	28511.77	20091.23	0	3331978.03	4.71
31. Aug	**1.26**	**3.5**	415098.97	0.00	8	8093972.764	28328.9	20048.68	0	3283375.03	4.70
01. Sep	**1.23**	**3.5**	413268.29	0.00	8	8041586.074	28145.55	20062.65	0	3234997.44	4.70
02. Sep	**1.14**	**3.5**	411445.02	0.00	8	7989001.968	27961.51	20419.43	0	3186789.24	4.69
03. Sep	**1.14**	**3.5**	409616.24	0.00	8	7935844.518	27775.46	20253.87	0	3138408.30	4.68
04. Sep	**1.1**	**3.5**	407801.76	0.00	8	7882689.249	27589.41	20315.9	0	3090378.97	4.68
05. Sep	**1.07**	**3.5**	405993.01	0.00	8	7829287.274	27402.51	20318.27	0	3042473.66	4.67
21. Sep	**1.53**	**3.5**	371886.45	0.00	8	6739663.085	23588.82	14773.7	0	2344807.46	4.57
22. Sep	**1.53**	**3.5**	370298.66	0.00	8	6684854.486	23396.99	14630.59	0	2306444.94	4.57
24. Sep	**1.5**	**3.5**	367118.08	0.00	8	6573895.262	23008.63	14484.35	0	2230391.81	4.56
25. Sep	**1.54**	**3.5**	365533.37	0.00	8	6518021.443	22813.08	14151.02	0	2192898.83	4.56
26. Sep	**1.58**	**3.5**	363959.73	0.00	8	6462145.993	22617.51	13821.39	0	2155934.74	4.55
27. Sep	**1.63**	**1.6**	362397.14	0.00	8	6406272.73	10250.04	13449.35	0	2119495.84	4.55
28. Sep	**1.66**	**1.6**	361374.64	0.00	8	6369499.839	10191.2	13220.28	0	2095796.45	4.54
29. Sep	**1.61**	**1.6**	360359.65	0.00	8	6332829.899	10132.53	13358.03	0	2072384.97	4.54
30. Sep	**1.58**	**1.6**	359336.21	0.00	8	6295685.517	10073.1	13401.49	0	2048894.42	4.54
16. Okt	**1.45**	**1.6**	331384.57	0.00	8	5211700.06	8338.72	11253.95	0	1700055.04	4.45
17. Okt	**1.63**	**1.6**	330250.38	0.00	8	5164718.856	8263.55	10469.66	0	1680462.37	4.45
18. Okt	**1.93**	**1.6**	329156.39	0.00	8	5119168.917	8190.67	9258.655	0	1661729.16	4.44
31. Okt	2.96	1.6	318264.29	0.00	8	4652780.154	7444.45	4846.48	0	1483831.06	4.41

In a next step, the broad-crested weir for 2003 was computed.

2003			Cd=	0.50			Distance Danube-lakes [m]:			
Broad-crested weir			hweir=	2.98			1200			
sigma	hu/h	Manning	h0	Lw	Surface inundated	ET/P	GW loss	Surface Q	Volumen lakes	H,island
-	-	m³/s	m	m	m²	m³/d	m³/d	m³/d	m³	m
0.30	1.00	896436.00	0.39	8	14172818.97	-17007.38	0	74567.59592	15875119.05	5.77
1.00	0.00	898057.03	0.39	8	14180034.76	-17016.04	1153.06	251373.1322	15817558.83	5.77
1.00	0.00	889019.78	0.38	8	14139285.33	-16967.14	2509.605	235780.2332	15582048.68	5.76
1.00	0.00	880527.12	0.36	8	14099807	-16919.77	4070.831	221350.8276	15360725.99	5.74
1.00	0.00	872526.16	0.35	8	14061525.2	-16873.83	5935.763	207964.7018	15152224.10	5.73
1.00	0.00	864964.95	0.33	8	14024342.5	-16829.21	6788.76	195508.1943	14955197.46	5.71
1.00	0.00	857846.53	0.32	8	13988415.66	-16786.1	7443.981	183960.9617	14769729.72	5.70
1.00	0.00	851143.57	0.31	8	13953743.63	-16744.49	8003.164	173253.9179	14595110.88	5.69
1.00	0.00	844827.55	0.29	8	13920304.33	-16704.37	8166.033	163318.5992	14430598.29	5.67
1.00	0.00	838884.17	0.28	8	13888138.36	-13888.14	8035.314	154110.9808	14275818.02	5.66
1.00	0.00	776501.45	0.16	8	13505049.65	-13505.05	5963.063	67317.73629	12653403.95	5.54
1.00	0.00	774199.48	0.16	8	13489163.41	-13489.16	6688.869	64525.3578	12593628.20	5.54
1.00	0.00	771976.22	0.15	8	13473691	-13473.69	7608.632	61861.62924	12535903.13	5.53
1.00	0.00	769819.27	0.15	8	13458557.58	-13458.56	8818.388	59309.18151	12479906.56	5.53
1.00	0.00	767713.22	0.15	8	13443663.75	-13443.66	10994.44	56847.84061	12425237.55	5.53
1.00	0.00	765617.35	0.14	8	13428725.64	-13428.73	12585.61	54429.32688	12370838.94	5.52
1.00	0.00	763552.54	0.14	8	13413894.6	-13413.89	13497.8	52077.47958	12317252.72	5.52
1.00	0.00	761542.41	0.13	8	13399346.33	-13399.35	14795.14	49817.92472	12265091.34	5.51
1.00	0.00	759568.58	0.13	8	13384954.37	-13384.95	16090.46	47628.61122	12213877.62	5.51
1.00	0.00	757628.44	0.13	8	13370704.46	-13370.7	16806.12	45505.701	12163543.50	5.51
1.00	0.00	714527.10	0.04	8	13025876.05	8206.3019	4389.063	7555.426441	11046728.83	5.42
1.00	0.00	713748.49	0.04	8	13019117.72	8202.0442	4746.614	7079.235962	11026578.04	5.42
1.00	0.00	712974.60	0.03	8	13012380.58	8197.7998	5291.26	6615.992729	11006550.14	5.41
1.00	0.00	712197.69	0.03	8	13005597.34	8193.5263	5647.969	6161.293885	10986445.09	5.41
1.00	0.00	711424.71	0.03	8	12998828.51	8189.262	6191.561	5719.452682	10966442.30	5.41
1.00	0.00	710647.93	0.03	8	12992006.43	8184.9641	6828.014	5286.34996	10946342.03	5.41
1.00	0.00	709863.42	0.03	8	12985096.13	8180.6106	7276.6	4860.365969	10926042.70	5.41
1.00	0.00	709078.18	0.03	8	12978158.75	14924.883	7724.665	4445.836375	10905725.12	5.41
1.00	0.00	708030.93	0.02	8	12968874.5	14914.206	8352.415	3912.131707	10878629.74	5.40
1.00	0.00	706980.41	0.02	8	12959524.11	14903.453	8885.823	3399.686716	10851450.99	5.40
1.00	0.00	691579.15	0.00	8	12818075.47	14740.787	3876.186	0	10453158.24	5.37
1.00	0.00	690858.98	0.00	8	12811256.52	14732.945	3583.373	0	10434541.27	5.37
1.00	0.00	690150.43	0.00	8	12804529.2	14725.209	3567.689	0	10416224.95	5.37
1.00	0.00	687973.06	0.00	8	12783742.46	14701.304	4531.972	0	10359943.39	5.36
1.00	0.00	687228.93	0.00	8	12776598.85	14693.089	5158.881	0	10340710.11	5.36
1.00	0.00	686460.84	0.00	8	12769203.92	14684.585	5692.557	0	10320858.14	5.36
1.00	0.00	685672.40	0.00	8	12761590.54	14675.829	6225.099	0	10300481.00	5.36
1.00	0.00	684863.67	0.00	8	12753757.38	14666.821	6848.306	0	10279580.07	5.36
1.00	0.00	664942.56	0.00	8	12552967.03	26110.171	11145.17	0	9764961.91	5.31
1.00	0.00	663499.79	0.00	8	12537821.8	26078.669	12006.3	0	9727706.57	5.31
1.00	0.00	662024.82	0.00	8	12522251.65	26046.283	12864.22	0	9689621.59	5.31
1.00	0.00	660517.80	0.00	8	12506251.91	26013.004	13268.61	0	9650711.09	5.30
1.00	0.00	658996.33	0.00	8	12490004.6	25979.21	13851.18	0	9611429.48	5.30
1.00	0.00	657453.52	0.00	8	12473432.27	25944.739	14161.94	0	9571599.08	5.30
1.00	0.00	655899.94	0.00	8	12456644.62	25909.821	15009.45	0	9531492.41	5.29
1.00	0.00	654314.80	0.00	8	12439412.38	25873.978	15763.83	0	9490573.14	5.29
1.00	0.00	652701.74	0.00	8	12421768.55	25837.279	16336.06	0	9448935.33	5.29
1.00	0.00	651067.86	0.00	8	12403784.99	25799.873	16637.76	0	9406762.00	5.28
1.00	0.00	626316.30	0.00	8	12117026.27	39259.165	13681.92	0	8768082.53	5.23
1.00	0.00	624264.11	0.00	8	12091995.73	39178.066	13874.86	0	8715141.45	5.22
1.00	0.00	622207.54	0.00	8	12066711.13	39096.144	14413.95	0	8662088.52	5.22
1.00	0.00	620133.20	0.00	8	12041002.98	39012.85	15643.27	0	8608578.43	5.21
1.00	0.00	618014.40	0.00	8	12014529.21	38927.075	16432.67	0	8553922.31	5.21

1.00	0.00	615868.29	0.00	8	11987491.23	38839.472	16958.08	0	8498562.57	5.20
1.00	0.00	613705.19	0.00	8	11960009.96	38750.432	17221.56	0	8442765.01	5.20
1.00	0.00	596098.51	0.00	8	11727500.5	37997.102	20009.61	0	7988594.95	5.16
1.00	0.00	593849.94	0.00	8	11696639.07	37897.111	20671.29	0	7930588.23	5.15
1.00	0.00	591579.67	0.00	8	11665203.08	37795.258	20739.71	0	7872019.83	5.15
1.00	0.00	589310.77	0.00	8	11633505.74	37692.559	21309.49	0	7813484.86	5.14
1.00	0.00	587023.85	0.00	8	11601270.34	37588.116	21540.28	0	7754482.80	5.14
1.00	0.00	543360.90	0.00	8	10926679.9	51136.862	23327.87	0	6627099.71	5.04
1.00	0.00	540480.41	0.00	8	10877938.02	50908.75	23638.93	0	6552634.98	5.03
1.00	0.00	537597.31	0.00	8	10828588.18	50677.793	24256.58	0	6478087.29	5.02
1.00	0.00	534699.89	0.00	8	10778417.71	50442.995	24865.28	0	6403152.92	5.01
1.00	0.00	531788.69	0.00	8	10727420.03	50204.326	25155.93	0	6327844.65	5.01
1.00	0.00	528876.18	0.00	8	10675801.62	49962.752	25133.56	0	6252484.39	5.00
1.00	0.00	525974.60	0.00	8	10623774.67	49719.265	25185.79	0	6177388.08	4.99
1.00	0.00	523081.18	0.00	8	10571287.47	49473.625	24702.4	0	6102483.02	4.99
1.00	0.00	520216.70	0.00	8	10518721.11	49227.615	24525.71	0	6028306.99	4.98
1.00	0.00	517369.35	0.00	8	10465865.63	48980.251	24198.33	0	5954553.67	4.97
1.00	0.00	474800.62	0.00	8	9598443.772	40889.37	21441.08	0	4848824.22	4.86
1.00	0.00	472409.02	0.00	8	9545091.91	40662.092	21141.36	0	4786493.77	4.86
1.00	0.00	470038.64	0.00	8	9491692.415	40434.61	20980.48	0	4724690.32	4.85
1.00	0.00	467684.17	0.00	8	9438131.973	40206.442	20819.9	0	4663275.23	4.84
1.00	0.00	465345.60	0.00	8	9384415.818	39977.611	20929.89	0	4602248.89	4.84
1.00	0.00	463012.63	0.00	8	9330308.038	39747.112	20834.82	0	4541341.39	4.83
1.00	0.00	460693.17	0.00	8	9275993.221	39515.731	20605.55	0	4480759.46	4.83
1.00	0.00	458392.39	0.00	8	9221597.686	39284.006	20377.57	0	4420638.18	4.82
1.00	0.00	456110.27	0.00	8	9167127.496	39051.963	20084.91	0	4360976.60	4.81
1.00	0.00	453849.29	0.00	8	9112649.799	38819.888	19663.32	0	4301839.72	4.81
1.00	0.00	419055.14	0.00	8	8205792.795	34956.677	20332.4	0	3387831.58	4.71
1.00	0.00	416960.57	0.00	8	8146825.328	28513.889	20093.08	0	3332542.50	4.71
1.00	0.00	415120.19	0.00	8	8094577.497	28331.021	19933.97	0	3283935.54	4.70
1.00	0.00	413293.76	0.00	8	8042317.588	28148.112	19775.37	0	3235670.55	4.70
1.00	0.00	411481.24	0.00	8	7990050.464	27965.177	19732.36	0	3187747.07	4.69
1.00	0.00	409678.26	0.00	8	7937654.134	27781.789	19745.14	0	3140049.53	4.68
1.00	0.00	407882.73	0.00	8	7885069.859	27597.745	20096.26	0	3092522.60	4.68
1.00	0.00	406081.90	0.00	8	7831921.428	27411.725	19931.81	0	3044828.60	4.67
1.00	0.00	404295.33	0.00	8	7778785.124	27225.748	19991.98	0	2997485.06	4.67
1.00	0.00	402514.53	0.00	8	7725411.883	27038.942	19993.26	0	2950267.34	4.66
1.00	0.00	368629.33	0.00	8	6626812.927	23193.845	14479.57	0	2266395.49	4.56
1.00	0.00	367047.75	0.00	8	6571423.762	22999.983	14335.95	0	2228722.07	4.56
1.00	0.00	363879.64	0.00	8	6459291.575	22607.521	14186.21	0	2154060.53	4.55
1.00	0.00	362301.18	0.00	8	6402828.79	22409.901	13855.67	0	2117266.80	4.55
1.00	0.00	360733.78	0.00	8	6346365.911	22212.281	13528.88	0	2081001.22	4.54
1.00	0.00	359177.41	0.00	8	6289906.862	10063.851	13160.55	0	2045260.06	4.54
1.00	0.00	358159.73	0.00	8	6252775.34	10004.441	12933.78	0	2022035.66	4.53
1.00	0.00	347561.45	0.00	8	5855792.074	9369.2673	12185.4	0	1999097.44	4.50
1.00	0.00	346460.16	0.00	8	5813437.882	9301.5006	12208.46	0	1977542.78	4.50
1.00	0.00	327999.02	0.00	8	5070727.522	8113.164	10909.92	0	1642085.61	4.44
1.00	0.00	326868.02	0.00	8	5023137.898	8037.0206	10143.36	0	1623062.53	4.43
1.00	0.00	325777.57	0.00	8	4977016.75	7963.2268	8962.597	0	1604882.14	4.43
1.00	0.00	314949.12	0.00	8	4506040.32	7209.66	4658.4	0	1432705.42	4.40

The next sheets represent the year 2005. First the bag weir is summarised.

			2005	Cd=	0.80			Distance Danube-lakes [m]:			
			Bag weir	hweir=	3.02			1200			
ET			Manning	h0	Lw	Surface inund.	ET/P	GW loss	Surface Q	Volumen lakes	H,island
mm/d	Date	2005	m³/s	m	m	m²	m³/d	m³/d	m³/d	m³	m
3.24	21. Jun	5.81	896436.00	0.35	8	14172818.97	45919.93	0	338106.8935	15875119.05	5.77
3.24	22. Jun	5.72	885529.58	0.33	8	14123202.48	45759.18	306.561	309751.8974	15491092.22	5.75
3.24	23. Jun	5.53	871875.72	0.31	8	14058365.49	45549.1	1974.7	275165.3067	15135274.58	5.73
3.24	24. Jun	5.36	859491.45	0.28	8	13996798.51	45349.63	3448.2	244736.6764	14812585.47	5.70
3.24	25. Jun	5.21	848223.58	0.26	8	13938378.13	45160.35	4728.1	217891.1661	14519050.96	5.68
3.24	26. Jun	5.12	837941.51	0.24	8	13882973.14	44980.83	5415.66	194145.3362	14251271.36	5.66
3.24	27. Jun	4.95	828548.81	0.22	8	13830535.65	44810.94	6910.96	173124.884	14006729.53	5.64
3.24	28. Jun	4.75	819909.76	0.21	8	13780705.81	44649.49	8707.15	154396.1705	13781882.75	5.63
3.24	29. Jun	4.59	811924.85	0.19	8	13733235.77	44495.68	10107.9	137635.5284	13574129.94	5.61
3.24	30. Jun	4.43	804533.74	0.18	8	13688045.33	44349.27	11511.1	122622.6575	13381890.85	5.60
4.68	17. Jul	6.13	726124.03	0.02	8	13124219.64	61421.35	0	5290.07087	11346961.95	5.44
4.68	18. Jul	6.2	723547.83	0.02	8	13102743.47	61320.84	0	3493.184081	11280250.53	5.44
4.68	19. Jul	6.25	721044.56	0.01	8	13081674.41	61222.24	0	2000.606936	11215436.51	5.43
4.68	20. Jul	6.32	718602.42	0.01	8	13060927.14	61125.14	0	838.5995688	11152213.67	5.43
4.68	21. Jul	6.34	716208.61	0.00	8	13040403.85	61029.09	0	91.67154577	11090249.93	5.42
4.68	22. Jul	6.41	713847.07	0.00	8	13019974.45	60933.48	0	0	11029129.17	5.42
4.68	23. Jul	6.42	711492.47	0.00	8	12999422.64	60837.3	0	0	10968195.69	5.41
4.68	24. Jul	6.4	709141.30	0.00	8	12978717.2	60740.4	0	0	10907358.39	5.41
4.68	25. Jul	6.33	706793.60	0.00	8	12957857.44	60642.77	0	0	10846617.99	5.40
4.68	26. Jul	6.27	704449.38	0.00	8	12936842.71	60544.42	0	0	10785975.22	5.40
4.26	21. Aug	5.73	645505.66	0.00	8	12341708.76	52575.68	0	0	9263205.95	5.27
4.26	22. Aug	5.98	643468.37	0.00	8	12318636.92	52477.39	0	0	9210630.27	5.27
4.26	23. Aug	6.04	641434.78	0.00	8	12295425.61	52378.51	0	0	9158152.88	5.26
4.26	24. Aug	6.08	639404.93	0.00	8	12272074.63	52279.04	0	0	9105774.37	5.26
4.26	25. Aug	6.08	637378.85	0.00	8	12248583.8	52178.97	0	0	9053495.33	5.25
4.26	26. Aug	6.16	635356.56	0.00	8	12224952.93	52078.3	0	0	9001316.36	5.25
4.26	27. Aug	6.22	633338.10	0.00	8	12201181.85	51977.03	0	0	8949238.06	5.24
4.26	28. Aug	6.26	631323.49	0.00	8	12177270.43	51875.17	0	0	8897261.03	5.24
4.26	29. Aug	6.3	629312.76	0.00	8	12153218.5	51772.71	0	0	8845385.85	5.23
4.26	30. Aug	6.32	627305.94	0.00	8	12129025.97	51669.65	0	0	8793613.14	5.23
3.5	15. Sep	5.75	600611.19	0.00	8	11788624.1	41260.18	0	0	8105004.78	5.17
3.5	16. Sep	5.52	599011.70	0.00	8	11767082.4	41184.79	0	0	8063744.60	5.17
3.5	17. Sep	5.28	597415.16	0.00	8	11745445.73	41109.06	0	0	8022559.81	5.16
3.5	20. Sep	4.68	592527.59	0.00	8	11678362.75	40874.27	3964.67	0	7896474.56	5.15
3.5	21. Sep	4.6	590789.53	0.00	8	11654196.62	40789.69	4594.06	0	7851635.62	5.15
3.5	22. Sep	4.65	589030.41	0.00	8	11629569.49	40703.49	4131.6	0	7806251.87	5.14
3.5	23. Sep	4.79	587292.61	0.00	8	11605073.6	40617.76	2919.45	0	7761416.78	5.14
3.5	24. Sep	4.98	585605.17	0.00	8	11581127.37	40533.95	1296.46	0	7717879.57	5.14
1.6	09. Okt	4.86	568921.92	0.00	8	11335633.25	18137.01	1929.33	0	7287335.39	5.10
1.6	10. Okt	4.85	568144.58	0.00	8	11323796.86	18118.07	1993.87	0	7267269.04	5.09
1.6	11. Okt	4.88	567365.51	0.00	8	11311897.44	18099.04	1732.43	0	7247157.10	5.09
1.6	12. Okt	4.95	566597.32	0.00	8	11300128.45	18080.21	1146.3	0	7227325.64	5.09
1.6	13. Okt	4.97	565852.59	0.00	8	11288684.7	18061.9	968.242	0	7208099.14	5.09
1.6	14. Okt	4.94	565115.49	0.00	8	11277324.99	18043.72	1196.67	0	7189069.00	5.09
1.6	15. Okt	4.93	564370.27	0.00	8	11265806.47	18025.29	1262.22	0	7169828.61	5.09
1.6	16. Okt	4.97	563623.25	0.00	8	11254226.02	18006.76	922.426	0	7150541.10	5.08
1.6	17. Okt	4.97	562890.13	0.00	8	11242827.78	17988.52	907.39	0	7131611.91	5.08
1.6	18. Okt	4.99	562158.32	0.00	8	11231416.97	17970.27	730.664	0	7112716.00	5.08
1.6	31. Okt	3.54	550610.36	0.00	8	11046906.47	17675	12032	0	6814446.08	5.05

Furthermore, the broad-crested weir is represented.

2005			Cd=	0.50			Distance Danube-lakes [m]:			
Borad-crested weir			hweir=	2.98			1200			
sigma	hu/h	Manning	h0	Lw	Surface inund.	ET/P	GW loss	Surface Q	Volumen lakes	H,island
-	-	m³/s	m	m	m²	m³/d	m³/d	m³/d	m³	m
0.30	1.00	896436.00	0.39	8	14172818.97	45919.93	0	74567.59592	15875119.05	5.77
1.00	0.72	895642.26	0.39	8	14169270.94	45908.44	495.403	247183.2886	15754631.52	5.77
1.00	0.00	884376.58	0.37	8	14117846.32	45741.82	2216.35	227863.6828	15461044.39	5.75
1.00	0.00	873792.46	0.35	8	14067655.93	45579.21	3733.66	210069.4889	15185222.53	5.73
1.00	0.00	863838.25	0.33	8	14018716.28	45420.64	5049.07	193668.6901	14925840.18	5.71
1.00	0.00	854467.59	0.31	8	13971041.22	45266.17	5761.93	178543.0049	14681701.78	5.69
1.00	0.00	845654.29	0.30	8	13924724.54	45116.11	7281.87	164610.3955	14452130.67	5.68
1.00	0.00	837321.33	0.28	8	13879565.32	44969.79	9100.15	151713.2399	14235122.30	5.66
1.00	0.00	829417.36	0.27	8	13835459.62	44826.89	10516	139741.4863	14029339.12	5.65
1.00	0.00	821922.25	0.25	8	13792453.83	44687.55	11930.5	128636.6045	13834254.74	5.63
0.30	1.00	733777.67	0.08	8	13186807.59	61714.26	0	6612.220766	11545210.42	5.46
0.30	1.00	731140.20	0.07	8	13165442.88	61614.27	0	5935.627854	11476883.94	5.45
0.30	1.00	728532.33	0.07	8	13144108.43	61514.43	0	5289.681373	11409334.04	5.45
0.30	1.00	725952.89	0.06	8	13122799.4	61414.7	0	4674.409081	11342529.93	5.44
0.30	1.00	723400.70	0.06	8	13101510.62	61315.07	0	4089.948128	11276440.82	5.44
0.30	1.00	720874.58	0.05	8	13080236.54	61215.51	0	3536.564944	11211035.80	5.43
0.30	1.00	718373.34	0.05	8	13058971.19	61115.99	0	3014.68213	11146283.73	5.43
0.30	1.00	715895.78	0.04	8	13037708.12	61016.47	0	2524.915721	11082153.06	5.42
0.30	1.00	713440.67	0.04	8	13016440.32	60916.94	0	2068.128428	11018611.67	5.42
0.30	1.00	711006.74	0.03	8	12995160.16	60817.35	0	1645.508676	10955626.60	5.41
0.30	1.00	651525.64	0.00	8	12408834.95	52861.64	0	0	9418577.74	5.28
0.30	1.00	649477.59	0.00	8	12386172.48	52765.09	0	0	9365716.11	5.28
0.30	1.00	647433.17	0.00	8	12363371.2	52667.96	0	0	9312951.01	5.28
0.30	1.00	645392.40	0.00	8	12340430.88	52570.24	0	0	9260283.05	5.27
0.30	1.00	643355.31	0.00	8	12317351.3	52471.92	0	0	9207712.82	5.27
0.30	1.00	641321.93	0.00	8	12294132.24	52373	0	0	9155240.90	5.26
0.30	1.00	639292.29	0.00	8	12270773.5	52273.5	0	0	9102867.90	5.26
0.30	1.00	637266.42	0.00	8	12247274.89	52173.39	0	0	9050594.40	5.25
0.30	1.00	635244.35	0.00	8	12223636.23	52072.69	0	0	8998421.01	5.25
0.30	1.00	633226.10	0.00	8	12199857.37	51971.39	0	0	8946348.32	5.24
0.30	1.00	606368.45	0.00	8	11865058.49	41527.7	0	0	8253514.78	5.18
0.30	1.00	604758.54	0.00	8	11843857.59	41453.5	0	0	8211987.08	5.18
0.30	1.00	603151.51	0.00	8	11822561.56	41378.97	0	0	8170533.58	5.18
1.00	0.00	598222.74	0.00	8	11756407.11	41147.42	4102.13	0	8043392.46	5.16
1.00	0.00	596468.64	0.00	8	11732554.44	41063.94	4735.56	0	7998142.90	5.16
1.00	0.00	594693.25	0.00	8	11708245.23	40978.86	4269.81	0	7952343.40	5.16
1.00	0.00	592939.26	0.00	8	11684062.59	40894.22	3049.22	0	7907094.73	5.15
1.00	0.00	591235.90	0.00	8	11660418.68	40811.47	1414.88	0	7863151.28	5.15
1.00	0.00	574415.81	0.00	8	11418262.13	18269.22	2049.81	0	7429140.37	5.11
1.00	0.00	573628.53	0.00	8	11406530.9	18250.45	2114.63	0	7408821.34	5.11
1.00	0.00	572839.49	0.00	8	11394736.84	18231.58	1851.09	0	7388456.25	5.11
1.00	0.00	572061.42	0.00	8	11383070.69	18212.91	1260.48	0	7368373.58	5.10
1.00	0.00	571306.96	0.00	8	11371724.57	18194.76	1080.91	0	7348900.19	5.10
1.00	0.00	570560.19	0.00	8	11360460.67	18176.74	1310.83	0	7329624.52	5.10
1.00	0.00	569805.23	0.00	8	11349039.5	18158.46	1376.67	0	7310136.95	5.10
1.00	0.00	569048.45	0.00	8	11337556.6	18140.09	1034.16	0	7290601.83	5.10
1.00	0.00	568305.68	0.00	8	11326252.77	18122	1018.82	0	7271427.57	5.09
1.00	0.00	567564.21	0.00	8	11314935.89	18103.9	840.578	0	7252286.75	5.09
1.00	0.00	555874.01	0.00	8	11132055.71	17811.3	12226	0	6950422.32	5.07